

AD-A210 322

REPORT DOCUMENTATION PAGE

DTIC
ELECTE
D
JUL 19 1989
B

2a. SECURITY CLASSIFICATION AUTHORITY		1b. RESTRICTIVE MARKINGS	
2b. DECLASSIFICATION / DOWNGRADING SCHEDULE		3. DISTRIBUTION / AVAILABILITY OF REPORT	
4. PERFORMING ORGANIZATION REPORT NUMBER(S)		5. MONITORING ORGANIZATION REPORT NUMBER(S)	
6a. NAME OF PERFORMING ORGANIZATION		6b. OFFICE SYMBOL (if applicable)	
6c. ADDRESS (City, State, and ZIP Code)		7a. NAME OF MONITORING ORGANIZATION	
8a. NAME OF FUNDING / SPONSORING ORGANIZATION		8b. OFFICE SYMBOL (if applicable)	
8c. ADDRESS (City, State, and ZIP Code)		9. PROCUREMENT INSTRUMENT IDENTIFICATION NUMBER	
		10. SOURCE OF FUNDING NUMBERS	
		PROGRAM ELEMENT NO.	PROJECT NO.
		TASK NO.	WORK UNIT ACCESSION NO.
11. TITLE (Include Security Classification)			
12. PERSONAL AUTHOR(S)			
13a. TYPE OF REPORT	13b. TIME COVERED	14. DATE OF REPORT (Year, Month, Day)	15. PAGE COUNT
16. SUPPLEMENTARY NOTATION			
17. COSATI CODES		18. SUBJECT TERMS (Continue on reverse if necessary and identify by block number)	
FIELD	GROUP	Cationic Polymerization/Energetic Polymers/Oxetanes/Quantum Chemical Calculations/Configuration Interaction (CI)/Multireference Double Excitation - Configuration Interaction(cont)	
19. ABSTRACT (Continue on reverse if necessary and identify by block number)			
<p>I. New Program Developments on the CRAY Supercomputer</p> <p>II. MRD-CI Calculations for Cationic Polymerization of Energetic Oxetanes</p> <p>III. Ab-Initio MRD-CI Calculations for Breaking a Chemical Bond in a Molecule in a Crystal or Other Solid Environment</p> <p>IV. Ab-Initio Multireference Coupled Cluster and Multireference CI Calculations for Protonation NH_3^+ / Deprotonation NH_2^-</p> <p>V. MR-CC (Multireference-Coupled Cluster)</p> <p>A state-of-the-theoretical-art multireference coupled cluster (for both closed and open shell systems) was rewritten, vectorized and adapted for the CRAY XMP supercomputer.</p> <p>B. MRD-CI (Multireference Double Excitation-Configuration Interaction)</p> <p>In order to be able to handle the transformations for the MRD-CI calculations for larger</p>			
20. DISTRIBUTION / AVAILABILITY OF ABSTRACT		21. ABSTRACT SECURITY CLASSIFICATION	
22a. NAME OF RESPONSIBLE INDIVIDUAL		22b. TELEPHONE (Include Area Code)	
22c. OFFICE SYMBOL			

A 89 7 19 047

18. (continued) (MRD-CI)/Energetic Compounds/MRD-CI for breaking Chemical Bond in Crystal/MR-CC Multireference Coupled Cluster/ NH_4^+ MR-CC and MRD-CI Potential Surfaces

19. Abstract (continued)

systems we are rewriting the integral transformation program from integrals over atomic orbitals to integrals over molecular orbitals.

II. Our major emphasis this past year has been to carry out in-depth detailed ab-initio MRD-CI (multireference double excitation - configuration interaction) calculations on the propagation step of cationic polymerization of oxetane (or an energetic substituted oxetane) reacting with protonated oxetane (or a protonated energetic substituted oxetane). MRD-CI calculations (based on localized orbitals) along the potential energy surfaces have been carried out for a very large number of geometry variations. These have enabled us to map out the reaction coordinates of the propagation step reaction of oxetane (or an energetic substituted oxetane) reacting with protonated oxetane (or with a protonated energetic substituted oxetane), to identify the transition state of the propagation step and to identify when the $\text{C}_{4A}-\text{O}_{1A}$ bond in the protonated ring will start to open as a function of inter-ring distance and angle for each different pair of substituted reactants. This year we carried out the MRD-CI calculations for the propagation step of cationic polymerization involving BAMO and BAMOH⁺ species: BAMO + OXETH⁺, BAMO + AMMOH⁺ and OXET + BAMOH⁺. We are also carrying out the MRD-CI calculations for AMMO + BAMOH⁺ (which should be completed in the next quarter). We have run the SCF calculations for BAMO + BAMOH⁺. For certain of the intermolecular geometries of BAMO + BAMOH⁺ there are more integrals than the available peripheral disk space can handle with the transformation program (needed to run the subsequent MRD-CI calculations). The results of our calculations to date suggest some general postulates concerning propensities of various substituted oxetane partners for homopolymerization and copolymerization.

III. A. Nitromethane $\text{H}_3\text{C} - \text{NO}_2$

This past year, we have carried out extensive further MRD-CI calculations on breaking the $\text{H}_3\text{C} - \text{NO}_2$ bond in nitromethane in a nitromethane crystal in the presence of voids. (RW)

B. Dimethylnitramine $\text{Me}_2\text{N} - \text{NO}_2$

As a prototype for breaking $>\text{N} - \text{NO}_2$ bonds we initiated MRD-CI calculations for breaking the $\text{Me}_2\text{N} - \text{NO}_2$ bond. In the ground and several electronically excited states $\text{Me}_2\text{N} - \text{NO}_2$ is not describable properly as a single determinant and requires more reference configurations than any other molecule we have ever investigated.

IV. We carried out both MR-CC and, for comparison, MRD-CI calculations for the dissociation of NH_4^+ (which itself is the cation in several energetic species). The lowest 1A_1 state of NH_4^+ at equilibrium dissociates adiabatically to $\text{NH}_3(\bar{X} \ ^2A_1) + \text{H}$ not to $\text{NH}_3(\bar{X} \ ^1A_1) + \text{H}^+$. The curve arising at the asymptote from $\text{NH}_3(\bar{X} \ ^1A_1) + \text{H}^+$ is a repulsive $\bar{A} \ ^1A_1$ curve and does not cross the other 1A_1 curve. Only the SCF (or unrestricted Hartree-Fock UHF) lowest $\bar{X} \ ^1A_1$ curve dissociates incorrectly adiabatically to $\text{NH}_3(\bar{X} \ ^1A_1) + \text{H}^+$. This is significant because it implies UHF curves [whether or not subsequently corrected by MP (Møller-Plesset perturbation correlation energy corrections)] do not give correct physical results for certain dissociations.

Report Number ONR-NR093964-TR9

SUMMARY

ANNUAL REPORT

QUANTUM CHEMICAL INVESTIGATIONS OF THE MECHANISM OF CATIONIC
POLYMERIZATION

and

THEORETICAL PREDICTION OF CRYSTAL DENSITIES

and

DECOMPOSITION PATHWAYS OF ENERGETIC MOLECULES

Joyce J. Kaufman, Principal Investigator
Department of Chemistry
The Johns Hopkins University

Contract N00014-80-C-0003
Office of Naval Research

Dr. Richard Miller, ONR Contract Monitor

Period Covered October 1, 1987 - September 30, 1988

November 15, 1988

Approved for public release; distribution limited

Reproduction in whole or in part is permitted for any purpose of the United
States Government

QUANTUM CHEMICAL INVESTIGATIONS OF THE MECHANISM OF CATIONIC
POLYMERIZATION
and
THEORETICAL PREDICTION OF CRYSTAL DENSITIES
and
DECOMPOSITION PATHWAYS OF ENERGETIC MOLECULES

Joyce J. Kaufman, Principal Investigator
Department of Chemistry
The Johns Hopkins University

TABLE OF CONTENTS

CONCISE SUMMARY	1
I. New Program Developments on the CRAY Supercomputer	9
A. MR-CC (Multireference - Coupled Cluster)	9
B. MRD-CI (Multireference Double Excitation - Configuration Interaction)	11
II. MRD-CI Calculations for Cationic Polymerization of Energetic Oxetanes	12
A. Ab-Initio MRD-CI Calculations for the Propagation Step	13
1. Discussion of Calculation Procedure and Pathways of Attack	13
B. Detailed Results	18
1. Energies	18
a. 3,3-Bis(azidomethyl)oxetane (BAMO) + protonated oxetane (OXETH ⁺)	18
b. 3,3-Bis(azidomethyl)oxetane (BAMO) + protonated 3-azidomethyl-3-methyloxetane (AMMOH ⁺)	28
c. Oxetane (OXET) + protonated 3,3-bis(azidomethyl)-oxetane (BAMOH ⁺)	39
d. 3-Azidomethyl-3-methyloxetane (AMMO) + protonated 3,3-bis(azidomethyl)oxetane (BAMOH ⁺)	49
e. 3,3-Bis(azidomethyl)oxetane (BAMO) + protonated 3,3-bis(azidomethyl)oxetane (BAMOH ⁺)	50
2. Recap of Reaction Energies for Cationic Polymerization of Energetic Oxetanes for Initiation and Reaction	51
3. Population Analyses	53
III. Ab-Initio MRD-CI Calculations for Breaking a Chemical Bond in a Crystal or Other Solid Environment	73
A. Methodology	73
B. Calculations Carried Out for Nitromethane	74
C. Calculations Carried Out for Dimethylnitramine	89

IV. Ab-Initio Multireference Coupled Cluster and Multireference MRD-CI Calculations for Protonation NH ₃ / Deprotonation NH ₄ ⁺	102
A. Methodology - Multireference - Coupled Cluster Method (MR-CCM)	103
1. General Discussion of Coupled Cluster Method	103
2. Specific Methodology	104
3. Computational Details of the (H ₃ N --- H) ⁺ MR-CCM Calculations	107
B. Results and Discussion	108
C. Conclusion	110
V. Lectures Presented and Publications on This ONR Research	121
A. Presentations Given Dr. Joyce J. Kaufman	121
B. Publications	122
VI. Project Personnel	124
Distribution List	125



Accession For	
NTIS GRA&I	<input checked="" type="checkbox"/>
DTIC TAB	<input type="checkbox"/>
Unannounced	<input type="checkbox"/>
Justification	
By _____	
Distribution/	
Availability Codes	
Dist	Avail and/or Special
A-1	

QUANTUM CHEMICAL INVESTIGATIONS OF THE MECHANISM OF CATIONIC
POLYMERIZATION
and
THEORETICAL PREDICTION OF CRYSTAL DENSITIES
and
DECOMPOSITION PATHWAYS OF ENERGETIC MOLECULES

Joyce J. Kaufman, Principal Investigator
Department of Chemistry
The Johns Hopkins University

CONCISE SUMMARY

I. New Program Developments on the CRAY Supercomputer

A. MR-CC (Multireference - Coupled Cluster)

We have a long standing interest in comparing the reliability of multireference configuration interaction (MRD-CI) calculations with multireference coupled cluster (MR-CC) calculations. With the collaboration of Professor Uzi Kaldor, University of Tel Aviv, (a visiting scientist to our group at the Johns Hopkins University), his state-of-the-theoretical-art multireference coupled cluster program (for both closed shell and open shell systems) was rewritten, adapted and vectorized for the CRAY XMP supercomputer.

The reason for our considerable interest in this problem is described briefly below and will be described in more detail in the body of this report.

When making or breaking chemical bonds such as in molecular decompositions or intermolecular reactions it is necessary to use multiconfigurational wave functions. In this ONR research on energetic compounds we have demonstrated the necessity for such multiconfigurational wave functions by tracing the contribution of each significant configuration to every point on each potential surface.

When breaking a chemical bond in molecular decompositions or intermolecular reactions, to get reliable dissociation energies, desirably the calculation should be size extensive.

There are several approaches to try in order to have the calculations for dissociation or intermolecular reactions be size extensive (or approximately size extensive): MRD-CI (multireference double excitation-interaction) calculations with a "Davidson" type correction to remove unlinked double excitations and MR-CC (multireference-coupled cluster) calculations.

B. MRD-CI (Multireference Double Excitation - Configuration Interaction)

In order to be able to handle the transformations for the MRD-CI calculations for larger systems (such as BAMO + BAMOH⁺ or several dimethylnitramine molecules or larger energetic molecules as in the crystal) we are rewriting the transformation program. This program transforms integrals over atomic orbitals to integrals over molecular orbitals (the most computer time- and computer-memory and peripheral resource consuming portion of the MRD-CI calculations).

C. San Diego Supercomputer Center Allocation Committee

We continue to serve on the San Diego Supercomputer Center (SDSC) Allocation Committee. Dr. Joyce Kaufman served on the December 1987 and Dr. Walter Koski served on the April, June and September 1988 Allocation Committee Meetings. Of great pertinence for our entire ONR project on energetic compounds is that SDSC has granted us two substantial allocations of supercomputer CRAY XMP time, totalling several hundred hours for the year.

II. MRD-CI Calculations for Cationic Polymerization of Energetic Oxetanes

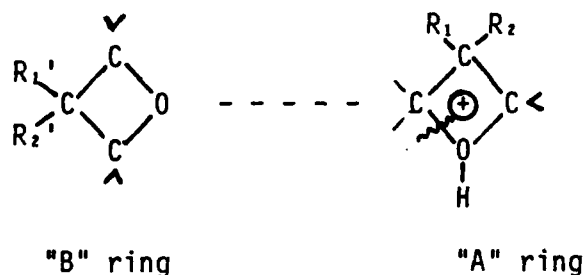
Our major emphasis this past year has been to carry out in-depth detailed ab-initio MRD-CI (multireference double excitation - configuration interaction) calculations on the propagation step of cationic polymerization of prototypal substituted energetic oxetanes.

Cationic polymerization consists essentially of two major steps: initiation and then propagation. There is considerable Navy interest in energetic polymers made by cationic polymerization of oxetanes substituted or disubstituted by exotic energetic substituents such as azido, azidomethyl, nitrate, nitraminomethyl, nitromethyl, NF₂, etc. as well as fluoro and nitro groups. The initiation step (which is crucial for cationic polymerization to take place) is governed by the propensity of the substituted oxetane to undergo protonation. Our previous ab-initio quantum chemical SCF calculations on the energetic oxetane monomers and electrostatic molecular potential contour (EMPC) maps we generated from these electronic wave functions, which predict the order of protonation and hence initiation, were able to predict correctly the propensity of the energetic substituted oxetane monomers to undergo polymerization even prior to the synthesis of the monomers.

A. Ab-Initio MRD/CI Calculations for the Propagation Step

1. Discussion of Calculation Procedure and Pathways of Attack

As was suggested to us by several different experimentalists in cationic polymerization (primarily Gerry Manser) the mechanism for the propagation step seems to be attack of protonated oxetanes on oxetanes (or vice versa) with concomitant ring opening of the protonated oxetane according to the following general scheme



We have carried out this past year and are continuing to carry out ab-initio MRD-CI calculations on the subsequent propagation step of oxetane (or an energetic substituted oxetane) reacting with protonated oxetane (or a protonated energetic substituted oxetane).

MRD-CI calculations along the potential energy surfaces have been carried out for a very large number of geometry variations for the angles between the planes of the substituted oxetane and protonated substituted oxetane rings (which can be different in each direction in the case of substituted rings), the inter-ring distance ($O_{1B}-C_{4A}$) (where the A ring is the protonated ring and the B ring is the non-protonated ring), the angle of opening the $C_{4A}-O_{1A}$ ring and the orientation of the H atoms on C_{4A} .

The preferred direction of attack appears to be the reaction of the oxygen of the unprotonated oxetane ring (which we call O_{1B}) with the α carbon (which we call C_{4A}) of the protonated substituted oxetane ring along the $C_{4A}-O_{1A}$ bond direction with concomitant pulling back (inversion of the H atoms on C_{4A}) and opening of the $C_{4A}-O_{1A}$ bond in the protonated oxetane ring and formation of an $O_{1B}-C_{4A}$ bond.

The ab-initio MRD-CI calculations on the propagation step of the protonated oxetane ring opening in the course of interaction with oxetane were carried out based on localized orbitals on the pertinent regions involved in the reaction.

These MRD-CI calculations have enabled us to map out the reaction coordinates of the propagation step reaction of oxetane (or an energetic substituted oxetane) reacting with protonated oxetane (or with a protonated energetic substituted oxetane), to identify the transition state of the propagation step and to identify when the $C_{4A}-O_{1A}$ bond in the protonated ring will start to open as a function of inter-ring distance and angle for each different pair of substituted reactants.

By comparing these results for different pairs of reacting substituted oxetanes and protonated substituted oxetanes we have been able to gain insight into preference toward copolymer candidates. In all cases we have studied to date our calculated predictions agree with the order of Gerry Manser's experimental polymerization reactivities ratios.

B. Detailed Results

This past year we carried out the MRD-CI calculations for the propagation step of cationic polymerization involving BAMO and BAMOH⁺ species: BAMO + OXETH⁺, BAMO + AMMOH⁺ and OXET + BAMOH⁺. We are also carrying out the MRD-CI calculations for AMMO + BAMOH⁺ (which should be completed in the next quarter).

Because there are bulky bis(azidomethyl) substituents in the 3,3-position of the BAMOH⁺ being attacked we explored considerably more geometry variations than usual. There is more steric hindrance when the C_{4A} of BAMOH⁺ is being attacked by the O_{1B} of AMMO than when the C_{4A} of AMMOH⁺ is being attacked by the O_{1B} of BAMO.

ΔE for the polymerization reaction has two components: ΔE (protonation) + ΔE (addition). ΔE for BAMO + AMMOH⁺ is quite close to that of AMMO + AMMOH⁺ (just a very little bit lower). Our previous calculations indicated that AMMO would have somewhat more of a tendency to protonate than would BAMO. Thus, in a mixture of AMMO + BAMO, AMMO will initiate first. Also AMMOH⁺ will have somewhat more of a tendency to react with itself (AMMO) than with BAMO. This is in accord with Gerry Manser's experimental polymerization results.

We have run the SCF calculations for BAMO + BAMOH⁺. For this latter case because of the steric hindrance we have examined a large number of intermolecular geometries. For certain of the intermolecular geometries of BAMO + BAMOH⁺ there are more integrals than the available peripheral disk space can handle with the transformation program (needed to run the subsequent MRD-CI calculations) in its current form. We are currently rewriting the transformation program. There is more steric hindrance when the C_{4A} of BAMOH⁺ is being attacked by OXET or AMMO than when the C_{4A} of OXETH⁺ or AMMOH⁺ is being attacked by BAMO. The attack of BAMO on BAMOH⁺ is even more sterically hindered than any of the other cases we have examined to date. This finding adds further evidence to our hypothesis that the steric hindrance could be a contributing factor to Gerry Manser's observations that bis compounds are more difficult to polymerize and copolymerize. This effect of bulky bis 3,3-substituents on the protonated oxetane being attacked could also be a contributing factor to Gerry Manser's comments that certain compounds will not undergo cationic polymerization or will undergo cationic polymerization only slowly or with difficulty.

The results of our calculations to date suggest some general postulates concerning propensities of various substituted oxetane partners for homopolymerization and copolymerization. For the oxetanes A and B, the species with the highest quantum chemically calculated proton affinity will initiate first. (It does not appear possible to measure directly

experimentally the proton affinities of oxetanes. Our experimental colleague, Dr. Walter S. Koski, had already tried a number of different experimental techniques for us on this problem, including proton transfer in a tandem mass spectrometer.) It is desirable that the species that initiates first have the lowest intrinsic steric hindrance [the least bulky 3,3-substituent(s) and the least number of these bulky 3,3-substituents]. The reason for this is that in the propagation step the 3,3-substituents on the protonated oxetane (designated here as molecule A) are on C_{3A} which is the neighbor of C_{4A} which is being attacked by O_{1B} of the neutral oxetane (designated here as molecule B). Thus the bulkiness of the 3,3-substituent(s) on A exert a profound influence on the steric hindrance to the propagation step. On the other hand the 3,3-substituents on the neutral oxetane are not neighbors to O_{1B} (the attacking atom of the neutral oxetane) and thus are expected to exert considerably less steric hindrance. The above discussion would also seem to indicate why certain compounds which cannot undergo homopolymerization can undergo copolymerization. A very sterically hindered 3,3-substituted oxetane may protonate and thus initiate but is so sterically hindered that it is very difficult for another like neutral 3,3-substituted oxetane to attack successfully the α position (C_{4A}) of the sterically hindered 3,3-substituted protonated oxetane.

We shall be continuing these MRD-CI calculations on the initiation and propagation steps in cationic polymerization. The species to be investigated and their partners will be chosen from Garry Manser's recent results.

III. Ab-Initio MRD-CI Calculations for Breaking a Chemical Bond in a Molecule in a Crystal or Other Solid Environment

MRD-CI (multireference double excitation-configuration interaction) calculations are necessary to describe bond breaking processes correctly. In the previous year, 1987, we derived, implemented and used successfully an extension of our MRD-CI technique based on localized/local orbitals to breaking of a chemical bond in a molecule in a crystal or other solid environment. This development has led to an important breakthrough which leads to crucial understanding of the initiation of detonation and the subsequent processes leading to detonation. Our method is completely general and applicable to any molecule in any kind of a crystal or other solid environment. The crystal can have voids, defects, deformations, dislocations, impurities, dopants, edges and surface boundaries, etc.

A. Nitromethane $H_3C - NO_2$

This past year, we have carried out extensive further MRD-CI calculations on breaking the $H_3C - NO_2$ bond in nitromethane in a nitromethane crystal in the presence of voids. To investigate the effect of voids we carried out a number more MRD-CI calculations of the energy necessary to break the $H_3C - NO_2$ bond in nitromethane in a nitromethane crystal as a function of voids in the nitromethane molecules represented by multipoles, in the nitromethane molecules treated explicitly in the SCF and in various combinations of voids in nitromethane multipoles and in

nitromethane molecules treated explicitly in the SCF. For each case of different types and combinations of voids the entire integral, SCF, MRD-CI calculation has to be carried out again. Our results to date indicate it still always takes more energy to break the $\text{H}_3\text{C} - \text{NO}_2$ bond when the nitromethane molecule is in a nitromethane crystal. However the relative energies for breaking the $\text{H}_3\text{C} - \text{NO}_2$ bond vary as function of the positions and types and combinations of the voids.

<Impurities and dopants can be treated in a manner completely analogous to our treatment of voids. In the cases of impurities and dopants the impurity or the dopant molecules can be in the space treated explicitly in the SCF or in the multipole environment.

B. Dimethylnitramine $\text{Me}_2\text{N} - \text{NO}_2$

As a prototype for breaking $>\text{N} - \text{NO}_2$ bonds we initiated MRD-CI calculations for breaking the $\text{Me}_2\text{N} - \text{NO}_2$ bond in dimethylnitramine. Dimethylnitramine has C_{2v} symmetry in the gas phase but not when the molecule is in a crystal. Thus in the MRD-CI for breaking the $\text{Me}_2\text{N} - \text{NO}_2$ bond in dimethylnitramine in a non-symmetrical environment only a combination of all singlet states or all triplet states can be solved.

This year we first investigated MRD-CI calculations for the isolated dimethylnitramine molecule (but without using symmetry) for the lowest and several electronically excited states. Each time a new configuration (not in the reference space) is found to be significant in any of the roots it is added to the reference configurations and the entire MRD-CI calculation is redone. Dimethylnitramine requires more reference configurations than any other molecule we have ever studied by MRD-CI. We have initiated MRD-CI investigations of the dissociation of dimethylnitramine in the crystal.

IV. Ab-Initio Multireference Coupled Cluster and Multireference CI Calculations for Protonation NH_3 / Deprotonation NH_4^+

The Coupled Cluster Methods are more sophisticated than the many-body-perturbation methods (including the Møller Plesset methods to any order). The coupled cluster method essentially corresponds to infinite order many-body perturbation theory.

The major problem in using the coupled cluster method for breaking or forming bonds is that a multiconfigurational wave function is necessary to describe these processes properly. We have carried out multireference coupled cluster (MR-CC) calculations (using the state-of-the-theoretical-art method of Kaldor). One of our interests in the MR-CC method is that it is size consistent and is supposed to give slightly more accurate dissociation energies.

We carried out both MR-CC and, for comparison, MRD-CI calculations for the dissociation of NH_4^+ (which itself is the cation in several energetic species and is the prototype of $\text{R}_1\text{R}_2\text{R}_3\text{NH}^+$ cations in other energetic species). We have carried out both the MR-CC and MRD-CI calculations at each point along the $(\text{H}_3\text{N} - - - \text{H})^+$ potential surface to compare the structures of the wave functions and their energies. At each point the geometry was optimized by MRD-CI calculations and the MR-CC calculations were carried out at the optimized geometry. Our results to date indicate that the agreement between the MR-CC and MRD-CI is quite close but more testing remains to be done on this and different systems. One important hypothesis we had made previously for protonation and deprotonation is confirmed. The lowest ${}^1\text{A}_1$ state of NH_4^+ at equilibrium dissociates adiabatically to $\text{NH}_3^+(\bar{\text{X}} {}^2\text{A}_1) + \text{H}$ not to $\text{NH}_3(\bar{\text{X}} {}^1\text{A}_1) + \text{H}^+$. The curve arising at the asymptote from $\text{NH}_3(\bar{\text{X}} {}^1\text{A}_1) + \text{H}^+$ is a repulsive $\bar{\text{A}} {}^1\text{A}_1$ curve and does not cross the other ${}^1\text{A}_1$ curve. Only the SCF (or unrestricted Hartree-Fock UHF) lowest $\bar{\text{X}} {}^1\text{A}_1$ curve dissociates incorrectly adiabatically to $\text{NH}_3(\bar{\text{X}} {}^1\text{A}_1) + \text{H}^+$. This is significant because it implies UHF curves [whether or not subsequently corrected by MP (Moeller-Plesset perturbation correlation energy corrections)] do not give correct physical results for certain dissociations. (MP corrections to any order cannot correct for this deficiency of the single determinant SCF or UHF wave function.)

We have had a great deal of interest in our new strategy of MRD-CI calculations based on localized/local orbitals for breaking a chemical bond in a molecule in a crystal or other solid environment. This same strategy is applicable for reactions in any type of environments. (Thus, this approach is relevant to initiation and subsequent processes leading to detonation.)

Dr. Kaufman presented a number of invited* papers on MRD-CI calculations for breaking the $\text{H}_3\text{C} - \text{NO}_2$ bond in nitromethane in a nitromethane crystal (* denotes invited lecture).

- *a. International Sanibel Symposium on Atomic, Molecular and Solid State Theory, Marineland, Florida, March 1988.
- *b. Working Group Meeting on Synthesis of High Energy Density Materials, U.S. Army Armament Research,

Development and Engineering Center, Dover, New Jersey, June 1988.

- c. American Chemical Society/North American Chemical Congress, Toronto, Canada June 1988.
- *d. Gordon Conference on Chemistry of Energetic Materials, New Hampton School, New Hampshire, June 1988.
- *e. 6th International Congress of Quantum Chemistry, Jerusalem Israel, August 1988.

Dr. Kaufman also presented an invited paper on MRD-CI calculations on the Propagation Step in Cationic Polymerization of Energetic Substituted Oxetanes at the ONR Energetic Materials Workshop, Great Oak Landing, Maryland, September 1988. During that presentation Dr. Kaufman also mentioned briefly our results on the $\text{H}_3\text{C} - \text{NO}_2$ decomposition in a nitromethane crystal including preliminary results on treating voids in the nitromethane crystal.

Dr. Kaufman also presented a paper on "Ab-Initio Multireference Coupled Cluster and Multireference CI Calculations for Protonation of NH_3 /Deprotonation of NH_4^+ Involve Multipotential Surfaces" at the American Chemical Society/North American Chemical Congress, Toronto, Canada, June 1988.

QUANTUM CHEMICAL INVESTIGATIONS OF THE MECHANISM OF CATIONIC
POLYMERIZATION
and
THEORETICAL PREDICTION OF CRYSTAL DENSITIES
and
DECOMPOSITION PATHWAYS OF ENERGETIC MOLECULES

Joyce J. Kaufman, Principal Investigator
Department of Chemistry
The Johns Hopkins University

I. New Program Developments on the CRAY Supercomputer

A. MR-CC (Multireference - Coupled Cluster)

We have a long standing interest in comparing the reliability of multireference configuration interaction (MRD-CI) calculations with multireference coupled cluster (MR-CC) calculations. With the collaboration of Professor Uzi Kaldor, University of Tel Aviv, (a visiting scientist to our group at the Johns Hopkins University), his state-of-the-theoretical-art multireference coupled cluster program (for both closed shell and open shell systems) was rewritten, adapted and vectorized for the CRAY XMP supercomputer.

The reason for our considerable interest in this problem is described below.

When making or breaking chemical bonds such as in molecular decompositions or intermolecular reactions it is necessary to use multiconfigurational wave functions. In this ONR research on energetic compounds we have demonstrated the necessity for such multiconfigurational wave functions by tracing the contribution of each significant configuration to every point on each potential surface.

When breaking a chemical bond in molecular decompositions or intermolecular reactions, to get reliable dissociation energies, desirably the calculation should be size extensive. That means that the fragments along the dissociative pathway and the asymptote should be treated with the same degree of correlation as the undissociated molecule. At the asymptote if single and double excitations are allowed in each of the fragments that would correspond to allowing quadruple excitations in the undissociated molecule.

There are several approaches to try in order to have the calculations for dissociation or intermolecular reactions be size extensive (or approximately size extensive). Since multiconfiguration potential energy surfaces are necessary, MRD-CI wave functions are well suited for describing properly the processes of molecular dissociations and reactions.

One approach to have MRD-CI calculations essentially size consistent or size extensive (which we often use for reactions and dissociations) is to

$$E(\text{full CI}) = E(\text{EXT}) + (1 - \sum_p c_p^{\text{ref}})^2 [E(\text{EXT}) - E(\text{Ref})]$$

$E(\text{Ref})$ = energy for only reference configurations

$E(\text{EXT})$ = energy extrapolated for all configurations

This correction has the effect of making the MRD-CI calculations essentially size consistent or size extensive.

Another approach is to carry out coupled cluster calculations which by their nature are size extensive.

Briefly,

$$\Psi = \Omega \Phi_0 \quad \Psi = \exp(T) \Phi_0 \quad T = T_1 + T_2 + \dots$$

$$T = \sum_{i,j \text{ conn}} a_i^+ a_j t_j^i + 1/2 \sum_{i,j,k,l \text{ conn}} a_i^+ a_j^+ a_l a_k t_{kl}^{ij} + \dots$$

CCSD ($T = T_1 + T_2$) also includes connected energy diagrams from disconnected triple and quadruple excitations such as T_2^2 (the most important such excitations)

Exponential form ensures size-consistency

Open shells

Define model space

$$\Psi^a = \Omega \Psi_0^a; \Psi_0^a \text{ in } P$$

$$\Psi_0^a = P \Psi^a$$

The Coupled Cluster Methods are more sophisticated than the many-body-perturbation methods (including the Møller Plesset methods to any order). The coupled cluster method essentially corresponds to infinite order many-body perturbation theory.

The major problem in using the coupled cluster method for breaking or forming bonds is that a multiconfigurational wave function is necessary to describe these processes properly. Most coupled cluster calculations operate on a single reference wave function. We developed and implemented a strategy several years ago where we carried out MRD-CI calculations first to obtain the multiconfiguration wave function at each point along a dissociation path and then applied a coupled cluster technique to those multiconfiguration wave functions. One had to take precautions to exclude in the coupled cluster treatment "intruder" states where the correlation

obtain the multiconfiguration wave function at each point along a dissociation path and then applied a coupled cluster technique to those multiconfiguration wave functions. One had to take precautions to exclude in the coupled cluster treatment "intruder" states where the correlation would be taken into account twice, once in the MRD-CI and once in the coupled cluster.

Professor Kaldor's recent state-of-the-theoretical-art approach to multireference coupled cluster takes a different approach and solves the multireference coupled cluster problem directly. Thus, we invited Professor Kaldor to visit with our group at the Johns Hopkins University and to collaborate with us in comparing multireference coupled cluster with multireference configuration interaction results.

We collaborate on this endeavor with Professor Uzi Kaldor. He has spent several months each summer as a visiting scientist with our group.

B. MRD-CI (Multireference Double Excitation - Configuration Interaction)

In order to be able to handle the transformations for the MRD-CI calculations for larger systems (such as BAMO + BAMOH⁺ or several dimethylnitramine molecules or larger energetic molecules as in the crystal) we are rewriting the transformation program. This program transforms integrals over atomic orbitals to integrals over molecular orbitals (the most computer time- and computer-memory and peripheral resource consuming portion of the MRD-CI calculations).

II. MRD-CI Calculations for Cationic Polymerization of Energetic Oxetanes

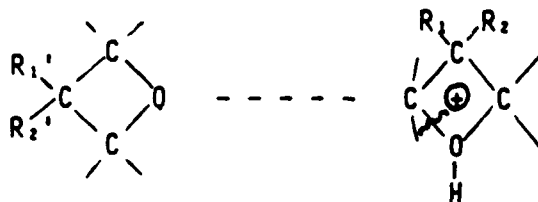
Our major emphasis this past year has been to carry out in-depth detailed ab-initio MRD-CI (multi-reference double excitation-configuration interaction) calculations on the propagation step of cationic polymerization of prototype substituted energetic oxetanes. Cationic polymerization consists essentially of two major steps: initiation and then propagation. There is considerable Navy interest in energetic polymers made by cationic polymerization of oxetanes substituted or disubstituted by exotic energetic substituents such as azido, azidomethyl, nitrate, nitraminomethyl, nitromethyl, NF_2 , etc. as well as fluoro and nitro groups. The initiation step (which is crucial for cationic polymerization to take place) is governed by the propensity of the substituted oxetane to undergo protonation. Our previous ab-initio quantum chemical SCF calculations on the energetic oxetane monomers and electrostatic molecular potential contour (EMPC) maps we generated from these electronic wave functions which predict the order of protonation and hence initiation, were able to predict correctly the propensity of the energetic substituted oxetane monomers to undergo polymerization even prior to the synthesis of the monomers.

Our previous and more recent ab-initio MRD-CI results for the propagation step involving various energetic oxetane partners suggest some general postulates concerning propensities of various substituted oxetane partners for homopolymerization and copolymerization. For the oxetanes A and B, the species with the highest quantum chemically calculated proton affinity will initiate first. (It does not appear possible to measure directly experimentally the proton affinities of oxetanes. Our experimental colleague, Dr. Walter S. Koski, had already tried a number of different experimental techniques for us on this problem, including proton transfer in a tandem mass spectrometer.) It is desirable that the species that initiates first have the lowest intrinsic steric hindrance [the least bulky 3,3-substituent(s) and the least number of these bulky 3,3-substituents]. The reason for this is that in the propagation step the 3,3-substituents on the protonated oxetane (designated here as molecule A) are on C_{3A} which is the neighbor of C_{4A} which is being attacked by O_{1B} of the neutral oxetane (designated here as molecule B). Thus the bulkiness of the 3,3-substituent(s) on A exert a profound influence on the steric hindrance to the propagation step. On the other hand the 3,3-substituents on the neutral oxetane are not neighbors to O_{1B} (the attacking atom of the neutral oxetane) and thus are expected to exert considerably less steric hindrance. The above discussion would also seem to indicate why certain compounds which cannot undergo homopolymerization can undergo copolymerization. A very sterically hindered 3,3-substituted oxetane may protonate and thus initiate but is so sterically hindered that it is very difficult for another like neutral 3,3-substituted oxetane to attack successfully the sterically hindered 3,3-substituted protonated oxetane.

A. Ab-Initio MRD/CI Calculations for the Propagation Step

1. Discussion of Calculation Procedure and Pathways of Attack

As was suggested to us by several different experimentalists in cationic polymerization (primarily Gerry Manser) the mechanism seems to be attack of protonated oxetanes on oxetanes (or vice versa) with concomitant ring opening of the protonated oxetane according to the following general scheme



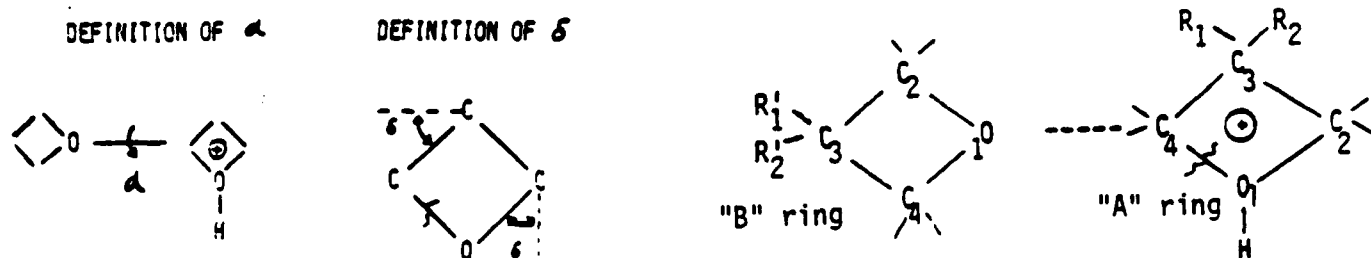
This year we continued to carry out ab-initio MRD-CI calculations on the subsequent propagation step of oxetane (or an energetic substituted oxetane) reacting with protonated oxetane (or a protonated energetic substituted oxetane).

In order to understand and to be able to predict copolymerization propensities of various energetic substituted oxetanes it is necessary to trace the reaction pathways of the propagation step in cationic polymerization.

These energetic oxetanes are large molecules for MRD-CI calculations and the systems of energetic oxetanes plus protonated oxetanes are even larger and thus beyond the size in which MRD-CI calculations can be carried out in the cpu memory and disc storage of current CRAY XMP supercomputers. Thus we had derived, implemented and tested a new computational strategy for MRD-CI calculations for intermolecular reactions and for molecular decompositions based on localized orbitals. (The strategy is described in more detail later in this section).

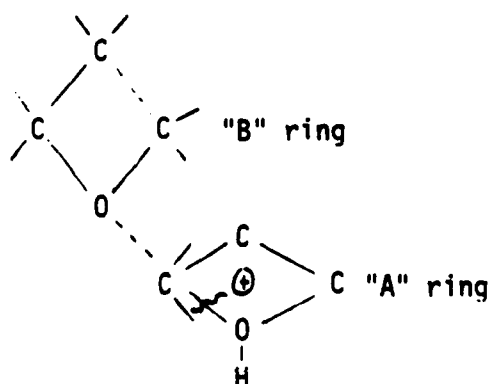
MRD-CI calculations along the potential energy surfaces have been carried out for a very large number (at least 25 separate MRD-CI calculated points at different geometries are necessary for each set of reacting partners) of α angles between the planes of the substituted oxetane and protonated substituted oxetane rings (which can be different in each direction in the case of substituted rings), the inter-ring distances ($O_{1B}-C_{4A}$) (where the A ring is the protonated ring and the B ring is the non-protonated ring), angles δ of opening the $C_{4A}-O_{1A}$ bond in ring A and the orientation of the H atoms on C_{4A} as a function of the inter-ring distance.

For the MRD-CI calculations on oxetanes and protonated oxetanes



we considered the localized bonds in the $C_{4A}-O_{1A}$ bond, the $C_{3A}-C_{4A}$ bond, the $C_{2A}-C_{4A}$ bond, the $O_{1A}-H^+$ bond, the lone pairs on O_{1A} and the bonds connecting hydrogens to C_{2A} and C_{4A} , the $O_{1B}-C_{4B}$ bond, the $O_{1B}-C_{2B}$ bond, the bonds connecting hydrogens to C_{2B} and C_{4B} and the inter-ring $O_{1B}-C_{4A}$ bond. This choice of localized orbitals has the great advantage since energetic oxetanes are substituted in the 3 position, that it preserves the similarity in the MRD-CI among all the energetic substituted oxetanes and protonated oxetanes and provides a sound basis for comparison.

The preferred direction of attack appears to be the reaction of the oxygen (which we call O_{1B}) of the unprotonated oxetane ring on the α carbon (which we call C_{4A}) of the protonated substituted oxetane ring along the $C_{4A}-O_{1A}$ bond direction with concomitant pulling back (inversion of the H atoms on C_{4A}) and opening of the $C_{4A}-O_{1A}$ bond in the protonated oxetane ring, similar to an S_N2 reaction mechanism.



The optimal angle α between the two rings is determined by SCF calculations for $R(O_{1B}-C_{4A}) = 2.6 - 2.9 - 3.4$ bohrs and is used for all other geometries.

Two bonds are essential. $C_{4A}-O_{1A}$ and $O_{1B}-C_{4A}$ are essential to describe the reaction pathway. The bond inside the protonated oxetane ring ($C_{4A}-O_{1A}$) varies from $R = 2.8$ to $R = 4.9$ bohrs which correspond to the fully closed and fully open ring of the protonated oxetane. This bond is described by the parameter δ which varies from 0° (fully closed ring) to 19° (fully open ring) and corresponds to the degree of openness of the ring.

The $O_{1B}-C_{4A}$ bond is changed from $R(O_{1B}-C_{4A})$ from $R = 2.1$ bohrs to $R = 10.0$ bohrs.

The opening ($C_{4A}-O_{1A}$) of the protonated oxetane ring starts at $R(O_{1B}-C_{4A}) = 4.6$ bohrs. Next both: $O_{1B}-C_{4A}$ and $C_{4A}-O_{1A}$ change simultaneously until the complex reaches the stabilization point at $R(O_{1B}-C_{4A})$ at 2.9 bohrs and $\delta = 19^\circ$ (fully open). Our investigations have shown that this holds true for all of the oxetane plus protonated oxetane systems we have investigated.

Positions of the proton H^+ and hydrogens connected to C_{4A} atom are the most affected by opening the ring and their positions were determined the previous year for the prototype system $OXET + FNOXH^+$. The positions of the pulled back hydrogens have been used for our subsequent studies of propagation reactions involving other protonated energetic oxetanes. The position of the proton is investigated each time but remains essentially the same for all systems studied.

We had previously shown that ab-initio MODPOT/VRDDO MRD-CI calculations for oxetanes and protonated oxetanes gave energy differences and MRD-CI coefficients very close to those from much larger basis set all-electron MRD-CI calculations.

Ab-initio MODPOT/VRDDO MRD-CI calculations have been carried out for each point of the potential surface of oxetanes reacting with protonated oxetanes in the propagation step of cationic polymerization. Because of the size of the intermolecular complex molecular orbitals selected from localized space are used in the MRD-CI calculations. The geometries studied include the most sensitive part of the complex in the the MRD-CI procedure. Ten of the most important main reference configurations have been used in MRD-CI treatment, and the same set of main reference configurations have been kept through whole potential surface. All single and double excitations were allowed relative to these main configurations. The energies of each of the thousands of contributing configurations is estimated by a perturbation procedure; a threshold is set for which contributions will be included explicitly in the MRD-CI; in the following tables, this MRD-CI energy is designated CI. Then the energies of all of

the other configurations generated but not included explicitly in the MRD-CI are extrapolated and added back in, this energy is designated EX. Finally a Davidson type correction (which has been shown to be a good correction) for size extensivity is added in.

$$E(\text{full CI estimate}) = E(\text{EX}) + (1 - \sum_p c_p^2) [E(\text{EX}) - E(\text{Ref})]$$

and the summation is over all reference species. The use of multiconfigurational scheme is to assure avoiding of possible artifacts.

Our MRD-CI results support the suggestions of Gerry Manser as to the mechanism of the propagation step in cationic polymerization of oxetanes. We discussed this with Gerry the previous year and he was quite gratified that our theoretical results were in accord with his hypothesis. We have spoken to Gerry Manser this year also and he felt that "our work complements each other." He hopes that we will continue to interact with him and to contribute in the area of polymerization mechanisms.

Our MRD-CI calculations have enabled us to map out the reaction coordinates of the propagation step reaction of oxetane (or an energetic substituted oxetane) reacting with protonated oxetane (or with a protonated energetic substituted oxetane), to identify the transition state of the propagation step and to identify when the C_{4A}-O_{1A} bond in the protonated oxetane will start to open as a function of inter-ring distance and angle for each different pair of substituted reactants.

By comparing these results for different pairs of reacting substituted oxetanes and protonated substituted oxetanes we have been able to gain insight into preference toward copolymer candidates. In all cases we have studied to date our calculated predictions agree with the order of Gerry Manser's experimental polymerization reactivities ratios.

For our calculations on the propagation step of (substituted) oxetane plus (substituted) protonated oxetane we have been using the new MRD-CI approach we previously developed, implemented and validated based on localized orbitals in the reaction/interaction region with the remainder of the non-participating localized occupied molecular orbitals being folded into an effective CI Hamiltonian. We had shown by test examples that the MRD-CI based on localized orbitals give a potential energy surface for molecular decomposition essentially parallel to that using the entire valence space MRD-CI. These MRD-CI calculations for the reaction of substituted protonated oxetanes with substituted oxetanes are a computationally and labor intensive project. For each different inter- and intra-molecular geometry point, first the SCF calculation must be run, then the resulting SCF canonical delocalized molecular orbitals must be localized. After localization a small single reference CI must be carried out to determine the major reference configurations to include in the subsequent MRD-CI. A great advantage in our carrying out the ab-initio MRD-CI calculations based on the important localized orbitals in the interaction/reaction region is the reasonable similarity of types of major

reference configurations for the variously energetic substituted oxetanes and energetic substituted protonated oxetanes.

We shall be continuing these MRD-CI calculations on the initiation and propagation steps in cationic polymerization. The species to be investigated and their partners will be chosen from Gerry Manser's recent results.

B. Detailed Results

1. Energies

a. 3,3-Bis(azidomethyl)oxetane (BAMO) + protonated oxetane (OXETH⁺)

Results

The stabilization point for the addition reaction BAMO + OXETH⁺ occurs at R(O1B-C4A) = 2.9 bohrs with the protonated oxetane ring fully open ($\delta = 19^\circ$). The MRD-CI stabilization energy was found to be -0.038896 a.u. = -24.41 kcal/mole. The reaction proceeds via a transition state with an estimated activation energy of 12.55 kcal/mole. The potential energy of surfaces and reaction potential map are presented in Figures II-1 to II-4.

Figure II-1: "MRD-CI Extrapolated Energy for BAMO Approaching Protonated Oxetane For Fixed Angle δ and Different Intermolecular Distances R(O1B- C4A)"

Figure II-2: "MRD-CI Extrapolated Energy for BAMO-Protonated Oxetane Complex for Fixed Intermolecular Distances R(O1B-C4A) and Different δ Angle Values"

Figure II-3: "MRD-CI Extrapolated Potential Energy Surface for BAMO Approaching OXETH⁺"

Figure II-4: "BAMO + OXETH⁺, Extrapolated MRD-CI Energy Along the Reaction Coordinate for BAMO + OXETH⁺ Addition Reaction"

The detailed Tables of Results follow in tables II-1 through II-5:

Table II-1: "BAMO + OXETH⁺ $\delta=0^\circ$ (fully closed), Energies (a.u.) as a function of R(O1B-C4A)"

Table II-2: "BAMO + OXETH⁺ $\delta=5^\circ$, Energies (a.u.) as a function of R(O1B-C4A)"

Table II-3: "BAMO + OXETH⁺ $\delta=10^\circ$, Energies (a.u.) as a function of R(O1B-C4A)"

Table II-4: "BAMO + OXETH⁺ $\delta=15^\circ$, Energies (a.u.) as a function of R(O1B-C4A)"

Table II-5: "BAMO + OXETH⁺ $\delta=19^\circ$ (fully open), Energies (a.u.) as a function of R(O1B-C4A)"

Figure II-1

MRD-CI EXTRAPOLATED ENERGY FOR BAMO APPROACHING PROTONATED OXETANE FOR FIXED ANGLE δ ($A=0^\circ$, $B=5^\circ$, $C=10^\circ$, $D=15^\circ$, $E=19^\circ$) AND DIFFERENT INTERMOLECULAR DISTANCES $R(O1B-C4A)$

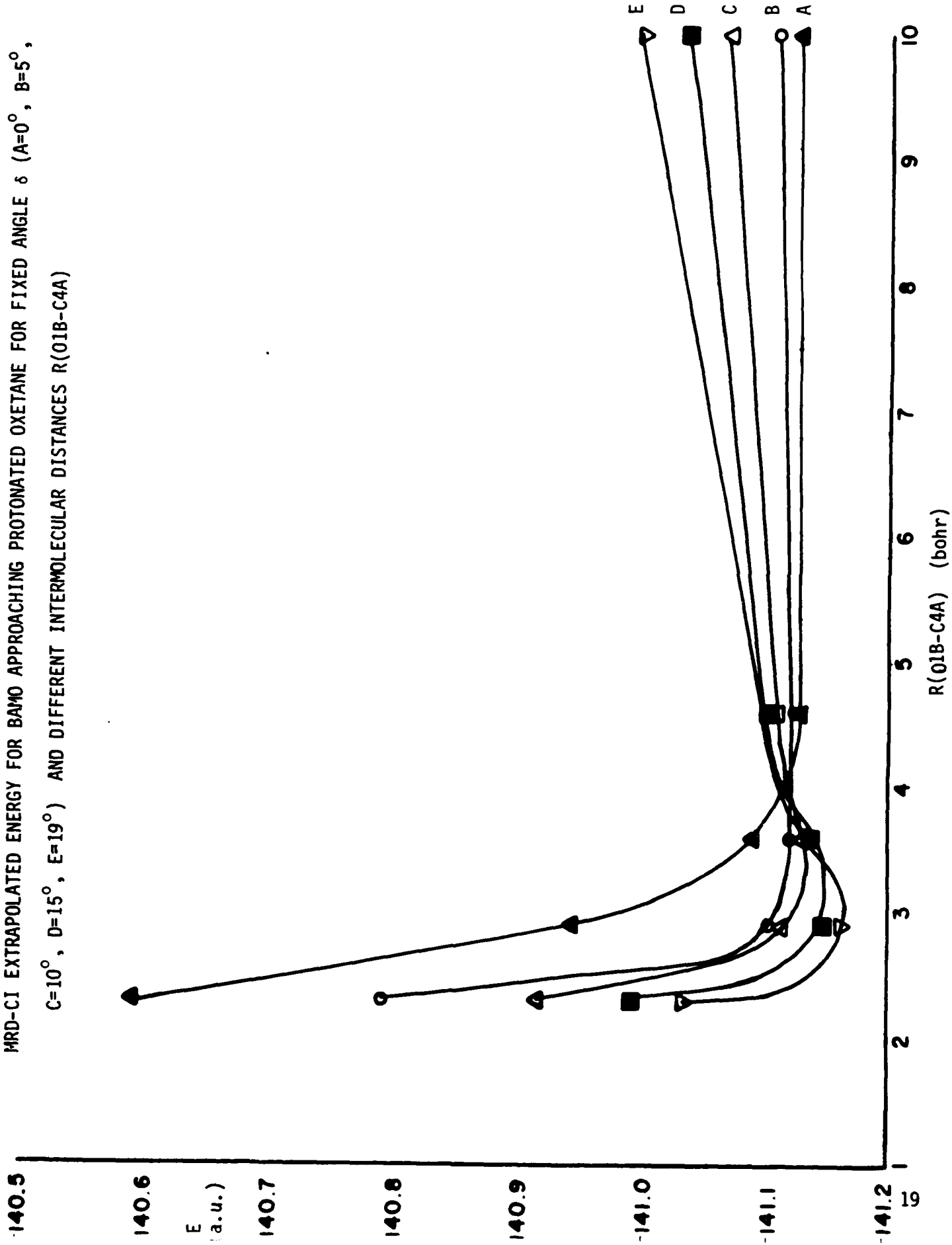


Figure 11-2
MRD-CI EXTRAPOLATED ENERGY FOR BAMO-PROTONATED OXETANE COMPLEX FOR FIXED INTERMOLECULAR DISTANCES AND
DIFFERENT δ ANGLE VALUES R(01B-C4A)

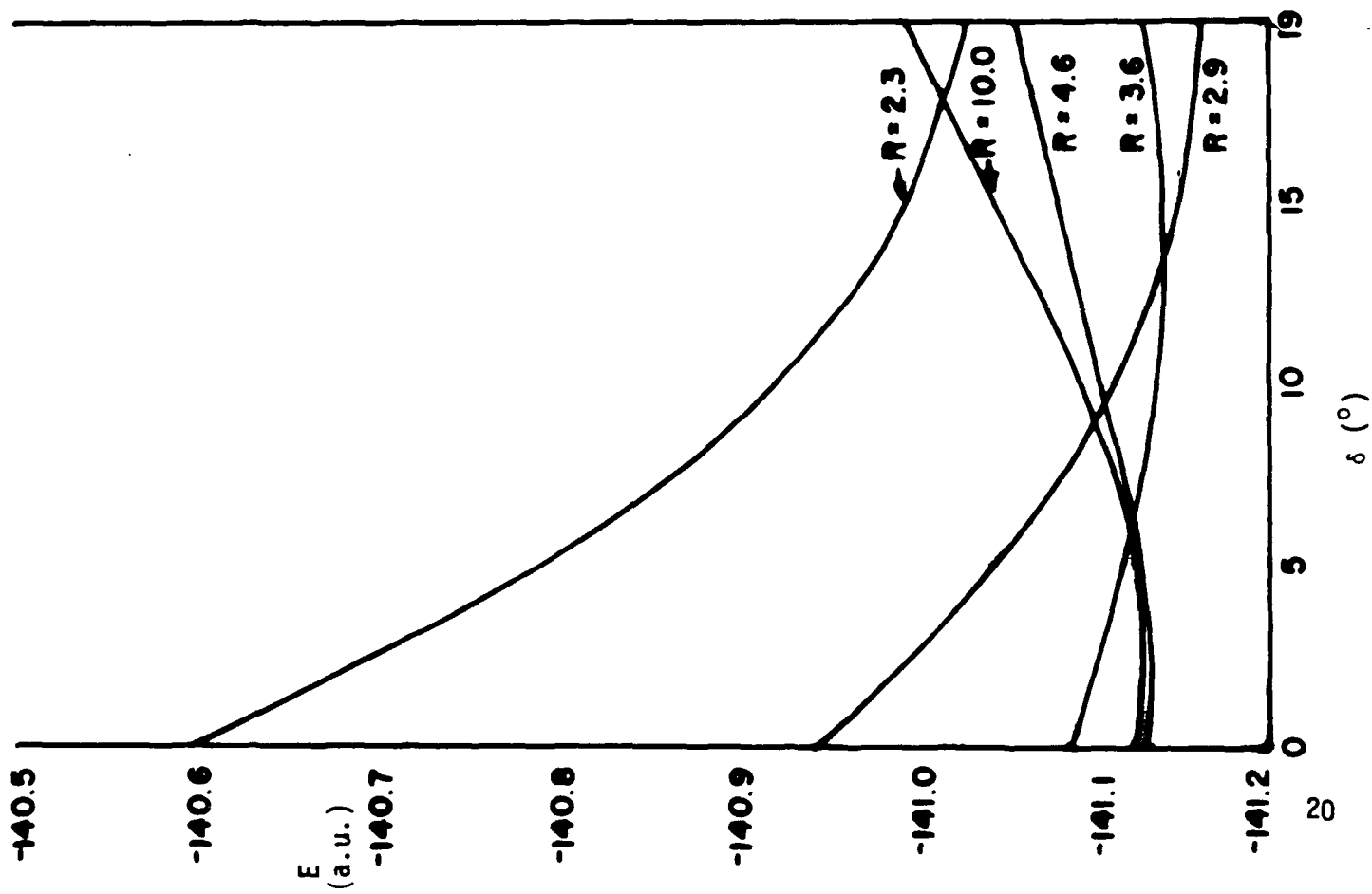


Figure II-3

THE POTENTIAL ENERGY SURFACE FOR BAMO APPROACHING PROTONATED OXETANE
MRD-CI (extrapolated)

THE DASHED LINE IS THE REACTION COORDINATE
THE VALUES ON THE GRAPH CORRESPOND TO EXTRAPOLATED ENERGY
BY EQUATION $E = -154.3 + a$ (a.u.)

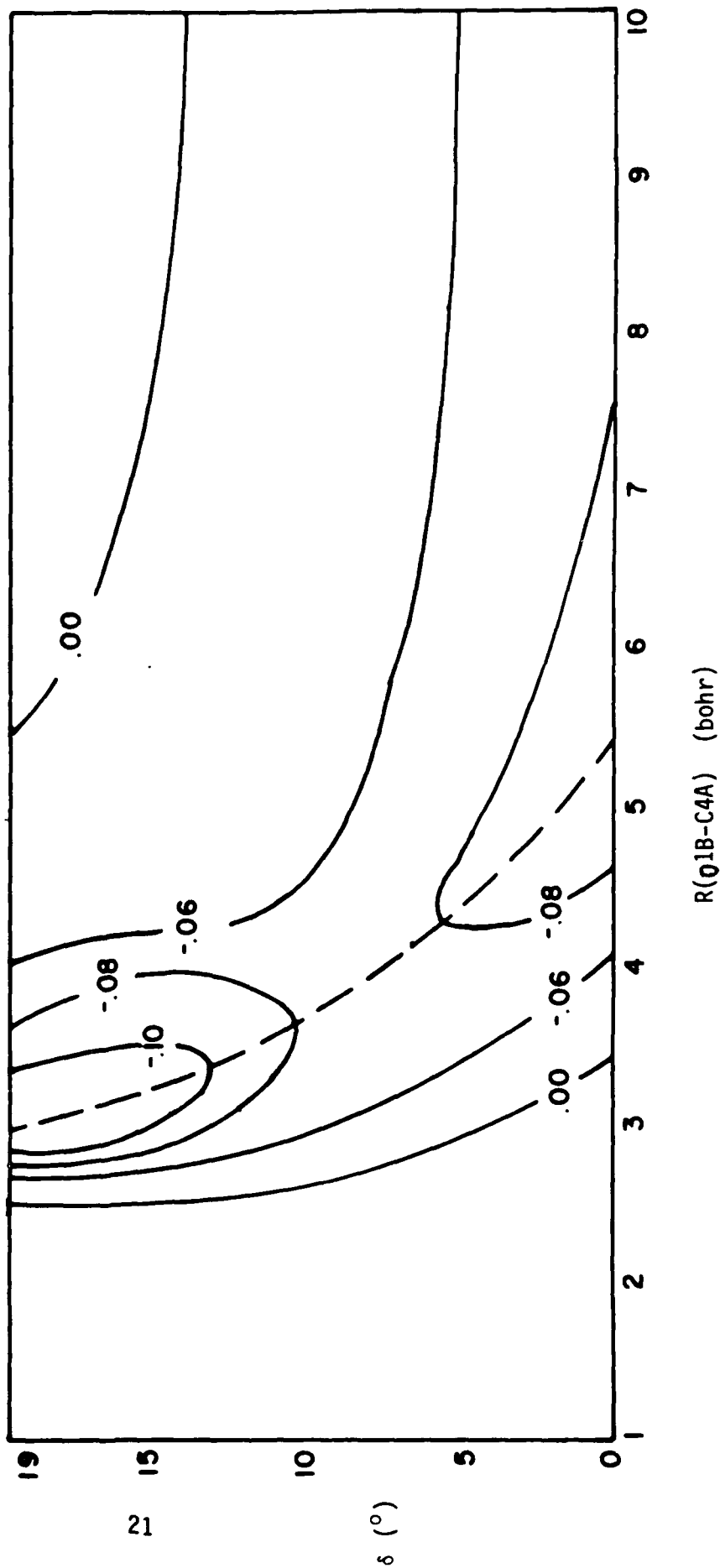


Figure II-4

BAMO-OXETH⁺ MRD-CI EXTRAPOLATED ENERGY ALONG THE REACTION COORDINATE FOR BAMO-PROTONATED OXETANE ADDITION REACTION

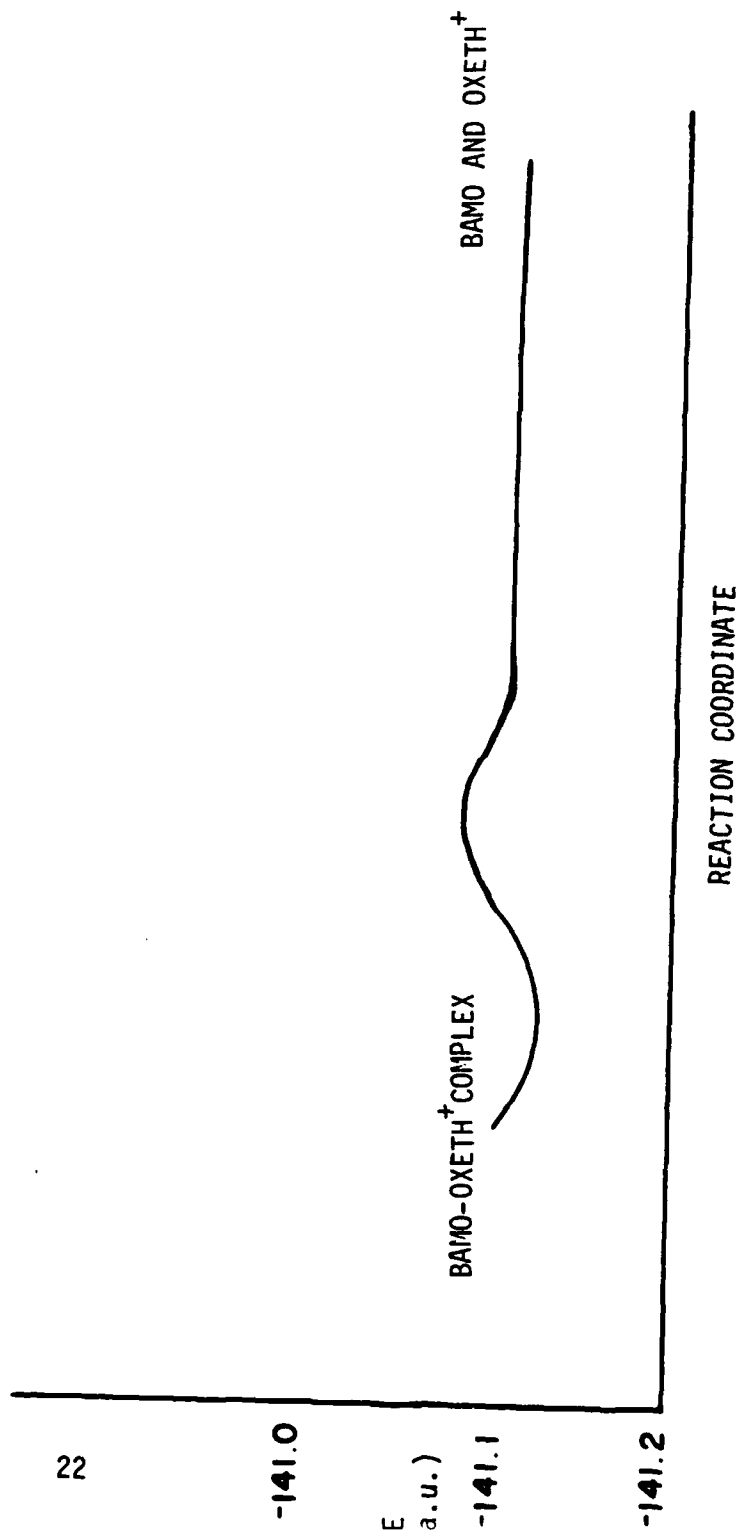


Table II-1

BAMO + OXETH⁺
 $\delta = 0^\circ$ (fully closed)
 $\alpha = -90^\circ$
ENERGIES (a.u.)

R(01B-C4A) (bohrs)	<u>2.3</u>	<u>2.9</u>	<u>3.6</u>
SCF	-140.394796	-140.750568	-140.900008
CI	-140.589875 (891)	-140.941911 (809)	-141.085247 (652)
EXT	-140.598322	-140.948674	-141.091835
DAV	-140.601648	-140.951656	-141.094343
# SAFs generated	37437	37437	37437
Σc^2	0.964	0.965	0.967
gs	0.905	0.906	0.905
R(01B-C4A) (bohrs)	<u>4.6</u>	<u>10.0</u>	
SCF	-140.943314	-140.936448	
CI	-141.124490 (520)	-141.118354 (473)	
EXT	-141.129670	-141.122238	
DAV	-141.131798	-141.124326	
# SAFs generated	37437	33881	
Σc^2	0.970	0.969	
gs	0.905	0.904	

Σc^2 is the contribution of all of the reference configurations
gs is the contribution of the ground state SCF wave function

Table II-2

BAMO + OXETH⁺

$\delta = 5^\circ$

$\alpha = -90^\circ$

ENERGIES (a.u.)

R(01B-C4A) (bohrs)	<u>2.3</u>	<u>2.9</u>	<u>3.6</u>
SCF	-140.604422	-140.858316	-140.932576
CI	-140.792276 (742)	-141.045479 (647)	-141.115297 (593)
EXT	-140.799310	-141.053570	-141.121027
DAV	-140.801814	-141.056355	-141.123726
# SAFs generated	37437	37437	37437
Σc^2	0.968	0.966	0.965
gs	0.906	0.905	0.904

R(01B-C4A) (bohrs)	<u>4.6</u>	<u>10.0</u>
SCF	-140.940389	-140.923863
CI	-141.121032 (529)	-141.104571 (425)
EXT	-141.125957	-141.107477
DAV	-141.128440	-141.113610
# SAFs generated	37437	37437
Σc^2	0.965	0.942
gs	0.901	0.900

Σc^2 is the contribution of all of the reference configurations
 gs is the contribution of the ground state SCF wave function

Table II-3

BAMO + OXETH⁺ $\delta = 10^\circ$ $\alpha = -90^\circ$

ENERGIES (a.u.)

R(01B-C4A) (bohrs)	2.3	2.9	3.6
SCF	-140.735359	-140.925031	-140.947167
CI	-140.916195 (645)	-141.107971 (594)	-141.126185 (531)
EXT	-140.921611	-141.113450	-141.132047
DAV	-140.923667	-141.115757	-141.134604
# SAFs generated	37437	37437	37437
Σc^2	0.971	0.968	0.965
gs	0.908	0.905	0.904
R(01B-C4A) (bohrs)	4.6	10.0	
SCF	-140.923098	-140.894267	
CI	-141.096484 (472)	-141.067411 (373)	
EXT	-141.101413	-141.070777	
DAV	-141.10376	-141.074795	
# SAFs generated	37437	37245	
Σc^2	0.965	0.952	
gs	0.904	0.901	

Σc^2 is the contribution of all of the reference configurations
 gs is the contribution of the ground state SCF wave function

Table II-4

BAMO + OXETH⁺ $\delta = 15^\circ$ $\alpha = -90^\circ$

ENERGIES (a.u.)

R(01B-C4A) (bohrs)	<u>2.3</u>	<u>2.9</u>	<u>3.6</u>
SCF	-140.813849	-140.964301	-140.954997
CI	-140.990047 (583)	-141.144169 (524)	-141.133012 (482)
EXT	-140.994875	-141.149155	-141.137881
DAV	-140.996733	-141.151208	-141.140190
# SAFs generated	37437	37437	37437
Σc^2	0.972	0.970	0.967
gs	0.911	0.906	0.903
R(01B-C4A) (bohrs)	<u>4.6</u>	<u>10.0</u>	
SCF	-140.908114	-140.867512	
CI	-141.078218 (439)	-141.034999 (337)	
EXT	-141.082423	-141.038348	
DAV	-141.084489	-141.040064	
# SAFs generated	37437	37437	
Σc^2	0.967	0.970	
gs	0.905	0.904	

Σc^2 is the contribution of all of the reference configurations
 gs is the contribution of the ground state SCF wave function

Table II-5

BAMO + OXETH⁺ $\delta = 19^\circ$ $\alpha = -90^\circ$

ENERGIES (a.u.)

R(01B-C4A) (bohrs)	2.3	2.9	3.6
SCF	-140.851821	-140.976943	-140.948700
CI	-141.025892 (547)	-141.156253 (507)	-141.128422 (476)
EXT	-141.030670	-141.161134	-141.132694
DAV	-141.032466	-141.163124	-141.134983
# SAFs generated	33881	37437	37437
Σc^2	0.973	0.971	0.967
gs	0.913	0.907	0.901
R(01B-C4A) (bohrs)	4.6	10.0	
SCF	-140.887304	-140.837856	
CI	-141.058652 (438)	-141.003788 (302)	
EXT	-141.062035	-141.006121	
DAV	-141.064146	-141.007550	
# SAFs generated	37437	37437	
Σc^2	0.966	0.973	
gs	0.903	0.905	

Σc^2 is the contribution of all of the reference configurations
 gs is the contribution of the ground state SCF wave function

- b. 3,3-Bis(azidomethyl)oxetane (BAMO) + protonated
3-azidomethyl-3-methyloxetane (AMMOH⁺)

Results

The stabilization point for the addition of BAMO to protonated AMMO occurs at $R = 2.9$ bohrs, $\delta = 19^\circ$ (fully open). The stabilization energy was found to be -0.019239 a.u. = 12.07 kcal/mole. The activation energy for the addition reaction was found to be approximately 12.55 kcal/mole.

ΔE for the polymerization reaction has two components: ΔE (protonation) + ΔE (addition). ΔE for BAMO + AMMOH⁺ is quite close to that of AMMO + AMMOH⁺ (just a very little bit lower). Our previous calculations indicated that AMMO would have somewhat more of a tendency to protonate than would BAMO. Thus, in a mixture of AMMO + BAMO, AMMO will initiate first. Also AMMOH⁺ will have somewhat more of a tendency to react with itself (AMMO) than with BAMO. This is in accord with Gerry Manser's experimental polymerization results.

The potential energy surfaces and reaction potential map are shown in Figures II-5 to II-8

Figure II-5: "MRD-CI Extrapolated Energy for BAMO Approaching Protonated AMMO for Fixed Angle δ and Different Intermolecular Distances R(O1B-C4A)"

Figure II-6: "MRD-CI Extrapolated Energy for BAMO - Protonated AMMO Complex for Fixed Intermolecular Distances R(O1B-C4A) and Different δ Angle Values"

Figure II-7: "Extrapolated CI Potential Energy Surface for BAMO Approaching Protonated AMMO"

Figure II-8: "BAMO + AMMOH⁺, Extrapolated MRD-CI Energy Along the Reaction Coordinate for BAMO - Protonated AMMO Addition Reaction"

The Detailed Tables of Results follow in Tables II-16 to II-20

Table II-6: "BAMO + AMMOH⁺ $\delta=0^\circ$ (fully closed), Energies (a.u.) as a function of R(O1B-C4A)"

Table II-7: "BAMO + AMMOH⁺ $\delta=5^\circ$, Energies (a.u.) as a function of R(O1B-C4A)"

Table II-8: "BAMO + AMMOH⁺ $\delta=10^\circ$, Energies (a.u.) as a function of R(O1B-C4A)"

Table II-9: "BAMO + AMMOH⁺ $\delta=15^\circ$, Energies (a.u.) as a function of R(01B-C4A)"

Table II-10: "BAMO + AMMOH⁺ $\delta=19^\circ$ (fully open), Energies (a.u.) as a function of R(01B-C4A)"

Figure II-5 MRD-CI EXTRAPOLATED ENERGY FOR BAMO APPROACHING PROTONATED ANMO FOR FIXED ANGLE δ ($A=0^\circ$, $B=5^\circ$, $C=10^\circ$, $D=15^\circ$, $E=19^\circ$) AND DIFFERENT INTERMOLECULAR DISTANCES R(01B-C4A)

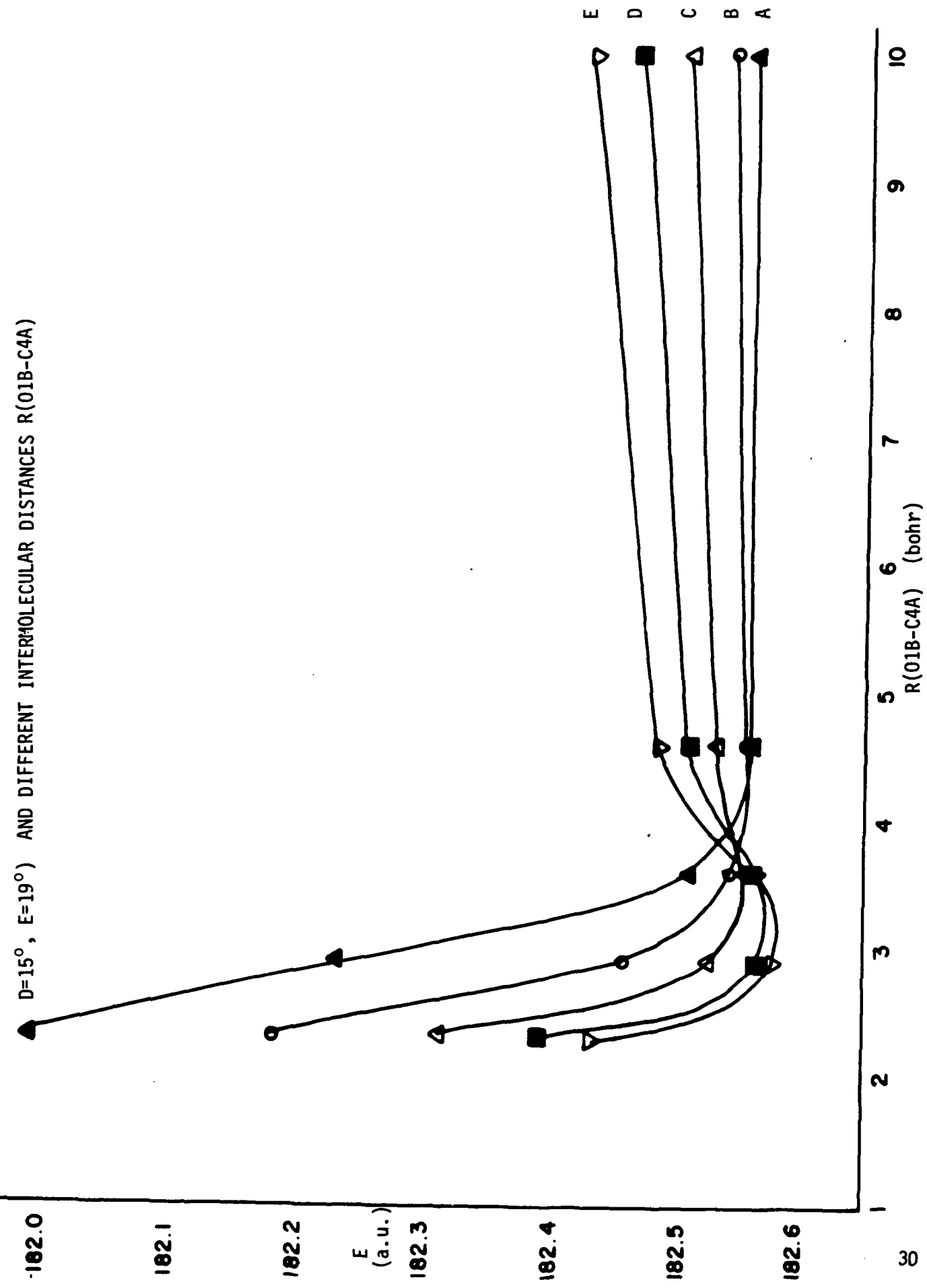


Figure II-6 MRD-CI EXTRAPOLATED ENERGY FOR BAMO-PROTONATED AMMO COMPLEX FOR FIXED INTERMOLECULAR DISTANCES R(01B-C4A) AND DIFFERENT δ ANGLE VALUES

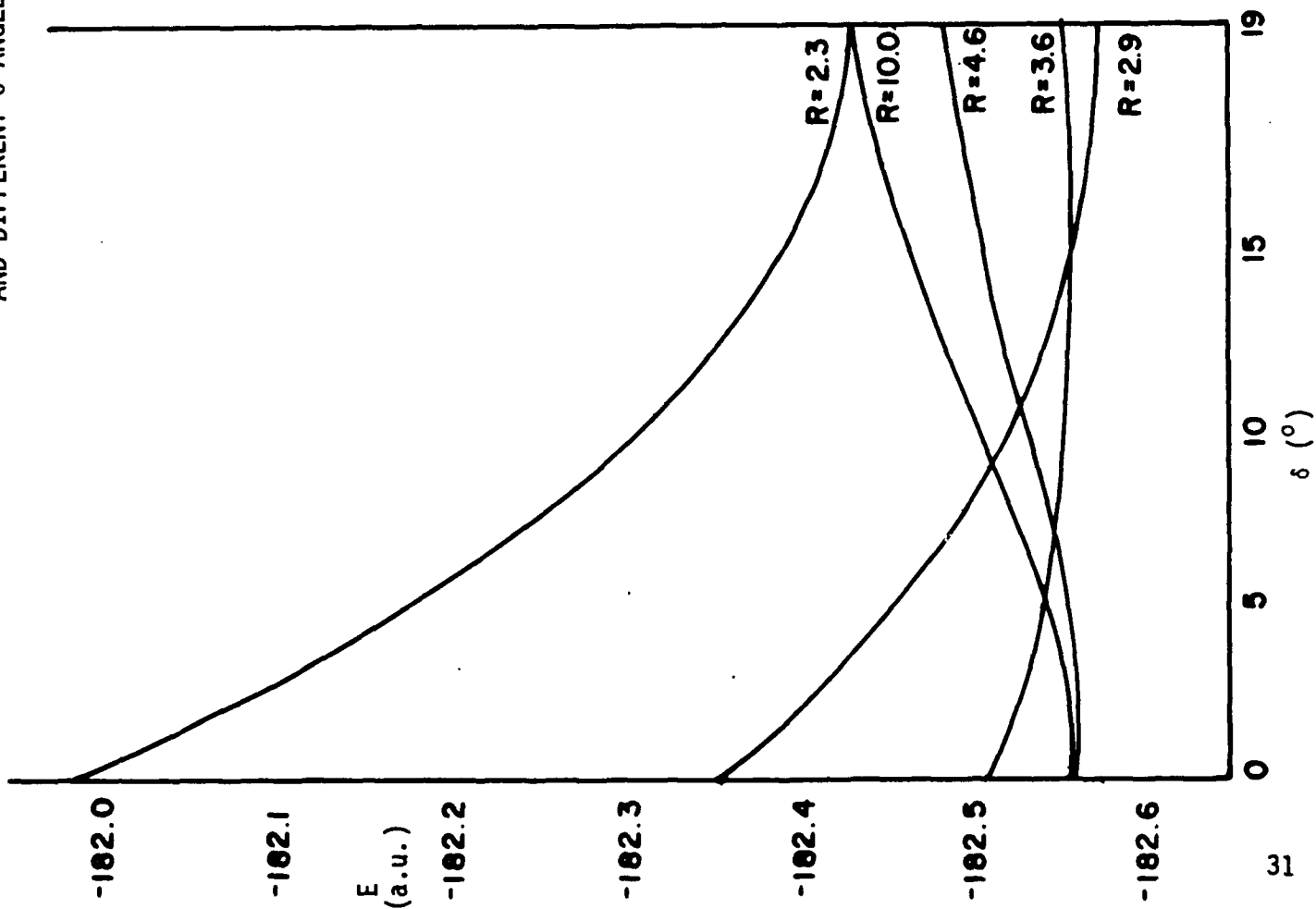


Figure II-7

THE POTENTIAL ENERGY SURFACE FOR BAMO APPROACHING PROTONATED AMMO
MRD-CI (extrapolated)

THE DASHED LINE IS THE REACTION COORDINATE
THE VALUES ON THE GRAPH CORRESPOND TO EXTRAPOLATED MRD-CI
ENERGY BY EQUATION $E = -154.3 + a$ (a.u.)

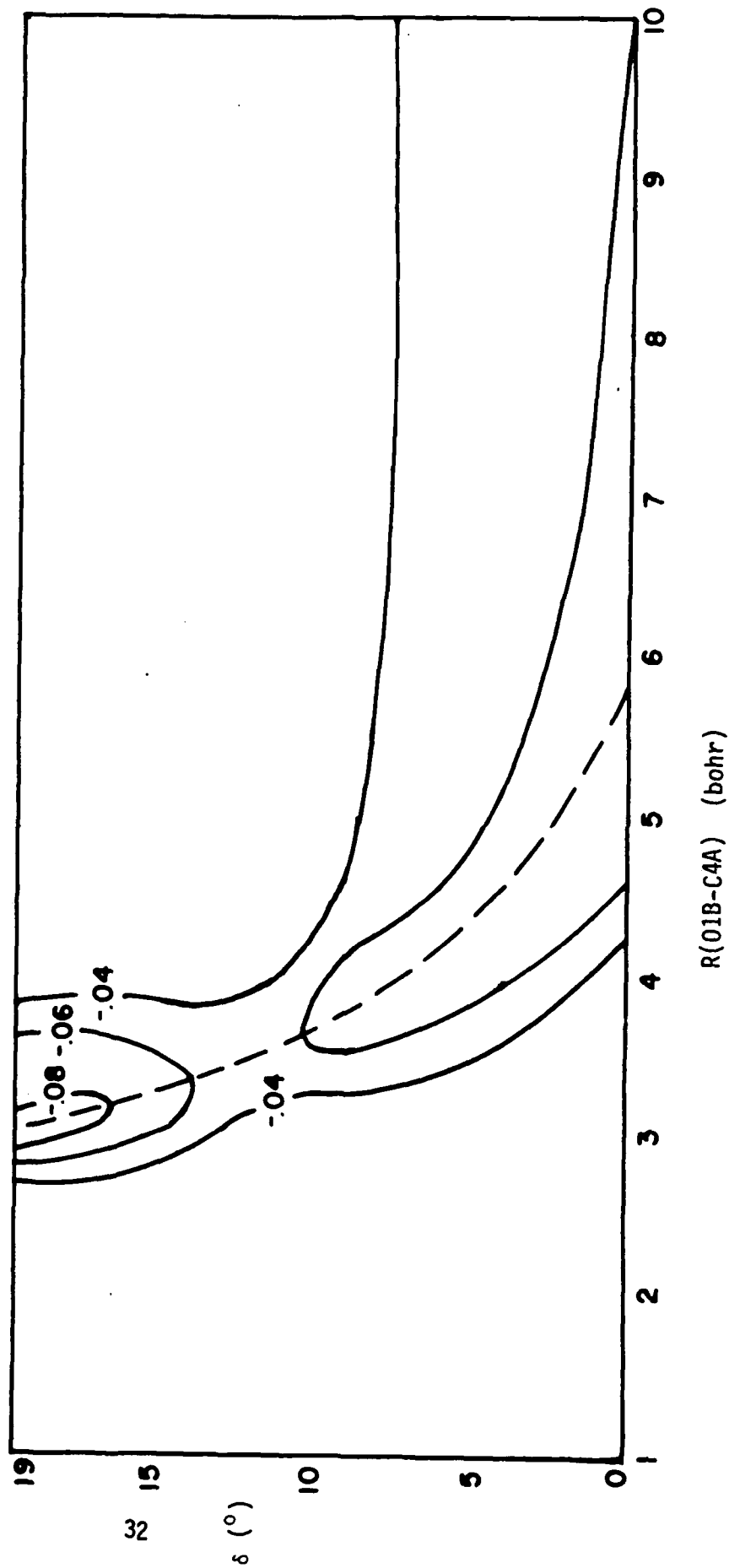


Figure II-8

BAMO-AMMOH⁺ MRD-CI EXTRAPOLATED ENERGY ALONG THE REACTION COORDINATE FOR BAMO-PROTONATED
AMMO ADDITION REACTION

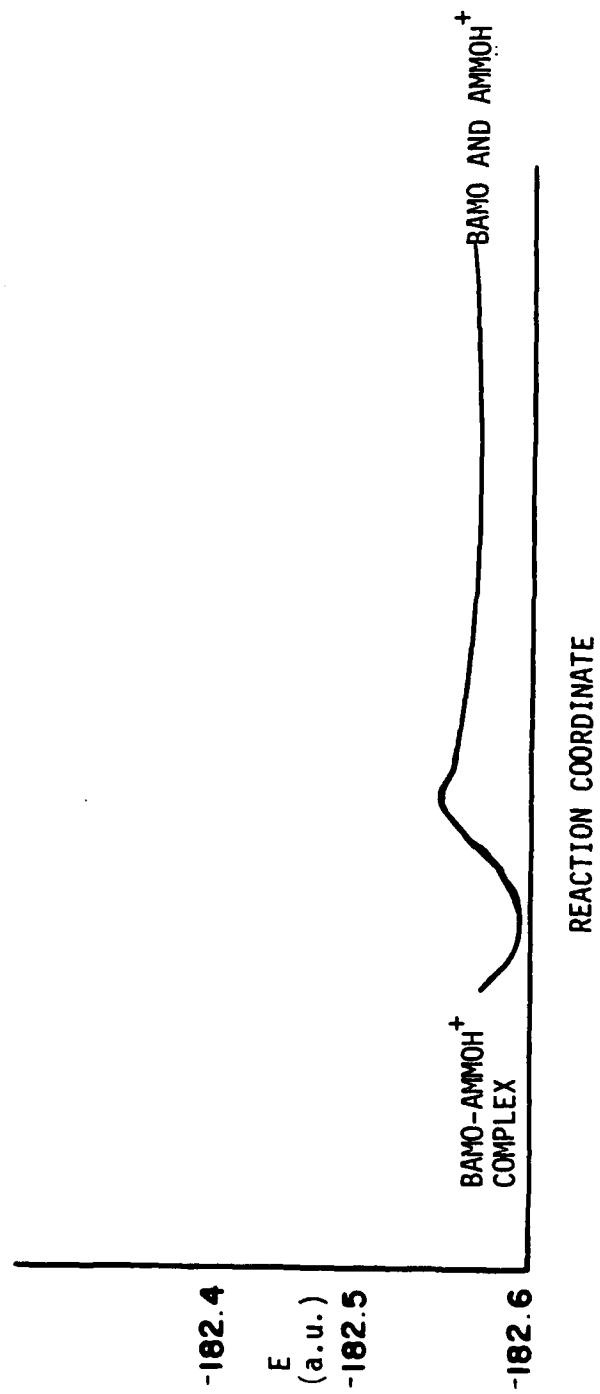


Table II-6

BAMO + AMMOH⁺
 $\delta = 0^\circ$ (fully closed)
 $\alpha = -90^\circ$
ENERGIES (a.u.)

<u>R(01B-C4A)</u> (bohrs)	<u>2.3</u>	<u>2.9</u>	<u>3.6</u>
SCF	-181.778080	-182.158030	-182.323246
CI	-181.972466 (889)	-182.348512 (800)	-182.507884 (649)
EXT	-181.980697	-182.355049	-182.514230
DAV	-181.983963	-182.358040	-182.516672
# SAFs generated	37437	37437	37437
Σc^2	0.964	0.965	0.968
gs	0.906	0.906	0.906
<u>R(01B-C4A)</u> (bohrs)	<u>4.6</u>	<u>10.0</u>	
SCF	-182.375635	-182.372309	
CI	-182.556438 (516)	-182.553866 (474)	
EXT	-182.561840	-182.557712	
DAV	-182.563944	-182.559763	
# SAFs generated	37437	37247	
Σc^2	0.970	0.970	
gs	0.906	0.904	

Σc^2 is the contribution of all of the reference configurations
gs is the contribution of the ground state SCF wave function

Table II-7

BAMO + AMMOH⁺ $\delta = 5^\circ$ $\alpha = -90^\circ$

ENERGIES (a.u.)

R(01B-C4A) (bohrs)	2.3	2.9	3.6
SCF	-181.995448	-182.269937	-182.357538
CI	-182.182539 (742)	-182.455236 (647)	-182.539786 (593)
EXT	-182.189510	-182.462829	-182.545773
DAV	-182.191977	-182.466964	-182.548438
# SAFs generated	37437	37272	37437
Σc^2	0.969	0.957	0.965
gs	0.907	0.908	0.905
R(01B-C4A) (bohrs)	4.6	10.0	
SCF	-182.373593	-182.360085	
CI	-182.554048 (529)	-182.541947 (425)	
EXT	-182.558766	-182.545584	
DAV	-182.561212	-182.547964	
# SAFs generated	37437	37437	
Σc^2	0.966	0.966	
gs	0.902	0.899	

Σc^2 is the contribution of all of the reference configurations
 gs is the contribution of the ground state SCF wave function

Table II-8

BAMO + AMMOH⁺
 $\delta = 10^\circ$
 $\alpha = -90^\circ$
ENERGIES (a.u.)

R(01B-C4A) (bohrs)	<u>2.3</u>	<u>2.9</u>	<u>3.6</u>
SCF	-182.132353	-182.339238	-182.372023
CI	-182.312344 (645)	-182.521461 (594)	-182.550209 (531)
EXT	-182.317808	-182.527164	-182.555465
DAV	-182.319828	-182.529448	-182.557940
# SAFs generated	37437	37437	37437
Σc^2	0.971	0.969	0.966
gs	0.909	0.906	0.905

R(01B-C4A) (bohrs)	<u>4.6</u>	<u>10.0</u>
SCF	-182.355018	-182.328791
CI	-182.528253 (472)	-182.503208 (373)
EXT	-182.533277	-182.507124
DAV	-182.535635	-182.509507
# SAFs generated	37437	37437
Σc^2	0.965	0.964
gs	0.904	0.900

Σc^2 is the contribution of all of the reference configurations
gs is the contribution of the ground state SCF wave function

Table II-9

BAMO + AMMOH⁺ $\delta = 15^\circ$ $\alpha = -90^\circ$

ENERGIES (a.u.)

R(01B-C4A) (bohrs)	2.3	2.9	3.6
SCF	-182.215199	-182.379878	-182.378767
CI	-182.390494 (583)	-182.559261 (524)	-182.556345 (482)
EXT	-182.395253	-182.564436	-182.561108
DAV	-182.397069	-182.566470	-182.563393
# SAFs generated	37437	37437	37437
Σc^2	0.973	0.970	0.967
gs	0.912	0.907	0.904
R(01B-C4A) (bohrs)	4.6	10.0	
SCF	-182.337244	-182.298430	
CI	-182.507114 (439)	-182.466346 (337)	
EXT	-182.511268	-182.469623	
DAV	-182.513311	-182.471384	
# SAFs generated	37437	37437	
Σc^2	0.968	0.970	
gs	0.905	0.904	

Σc^2 is the contribution of all of the reference configurations
 gs is the contribution of the ground state SCF wave function

Table II-10

BAMO + AMMOH⁺ $\delta = 19^\circ$ $\alpha = -90^\circ$

ENERGIES (a.u.)

R(01B-C4A) (bohrs)	2.3	2.9	3.6
SCF	-182.255598	-182.392872	-182.371160
CI	-182.429338 (547)	-182.571889 (507)	-182.555052 (476)
EXT	-182.433903	-182.576951	-182.555326
DAV	-182.435693	-182.578923	-182.557604
# SAFs generated	33881	37437	37437
Σc^2	0.973	0.971	0.967
gs	0.913	0.907	0.902
R(01B-C4A) (bohrs)	4.6	10.0	
SCF	-182.313706	-182.265085	
CI	-182.484825 (438)	-182.431655 (302)	
EXT	-182.488495	-182.434412	
DAV	-182.490581	-182.435891	
# SAFs generated	37437	37437	
Σc^2	0.967	0.973	
gs	0.904	0.905	

Σc^2 is the contribution of all of the reference configurations
 gs is the contribution of the ground state SCF wave function

c. Oxetane + protonated 3,3-bis(azidomethyl)-oxetane
(BAMOH⁺)

Results

The stabilization point R(O1B-C4A) = 2.9 bohrs, $\delta = 19^\circ$ (fully open), with the stabilization energy = -0.01389 a.u. = -8.72 kcal/mole. The activation energy for the addition reaction is estimated to be 15.69 kcal/mole.

The potential energy surfaces and reaction potential map are presented in Figures II-9 through II-12.

Figure II-9: "MRD-CI Extrapolated Energy for Oxetane Approaching Protonated BAMO for Fixed Angle δ and Different Intermolecular Distances R(O1B-C4A)"

Figure II-10: "MRD-CI Extrapolated Energy for Oxetane - Protonated BAMO Complex for Fixed Intermolecular Distances R(O1B-C4A) and Different δ Angle Values"

Figure II-11: "MRD-CI Extrapolated Potential Energy Surface for Oxetane Approaching Protonated BAMO"

Figure II-12: "OXET + BAMOH⁺, Extrapolated MRD-CI Energy Along the Reaction Coordinate for Oxetane - Protonated BAMO Addition Reaction"

The Detailed Tables of Results follow in Tables II-6 through II-10

Table II-11: "OXET + BAMOH⁺ $\delta=0^\circ$ (fully closed), Energies (a.u.) as a function of R(O1B-C4A)"

Table II-12: "OXET + BAMOH⁺ $\delta=5^\circ$, Energies (a.u.) as a function of R(O1B-C4A)"

Table II-13: "OXET + BAMOH⁺ $\delta=10^\circ$, Energies (a.u.) as a function of R(O1B-C4A)"

Table II-14: "OXET + BAMOH⁺ $\delta=15^\circ$, Energies (a.u.) as a function of R(O1B-C4A)"

Table II-15: "OXET + BAMOH⁺ $\delta=19^\circ$ (fully open), Energies (a.u.) as a function of R(O1B-C4A)"

Figure II-9

MRD-CI EXTRAPOLATED ENERGY FOR OXETANE APPROACHING PROTONATED BAMO FOR FIXED ANGLE δ ($A=0^\circ$, $B=5^\circ$, $C=10^\circ$, $D=15^\circ$, $E=19^\circ$) AND DIFFERENT INTERMOLECULAR DISTANCES $R(01B-C4A)$

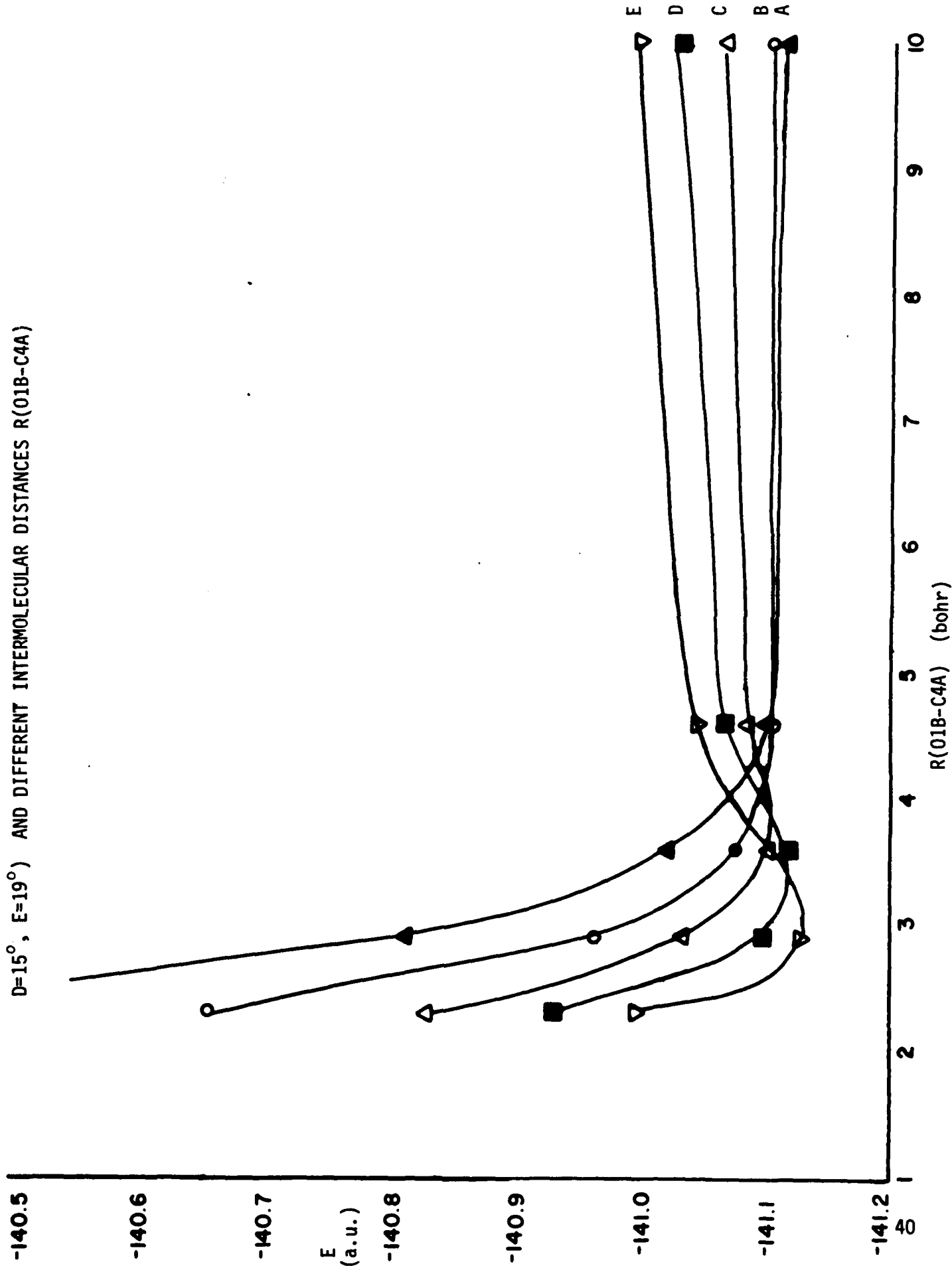


Figure II-10
MRD-CI EXTRAPOLATED ENERGY FOR OXETANE-PROTONATED BAMO COMPLEX FOR FIXED INTERMOLECULAR DISTANCES R(01B-C4A)
AND DIFFERENT δ ANGLE VALUES

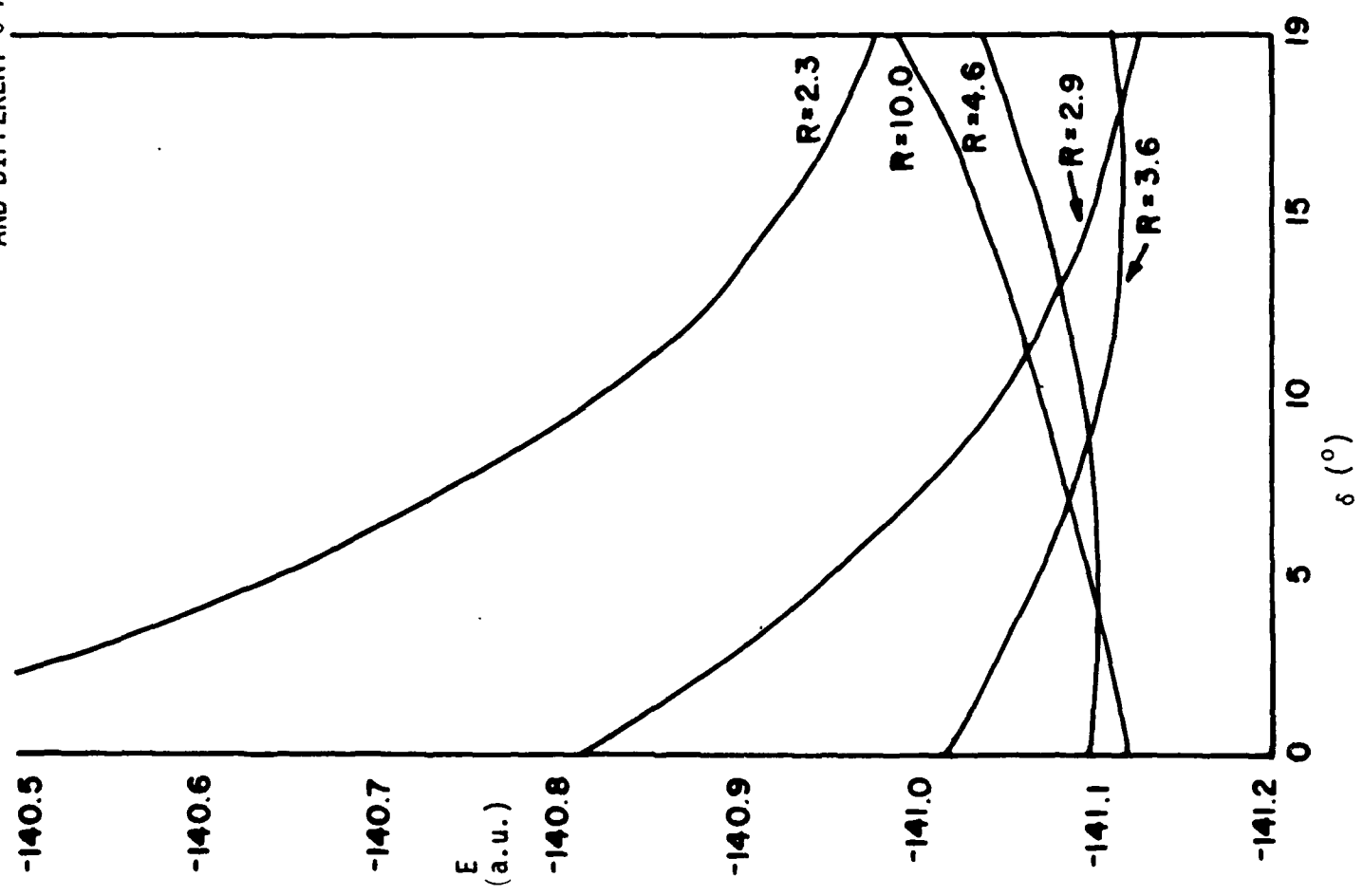


Figure II-11

THE POTENTIAL ENERGY SURFACE FOR OXETANE APPROACHING PROTONATED BAMO
MRD-CI (extrapolated)

THE DASHED LINE IS THE REACTION COORDINATE
THE VALUES ON THE GRAPH CORRESPOND TO EXTRAPOLATED MRD-CI
ENERGY BY EQUATION $E = -154.3 + a$ (a.u.)

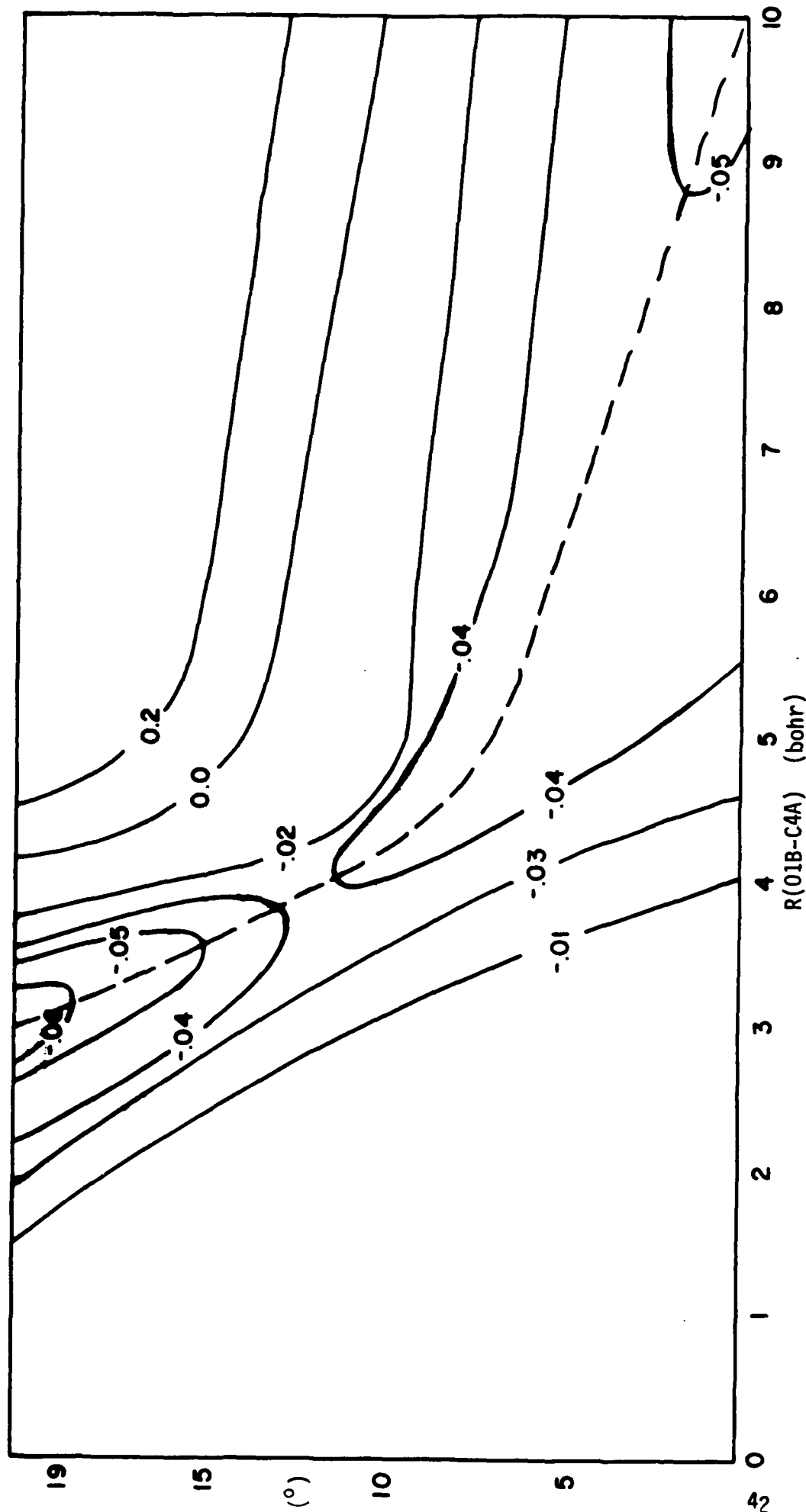


Figure II-12

OXETANE-BAMOH⁺ MRD-CI EXTRAPOLATED ENERGY ALONG THE REACTION COORDINATE FOR OXETANE-PROTONATED BAMO
ADDITION REACTION

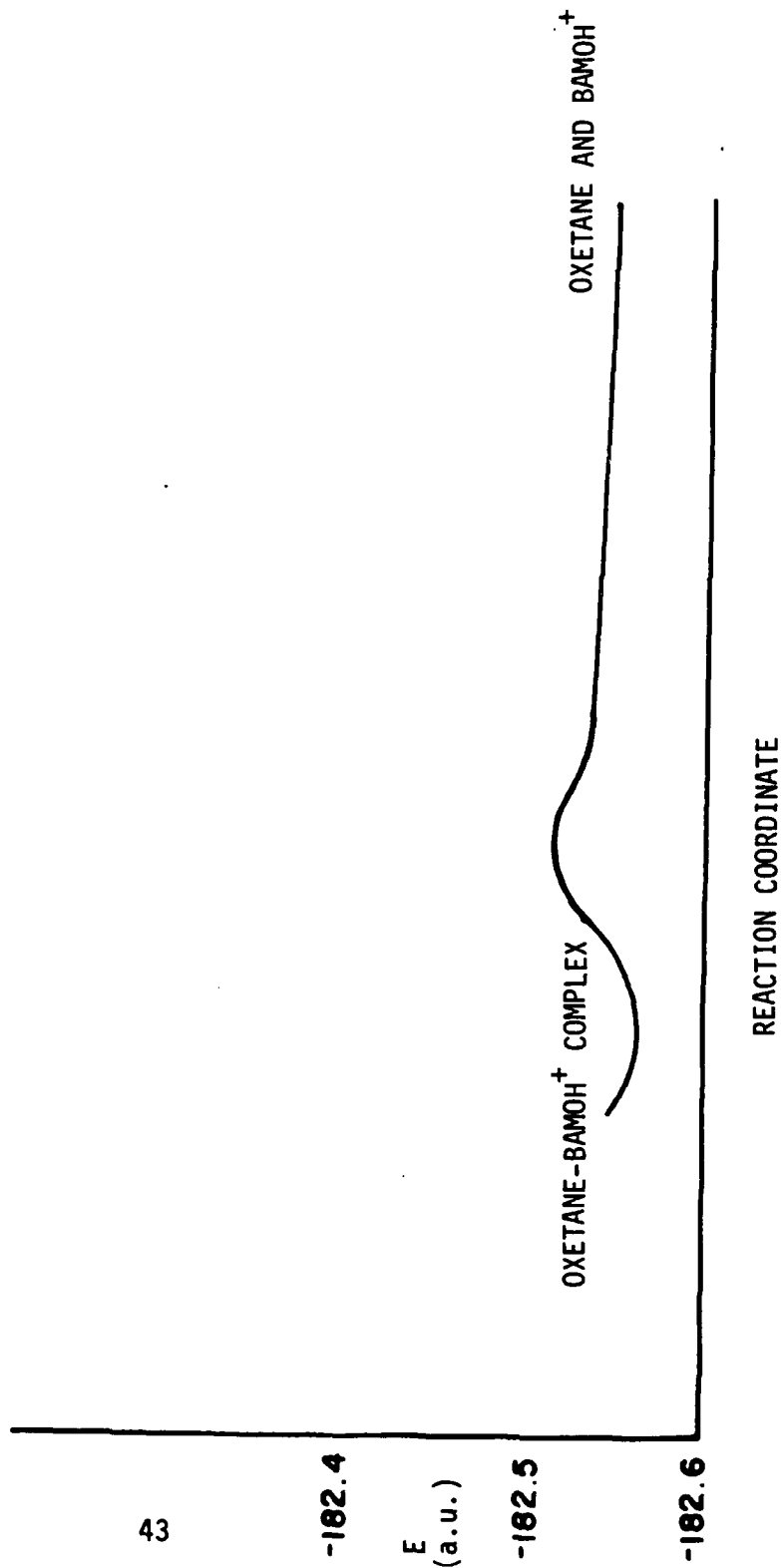


Table II-11

OXET + BAMOH⁺ $\delta = 0^\circ$ (fully closed) $\alpha = -90^\circ$

ENERGIES (a.u.)

R(01B-C4A) (bohrs)	<u>2.3</u>	<u>2.9</u>	<u>3.6</u>
SCF	-140.191550	-140.618884	-140.832071
CI	-140.384287 (871)	-140.808761 (806)	-141.016426 (648)
EXT	-140.392535	-140.815439	-141.023154
DAV	-140.395664	-140.818488	-141.025645
# SAFs generated	37437	37437	37437
Σc^2	0.965	0.965	0.967
gs	0.907	0.907	0.906
R(01B-C4A) (bohrs)	<u>4.6</u>	<u>10.0</u>	
SCF	-140.916659	-140.931042	
CI	-141.097773 (528)	-141.112675 (476)	
EXT	-141.103045	-141.116461	
DAV	-141.105177	-141.118524	
# SAFs generated	37437	37437	
Σc^2	0.970	0.970	
gs	0.906	0.904	

Σc^2 is the contribution of all of the reference configurations
 gs is the contribution of the ground state SCF wave function

Table II-12

OXET + BAMOH[†]

$\delta = 5^\circ$

$\alpha = -90^\circ$

ENERGIES (a.u.)

R(01B-C4A) (bohrs)	2.3	2.9	3.6
SCF	-140.466769	-140.771648	-140.887247
CI	-140.652682 (715)	-140.958037 (644)	-141.069740 (587)
EXT	-140.659569	-140.965615	-141.075686
DAV	-140.661966	-140.968316	-141.078407
# SAFs generated	37437	37437	37437
Σc^2	0.969	0.966	0.965
gs	0.907	0.906	0.905

R(01B-C4A) (bohrs)	4.6	10.0
SCF	-140.921208	-140.921030
CI	-141.101820 (536)	-141.102451 (433)
EXT	-141.106516	-141.105836
DAV	-141.108988	-141.108178
# SAFs generated	37437	37247
Σc^2	0.965	0.966
gs	0.902	0.899

Σc^2 is the contribution of all of the reference configurations
 gs is the contribution of the ground state SCF wave function

Table II-13

OXET + BAMOH⁺ $\delta = 10^\circ$ $\alpha = -90^\circ$

ENERGIES (a.u.)

R(01B-C4A) (bohrs)	2.3	2.9	3.6
SCF	-140.643183	-140.868583	-140.916703
CI	-140.822479 (637)	-141.051090 (585)	-141.096548 (534)
EXT	-140.827605	-141.056584	-141.101970
DAV	-140.829590	-141.058849	-141.104544
# SAFs generated	37437	37437	37437
Σc^2	0.972	0.967	0.965
gs	0.910	0.906	0.903

R(01B-C4A) (bohrs)	4.6	10.0
SCF	-140.908107	140.8916917
CI	-141.082086 (480)	-141.064964 (373)
EXT	-141.086959	-141.068972
DAV	-141.089354	-141.071255
# SAFs generated	37437	37247
Σc^2	0.965	0.965
gs	0.904	0.904

Σc^2 is the contribution of all of the reference configurations
 gs is the contribution of the ground state SCF wave function

Table II-14

OXET + BAMOH⁺ $\delta = 15^\circ$ $\alpha = -90^\circ$

ENERGIES (a.u.)

R(01B-C4A) (bohrs)	2.3	2.9	3.6
SCF	-140.751015	-140.925815	-140.932322
CI	-140.925764 (557)	-141.105482 (508)	-141.111688 (468)
EXT	-140.930515	-141.110667	-141.117464
DAV	-140.932315	-141.112690	-141.119847
# SAFs generated	37437	37437	37437
Σc^2	0.973	0.970	0.966
gs	0.912	0.907	0.902

R(01B-C4A) (bohrs)	4.6	10.0
SCF	-140.894065	-140.863017
CI	-141.065296 (442)	-141.030657 (338)
EXT	-141.069377	-141.033780
DAV	-141.071536	-141.035483
# SAFs generated	37437	37247
Σc^2	0.966	0.970
gs	0.904	0.904

Σc^2 is the contribution of all of the reference configurations
 gs is the contribution of the ground state SCF wave function

Table II-15

OXET + BAMOH⁺ $\delta = 19^\circ$ (fully open) $\alpha = -90^\circ$

ENERGIES (a.u.)

R(01B-C4A) (bohrs)	<u>2.3</u>	<u>2.9</u>	<u>3.6</u>
SCF	-140.803212	-140.945906	-140.928031
CI	-140.976305 (540)	-141.125366 (502)	-141.109421 (468)
EXT	-140.980849	-141.130357	-141.113757
DAV	-140.982607	-141.132331	-141.116090
# SAFs generated	37437	37437	37437
Σc^2	0.974	0.971	0.966
gs	0.914	0.907	0.900
R(01B-C4A) (bohrs)	<u>4.6</u>	<u>10.0</u>	
SCF	-140.871817	-140.830447	
CI	-141.044608 (424)	-140.996542 (303)	
EXT	-141.048147	-140.998771	
DAV	-141.050375	-141.000177	
# SAFs generated	37437	37437	
Σc^2	0.965	0.973	
gs	0.904	0.905	

Σc^2 is the contribution of all of the reference configurations
 gs is the contribution of the ground state SCF wave function

- d. 3-Azidomethyl-3-methyloxetane (AMMO) + protonated
3,3-bis(azidomethyl)oxetane (BAMOH⁺)

We are finishing the MRD-CI calculations for AMMO + BAMOH⁺. These will be completed in the next quarter (October - December 1988). The detailed results will be tabulated when the entire set of calculations is completed.

There is more steric hindrance for AMMO attacking BAMOH⁺ than for BAMO attacking AMMOH⁺.

This year we did finish the specific calculations needed to calculate ΔE (addition) for this system, AMMO + BAMOH⁺.

- e. 3,3-Bis(azidomethyl)oxetane (BAMO) + protonated
3,3-bis(azidomethyl)oxetane (BAMOH⁺)

We have run the SCF calculations for BAMO + BAMOH⁺. For this latter case because of the steric hindrance we have examined a large number of intermolecular geometries. For certain of the intermolecular geometries of BAMO + BAMOH⁺ there are more integrals than the available peripheral disk space on the CRAY XMP can handle with the transformation program (needed to run the subsequent MRD-CI calculations) in its current form. We are currently rewriting the transformation program. There is more steric hindrance when the C_{4A} of BAMOH⁺ is being attacked by OXET or AMMO than when the C_{4A} of OXETH⁺ or AMMOH⁺ is being attacked by BAMO. The attack of BAMO on BAMOH⁺ is even more sterically hindered than any of the other cases we have examined to date. This finding adds further evidence to our hypothesis that the steric hindrance could be a contributing factor to Gerry Manser's observations that bis compounds are more difficult to polymerize and copolymerize. This effect of bulky bis 3,3-substituents on the protonated oxetane being attacked could also be a contributing factor to Gerry Manser's comments that certain compounds will not undergo cationic polymerization or will undergo cationic polymerization only slowly or with difficulty.

2. Recap of Reaction Energies for Cationic Polymerization of Energetic Oxetanes for Initiation and Reaction

Cationic polymerization has two major steps: initiation and propagation. Initiation is governed by the propensity for protonation of the oxetane. The three dimensional electrostatic molecular potential contour (EMPC) maps we calculated earlier are very indicative of the propensity of the energetic substituted oxetanes to initiate. These EMPC maps are also indicative of the propensity of the energetic substituted oxetanes to polymerize. For a more quantitative comparison of propensity to initiate we calculated the MRD-CI energies of protonation [$\Delta E(\text{protonation})$] for all the energetic substituted oxetanes we have studied.

The next step in cationic polymerization is reaction between the oxetane (or substituted oxetanes) and the protonated oxetane (or protonated substituted oxetane). We have calculated the MRD-CI stabilization energy [$\Delta E(\text{addition})$] for several series of reactants as a function of the angle (α) between the rings, the inter-ring distance $R(\text{O1B-C4A})$ and the angle (δ) of opening the protonated ring. The stabilization point for all of the pairs of reactants we have studied to date is $R(\text{O1B-C4A}) = 2.9$ bohrs and $\delta = 19^\circ$. (See sketch page 14 for definition of δ angle)

In the Table (II-16) are tabulated the MRD-CI values for ΔE (protonation), ΔE (addition) and ΔE [ΔE (protonation) + ΔE (addition)] at the stabilization point for the new systems we studied this year [BAMO + OXETH⁺, BAMO + AMMOH⁺, OXET + BAMOH⁺, AMMO + BAMOH⁺] as well as for the systems we studied previously. The additional conclusions from our results of this year reinforce our general conclusions from last year.

The calculated for ΔE (protonation) indicate oxetane gives the most energy on protonation, AMMO next, then BAMO. Thus in mixtures they will initiate in this order.

The most favorable overall reactions involve OXETH⁺ reacting with OXET, AMMO and BAMO in that order. Next most favorable are OXET + AMMOH⁺ and AMMO + AMMOH⁺ (about the same) followed by BAMO + AMMOH⁺. The least favorable of the overall reactions are those involving BAMOH⁺ (we feel for the steric hindrance reasons we stated earlier): OXET + BAMOH⁺ and AMMO + BAMOH⁺.

We are continuing MRD-CI calculations for the potential surfaces of reactions involving BAMOH⁺ with various partners.

The results of calculations such as these enable one both to understand and then to predict copolymerization preferences. In all cases we have studied to date our calculated predictions agree with the order of Gerry Manser's experimental polymerization reactivity ratios.

TABLE II-16

CATIONIC POLYMERIZATION INITIATION AND PROPAGATION
 OXETANES (OXET) + PROTONATED OXETANES (OXETH⁺)
 AB-INITIO MODPOT/VRDDO MRD-CI

ENERGIES (a.u.)			
	$\Delta E(\text{protonation})$	$\Delta E(\text{addition})$	ΔE
OXET + OXETH ⁺	-0.31601	-0.04378	-0.35979
FNOX + OXETH ⁺	-0.31601	-0.01113	-0.32714
OXET + FNOXH ⁺	-0.27068	-0.06327	-0.33394
FNOX + FNOXH ⁺	-0.27068	-0.03157	-0.30225
AMMO + OXETH ⁺	-0.31601	-0.04362	-0.35963
OXET + AMMOH ⁺	-0.31548	-0.02386	-0.33934
AMMO + AMMOH ⁺	-0.31548	-0.02408	-0.33956
OXET + BAMOH ⁺	-0.30906	-0.01390	-0.32296
BAMO + OXETH ⁺	-0.31601	-0.03890	-0.35491
BAMO + AMMOH ⁺	-0.31548	-0.01924	-0.33472
AMMO + BAMOH ⁺	-0.30906	-0.01333	-0.32239

3. Population Analyses

Gerry Manser had expressed considerable interest in how the charges (corresponding to the gross atomic populations) on the O_{1A} (oxygen of protonated oxetane ring), C_{4A} (the α carbon of the protonated oxetane ring) and O_{1B} (oxygen of the oxetane ring) varied as a function of substituent and reaction pathway.

In our Annual Report 1986, Table III Page 24, showed that that as oxetane and protonated oxetane approached each other that the intra-ring TOP of the $C_{4A}-O_{1A}$ in the protonated ring got smaller as the oxetane ring approached, indicating a tendency for the protonated ring to open and the inter-ring TOP $O_{1B}-C_{4A}$ got larger indicating bond formation.

Similar trends in the TOPs were shown in last year's Annual Report 1987 in the Tables of population analyses of $OXET + OXETH^+$, $OXET + FNOXH^+$, $FNOX + OXETH^+$, $FNOX + FNOXH^+$, $AMMO + OXETH^+$, $OXET + AMMOH^+$, $AMMO + AMMOH^+$.

The general trends of the TOP population analysis of this year's calculations on $BAMO + OXETH^+$, $BAMO + AMMOH^+$ AND $OXET + BAMOH^+$ remain the same.

i) It is apparent from the TOPs in the tables that the two rings are repulsive when the protonated oxetane (or substituted protonated oxetane) ring is closed.

ii) the protonated oxetane (or substituted protonated oxetane) will open upon approach of the oxetane (or substituted oxetane) along the appropriate reaction pathway.

iii) The $O_{1B}-C_{4A}$ interring bond becomes stronger as the protonated (A) ring opens.

iv) Total overlap populations are a very sensitive criteria of the incipient making and breaking of bonds. The largest inter-ring TOP's occur when the energy is a minimum. As the protonated and unprotonated oxetane (energetic substituted oxetane) rings approach

a'. the intra-ring TOP ($C_{4A}-O_{1A}$) begins to get smaller even when the protonated ring is still fully closed. This indicates that the $C_{4A}-O_{1A}$ bond wants to lengthen.

b'. The TOP ($O_{1B}-C_{4A}$) begins to be noticeable at 4.6 bohrs and gets larger as the rings approach closer provided that the protonated ring is open by at least $\delta = 5^\circ$. The strongest TOP ($O_{1B}-C_{4A}$) occurs (as anticipated) at the most stable point energetically, $R(O_{1B}-C_{4A}) = 2.9$ bohrs and $\delta = 19^\circ$.

The behavior of these TOPs of BAMO + OXETH⁺, BAMO + AMMOH⁺ and OXET + BAMOH⁺ in the following Tables II-17 to II-19 is indicative of the same conclusion as that from the MRD-CI energy calculations.

The GAPs (gross atomic populations) show interesting behavior.

The general results in the systems investigated this year are:

- i) C_{2A} and C_{4A} (the α carbons in the original protonated ring) still carry about the same excess negative charge (-0.2 e) in spite of the fact that the entire protonated species itself carries a formal positive charge. As the protonated ring opens and the O_{1B} of the unprotonated ring begins to form a bond with C_{4A}, there is a slight drop in the charge on C_{4A} during the course of the reaction, but when the ring is finally open at the stabilization geometry of the system the charge on C_{4A} has gone back up again.
- ii) In the reactions of BAMO + OXETH⁺ and BAMO + AMMOH⁺ at the stabilization geometry of the system the charge on C_{2A} is higher than in the isolated protonated ring.
- iii) O_{1A} in the protonated ring (OXETH⁺, AMMOH⁺ and BAMOH⁺) carries an excess negative charge of -0.37 (or -0.38). O_{1B} in the unprotonated ring (OXET or AMMO) carries an excess negative charge of -0.35 (or -0.34). When the O_{1B}-C_{4A} bond forms, O_{1B} still carries an excess negative charge of -0.29 in BAMO + OXETH⁺ (just as in AMMO + OXETH⁺) and excess negative charges of 0.29 in BAMO + AMMOH⁺ and -0.28 in OXET + BAMOH⁺. This charge distribution is in contrast to the picture sketched by the experimentalists in cationic polymerization who draw a + charge on the O_{1B} when the reaction has taken place. The positive charge is distributed over the H atoms in both rings A and B.

Table II-20	GAPs	BAMO + OXETH ⁺
Table II-21	GAPs	BAMO + AMMOH ⁺
Table II-22	GAPs	OXET + BAMOH ⁺

Table II-17

BAMO + OXETH⁺Total Overlap Populations
Ab-Initio MODPOT/VRDDO

δ	R(bohrs)	0°		5°		10°		15°		19°	
		SCF	CI	SCF	CI	SCF	CI	SCF	CI	SCF	CI
<u>01B-C4A</u>											
2.3	-.1933	-.2043	.0978	.0728	.2381	.2044	.3148	.2761	.3650	.3232	
2.9	-.2297	-.2179	.0762	.0707	.2512	.2367	.3475	.3259	.4042	.3792	
3.6	-.1259	-.1175	.0490	.0555	.1833	.1907	.2670	.2731	.3150	.3162	
4.6	-.0211	-.0201	.0231	.0235	.0675	.0719	.1040	.1133	.1284	.1407	
10.0	.0000	.0000	.0000	.0000	.0000	.0000	.0000	.0000	.0000	.0000	
<u>C4A-01A</u>											
2.3	-.0218	-.0337	-.0380	-.0350	-.0394	-.0370	-.0297	-.0293	-.0219	-.0214	
2.9	.1704	.1466	.0800	.0801	.0118	.0146	-.0126	-.0122	-.0158	-.0155	
3.6	.3194	.2927	.1945	.1956	.0689	.0745	.0058	.0066	-.0105	-.0105	
4.6	.3902	.3642	.2690	.2730	.1199	.1359	.0249	.0320	-.0053	-.0034	
10.0	.4220	.3925	.3063	.3078	.1532	.1755	.0414	.0556	-.0005	.0042	

Table II- 18

BAMO + AMMOH⁺Total Overlap Populations
Ab-Initio MODPOT/VRDDO

δ R(bohrs)	01B-C4A				C4A-01A					
	0°	5°	10°	15°	19°	15°	10°	5°	0°	
	SCF	CI	SCF	CI	SCF	CI	SCF	CI	SCF	CI
2.3	-.2019	-.2123	.0971	.0723	.2428	.2090	.3239	.2854	.3770	.3358
2.9	-.2384	-.2260	.0727	.0671	.2528	.2383	.3532	.3317	.4125	.3874
3.6	-.1286	-.1207	.0452	.0512	.1811	.1881	.2680	.2741	.3185	.3199
4.6	-.0211	-.0205	.0215	.0214	.0648	.0679	.1019	.1106	.1277	.1395
10.0	.0000	.0000	.0000	.0000	.0000	.0000	.0000	.0000	.0000	.0000
2.3	-.0231	-.0345	-.0362	-.0327	-.0373	-.0347	-.0286	-.0281	-.0214	-.0208
2.9	.1760	.1530	.0861	.0863	.0162	.0190	-.0105	-.0100	-.0149	-.0146
3.6	.3275	.3009	.2034	.2042	.0763	.0828	.0096	.0109	-.0087	-.0087
4.6	.3972	.3711	.2771	.2804	.1290	.1458	.0313	.0395	-.0018	-.0004
10.0	.4276	.3978	.3126	.3124	.1620	.1836	.0499	.0654	.0054	.0116

Table II- 19

OXET + BAMOH⁺Total Overlap Populations
Ab-Initio MODPOT/VRDDO

δ	0°		5°		10°		15°		19°	
	SCF	CI								
2.3	-.1694	-.1789	.1203	.0947	.2590	.2240	.3350	.2954	.3845	.3423
2.9	-.2033	-.1905	.1025	.0957	.2732	.2558	.3664	.3417	.4212	.3932
3.6	-.1131	-.1041	.0666	.0743	.2015	.2077	.2841	.2874	.3307	.3285
4.6	-.0182	-.0171	.0276	.0286	.0738	.0789	.1115	.1219	.1360	.1490
10.0	.0000	.0000	.0000	.0000	.0000	.0000	.0000	.0000	.0000	.0000
<u>01B-C4A</u>										
2.3	-.0555	-.0669	-.0551	-.0481	-.0414	-.0392	-.0289	-.0288	-.0209	-.0204
2.9	.1485	.1238	.0685	.0680	.0095	.0114	-.0118	-.0121	-.0148	-.0146
3.6	.3113	.2843	.1887	.1878	.0680	.0719	.0070	.0070	-.0092	-.0094
4.6	.3897	.3643	.2698	.2731	.1226	.1374	.0278	.0342	-.0032	-.0017
10.0	.4223	.3938	.3082	.3096	.1571	.1784	.0452	.0597	.0021	.0069
<u>C4A-01A</u>										

Table II-20

BAMO + OXETH⁺Gross Atomic Populations
Ab-Initio MODPOT/VRDDO $\delta = 0^\circ$ (fully closed)

R(bohrs)	2.3		2.9		3.6		4.6		10.0	
	SCF	CI								
O1A	6.4478	6.3868	6.4612	6.3935	6.4593	6.3855	6.4517	6.3749	6.4442	6.3668
C2A	4.2391	4.2630	4.2266	4.2515	4.2126	4.2376	4.2030	4.2278	4.1963	4.2212
C3A	4.4581	4.4504	4.4404	4.4373	4.4388	4.4391	4.4409	4.4429	4.4460	4.4492
C4A	4.0771	4.0913	4.1216	4.1420	4.1458	4.1596	4.1709	4.1786	4.1924	4.1984
H2Aa	0.7388	0.7388	0.7268	0.7268	0.7150	0.7150	0.7066	0.7067	0.6995	0.6995
H2Ab	0.7382	0.7383	0.7263	0.7263	0.7146	0.7146	0.7063	0.7064	0.6994	0.6995
H4Aa	0.7454	0.7552	0.7307	0.7426	0.7117	0.7239	0.6990	0.7108	0.6996	0.7111
H4Ab	0.7451	0.7546	0.7303	0.7420	0.7112	0.7233	0.6985	0.7106	0.6994	0.7111
H+	0.5849	0.6068	0.5548	0.5762	0.5276	0.5480	0.5110	0.5306	0.5000	0.5199
O1B	6.3559	6.2987	6.3733	6.3157	6.3986	6.3499	6.4093	6.3701	6.3775	6.3435
C2B	4.2549	4.2780	4.2528	4.2711	4.2562	4.2750	4.2578	4.2764	4.2561	4.2728
C3B	4.0349	4.0345	4.0299	4.0298	4.0303	4.0300	4.0320	4.0316	4.0349	4.0345
C4B	4.2540	4.2773	4.2517	4.2710	4.2548	4.2744	4.2561	4.2756	4.2543	4.2718
H2Ba	0.7380	0.7381	0.7505	0.7506	0.7631	0.7631	0.7715	0.7716	0.7777	0.7777
H2Bb	0.7387	0.7387	0.7537	0.7537	0.7669	0.7670	0.7755	0.7756	0.7829	0.7829
H4Ba	0.7171	0.7172	0.7298	0.7299	0.7425	0.7425	0.7510	0.7511	0.7573	0.7574
H4Bb	0.7250	0.7250	0.7403	0.7404	0.7539	0.7540	0.7628	0.7629	0.7705	0.7706

Table II-20 (continued)

BAMO + OXETH⁺Gross Atomic Populations
Ab-Initio MODPOT/VRDDO $\delta = 5^\circ$

R (bohrs)	2.3		2.9		3.6		4.6		10.0	
	SCF	CI								
O1A	6.4757	6.4242	6.4844	6.4251	6.4811	6.4103	6.4708	6.3893	6.4609	6.3731
C2A	4.2526	4.2723	4.2451	4.2650	4.2332	4.2509	4.2227	4.2367	4.2151	4.2278
C3A	4.4432	4.4408	4.4404	4.4425	4.4450	4.4512	4.4491	4.4584	4.4532	4.4648
C4A	4.0894	4.0951	4.1066	4.1247	4.1100	4.1341	4.1155	4.1329	4.1362	4.1539
H2Aa	0.7526	0.7527	0.7420	0.7421	0.7296	0.7297	0.7191	0.7191	0.7110	0.7110
H2Ab	0.7520	0.7521	0.7415	0.7416	0.7292	0.7293	0.7187	0.7188	0.7109	0.7109
H4Aa	0.7524	0.7612	0.7333	0.7452	0.7053	0.7187	0.6845	0.7001	0.6785	0.6949
H4Ab	0.7514	0.7601	0.7325	0.7444	0.7046	0.7181	0.6840	0.6994	0.6783	0.6945
H+	0.6229	0.6460	0.5978	0.6204	0.5694	0.5878	0.5473	0.5617	0.5333	0.5462
O1B	6.3547	6.2912	6.3685	6.3021	6.3954	6.3377	6.4118	6.3683	6.3783	6.3453
C2B	4.2200	4.2456	4.2274	4.2465	4.2420	4.2590	4.2537	4.2726	4.2562	4.2724
C3B	4.0340	4.0336	4.0315	4.0314	4.0315	4.0314	4.0322	4.0318	4.0348	4.0344
C4B	4.2199	4.2457	4.2268	4.2466	4.2408	4.2586	4.2521	4.2719	4.2544	4.2714
H2Ba	0.7272	0.7273	0.7398	0.7399	0.7556	0.7556	0.7688	0.7689	0.7776	0.7777
H2Bb	0.7293	0.7293	0.7431	0.7432	0.7590	0.7591	0.7724	0.7724	0.7828	0.7828
H4Ba	0.7063	0.7063	0.7191	0.7191	0.7349	0.7350	0.7483	0.7484	0.7573	0.7574
H4Bb	0.7154	0.7155	0.7296	0.7296	0.7459	0.7459	0.7596	0.7597	0.7704	0.7705

Table II-20 (continued)

BAMO + OXETH⁺Gross Atomic Populations
Ab-Initio MODPOT/VRDDO $\delta = 10^\circ$

R(bohrs)	2.3		2.9		3.6		4.6		10.0	
	SCF	CI								
O1A	6.4871	6.4442	6.4956	6.4484	6.4986	6.4450	6.4946	6.4289	6.4875	6.4110
C2A	4.2623	4.2776	4.2591	4.2745	4.2516	4.2661	4.2421	4.2521	4.2338	4.2399
C3A	4.4368	4.4371	4.4419	4.4467	4.4507	4.4596	4.4567	4.4675	4.4602	4.4733
C4A	4.1190	4.1176	4.1195	4.1286	4.0997	4.1178	4.0719	4.0836	4.0756	4.0863
H2Aa	0.7608	0.7609	0.7525	0.7525	0.7419	0.7420	0.7306	0.7307	0.7212	0.7212
H2Ab	0.7602	0.7603	0.7519	0.7520	0.7415	0.7416	0.7303	0.7304	0.7211	0.7211
H4Aa	0.7419	0.7496	0.7256	0.7369	0.6968	0.7114	0.6685	0.6831	0.6538	0.6694
H4Ab	0.7406	0.7484	0.7246	0.7359	0.6960	0.7106	0.6679	0.6826	0.6537	0.6692
H+	0.6454	0.6703	0.6295	0.6543	0.6097	0.6329	0.5896	0.6083	0.5742	0.5892
O1B	6.3619	6.2961	6.3645	6.2937	6.3871	6.3174	6.4113	6.3610	6.3796	6.3454
C2B	4.1978	4.2249	4.2088	4.2289	4.2274	4.2416	4.2475	4.2646	4.2563	4.2730
C3B	4.0340	4.0336	4.0331	4.0330	4.0331	4.0332	4.0327	4.0325	4.0347	4.0343
C4B	4.1981	4.2253	4.2087	4.2291	4.2267	4.2415	4.2461	4.2640	4.2545	4.2721
H2Ba	0.7207	0.7207	0.7317	0.7318	0.7471	0.7472	0.7643	0.7643	0.7776	0.7776
H2Bb	0.7241	0.7241	0.7355	0.7356	0.7508	0.7508	0.7678	0.7678	0.7826	0.7827
H4Ba	0.6998	0.6998	0.7110	0.7110	0.7264	0.7265	0.7437	0.7437	0.7572	0.7573
H4Bb	0.7101	0.7102	0.7219	0.7219	0.7375	0.7375	0.7549	0.7549	0.7703	0.7703

Table II- 20 (continued)

BAM0 + OXETH⁺Gross Atomic Populations
Ab Initio MODPOT/VRDDO $\delta = 15^\circ$

R (bohrs)	2.3		2.9		3.6		4.6		10.0	
	SCF	CI								
O1A	6.4831	6.4447	6.4895	6.4498	6.4945	6.4524	6.4965	6.4513	6.4951	6.4443
C2A	4.2687	4.2810	4.2678	4.2799	4.2640	4.2756	4.2571	4.2655	4.2496	4.2546
C3A	4.4348	4.4366	4.4441	4.4500	4.4552	4.4658	4.4627	4.4739	4.4661	4.4775
C4A	4.1497	4.1458	4.1453	4.1490	4.1151	4.1287	4.0619	4.0636	4.0380	4.0230
H2Aa	0.7641	0.7642	0.7570	0.7571	0.7482	0.7483	0.7372	0.7373	0.7264	0.7265
H2Ab	0.7635	0.7635	0.7565	0.7566	0.7478	0.7479	0.7369	0.7369	0.7263	0.7264
H4Aa	0.7341	0.7407	0.7221	0.7322	0.6964	0.7109	0.6639	0.6781	0.6396	0.6527
H4Ab	0.7328	0.7394	0.7210	0.7312	0.6956	0.7101	0.6634	0.6775	0.6395	0.6525
H+	0.6546	0.6803	0.6447	0.6711	0.6326	0.6597	0.6184	0.6433	0.6049	0.6276
O1B	6.3715	6.3044	6.3615	6.2895	6.3767	6.3008	6.4054	6.3471	6.3805	6.3457
C2B	4.1838	4.2119	4.1970	4.2182	4.2165	4.2289	4.2410	4.2547	4.2564	4.2735
C3B	4.0345	4.0340	4.0344	4.0343	4.0344	4.0347	4.0334	4.0335	4.0347	4.0343
C4B	4.1844	4.2124	4.1971	4.2187	4.2161	4.2290	4.2398	4.2545	4.2546	4.2725
H2Ba	0.7171	0.7171	0.7268	0.7268	0.7407	0.7407	0.7594	0.7594	0.7775	0.7775
H2Bb	0.7212	0.7213	0.7309	0.7310	0.7446	0.7447	0.7631	0.7631	0.7825	0.7826
H4Ba	0.6962	0.6963	0.7060	0.7061	0.7200	0.7200	0.7388	0.7388	0.7571	0.7572
H4Bb	0.7073	0.7073	0.7172	0.7172	0.7312	0.7312	0.7501	0.7501	0.7702	0.7702

Table II- 20 (continued)

BAMO + OXETH⁺Gross Atomic Populations
Ab-Initio MOPOT/VRDDO $\delta = 19^\circ$ (fully open)

R(bohrs)	2.3		2.9		3.6		4.6		10.0	
	SCF	CI								
O1A	6.4744	6.4377	6.4780	6.4412	6.4812	6.4440	6.4830	6.4467	6.4829	6.4458
C2A	4.2745	4.2849	4.2741	4.2839	4.2715	4.2807	4.2660	4.2730	4.2590	4.2639
C3A	4.4342	4.4366	4.4451	4.4509	4.4564	4.4685	4.4638	4.4765	4.4665	4.4769
C4A	4.1779	4.1734	4.1752	4.1798	4.1444	4.1574	4.0817	4.0840	4.0367	4.0064
H2Aa	0.7648	0.7649	0.7584	0.7585	0.7503	0.7503	0.7390	0.7391	0.7261	0.7262
H2Ab	0.7642	0.7643	0.7579	0.7580	0.7498	0.7499	0.7387	0.7388	0.7261	0.7261
H4Aa	0.7276	0.7336	0.7206	0.7293	0.6998	0.7142	0.6677	0.6826	0.6368	0.6489
H4Ab	0.7264	0.7324	0.7196	0.7284	0.6990	0.7135	0.6672	0.6821	0.6367	0.6488
H+	0.6571	0.6833	0.6498	0.6765	0.6410	0.6688	0.6297	0.6571	0.6170	0.6445
O1B	6.3801	6.3134	6.3593	6.2863	6.3674	6.2874	6.3970	6.3318	6.3808	6.3460
C2B	4.1750	4.2035	4.1893	4.2116	4.2091	4.2215	4.2357	4.2461	4.2564	4.2735
C3B	4.0352	4.0347	4.0355	4.0353	4.0355	4.0358	4.0341	4.0344	4.0346	4.0342
C4B	4.1757	4.2041	4.1897	4.2121	4.2088	4.2217	4.2346	4.2458	4.2546	4.2726
H2Ba	0.7150	0.7151	0.7237	0.7237	0.7363	0.7363	0.7553	0.7554	0.7774	0.7775
H2Bb	0.7196	0.7197	0.7280	0.7281	0.7405	0.7406	0.7594	0.7594	0.7825	0.7826
H4Ba	0.6942	0.6942	0.7029	0.7029	0.7156	0.7156	0.7347	0.7347	0.7570	0.7571
H4Bb	0.7056	0.7057	0.7143	0.7143	0.7270	0.7271	0.7463	0.7463	0.7702	0.7702

Table II-21

BAMO + AMMOH⁺Gross Atomic Populations
Ab-Initio MODPOT/VRDDO $\delta = 0^\circ$ (fully closed)

R(bohrs)	2.3		2.9		3.6		4.6		10.0	
	SCF	CI								
O1A	6.4526	6.3911	6.4657	6.3975	6.4631	6.3888	6.4553	6.3783	6.4481	6.5704
C2A	4.2173	4.2418	4.2043	4.2297	4.1902	4.2157	4.1814	4.2064	4.1760	4.2012
C3A	4.0603	4.0530	4.0405	4.0381	4.0370	4.0382	4.0379	4.0408	4.0426	4.0468
C4A	4.0679	4.0819	4.1112	4.1311	4.1357	4.1489	4.1613	4.1682	4.1830	4.1885
H2Aa	0.7395	0.7396	0.7282	0.7282	0.7172	0.7173	0.7101	0.7102	0.7047	0.7048
H2Ab	0.7442	0.7442	0.7327	0.7328	0.7217	0.7217	0.7145	0.7145	0.7088	0.7089
H4Aa	0.7456	0.7549	0.7314	0.7430	0.7134	0.7255	0.7017	0.7136	0.7035	0.7149
H4Ab	0.7499	0.7593	0.7366	0.7481	0.7192	0.7309	0.7079	0.7192	0.7096	0.7206
H+	0.5868	0.6082	0.5567	0.5776	0.5299	0.5498	0.5140	0.5333	0.5039	0.5236
O1B	6.3608	6.3035	6.3774	6.3195	6.4005	6.3521	6.4108	6.3717	6.3794	6.3452
C2B	4.2453	4.2684	4.2472	4.2656	4.2549	4.2736	4.2592	4.2778	4.2566	4.2733
C3B	4.0381	4.0378	4.0317	4.0316	4.0311	4.0308	4.0319	4.0315	4.0347	4.0343
C4B	4.2400	4.2637	4.2426	4.2627	4.2506	4.2706	4.2553	4.2751	4.2542	4.2719
H2Ba	0.7472	0.7473	0.7597	0.7598	0.7707	0.7708	0.7764	0.7764	0.7782	0.7782
H2Bb	0.7404	0.7404	0.7534	0.7535	0.7655	0.7655	0.7737	0.7738	0.7827	0.7828
H4Ba	0.7191	0.7191	0.7328	0.7329	0.7450	0.7450	0.7520	0.7521	0.7570	0.7570
H4Bb	0.7268	0.7268	0.7399	0.7399	0.7520	0.7520	0.7603	0.7604	0.7699	0.7700

Table II-21 (continued)

BAMO + AMMOH⁺Gross Atomic Populations
Ab-Initio MODPOT/VRDDO $\delta = 5^\circ$

R (bohrs)	2.3		2.9		3.6		4.6		10.0	
	SCF	CI								
O1A	6.4837	6.4312	6.4922	6.4318	6.4881	6.4165	6.4773	6.3940	6.4675	6.3786
C2A	4.2294	4.2503	4.2209	4.2410	4.2082	4.2266	4.1980	4.2131	4.1917	4.2056
C3A	4.0480	4.0458	4.0430	4.0456	4.0460	4.0527	4.0489	4.0589	4.0525	4.0648
C4A	4.0775	4.0834	4.0933	4.1119	4.0971	4.1198	4.1043	4.1219	4.1267	4.1447
H2Aa	0.7531	0.7532	0.7434	0.7434	0.7322	0.7323	0.7235	0.7235	0.7173	0.7174
H2Ab	0.7578	0.7579	0.7479	0.7480	0.7366	0.7367	0.7278	0.7278	0.7214	0.7214
H4Aa	0.7583	0.7666	0.7401	0.7515	0.7131	0.7269	0.6939	0.7089	0.6890	0.7050
H4Ab	0.7514	0.7602	0.7330	0.7449	0.7061	0.7195	0.6869	0.7025	0.6823	0.6986
H+	0.6267	0.6494	0.6014	0.6234	0.5730	0.5905	0.5516	0.5652	0.5385	0.5505
O1B	6.3598	6.2960	6.3729	6.3064	6.3983	6.3413	6.4140	6.3708	6.3800	6.3458
C2B	4.2109	4.2365	4.2227	4.2421	4.2417	4.2588	4.2555	4.2746	4.2567	4.2734
C3B	4.0368	4.0363	4.0330	4.0329	4.0320	4.0319	4.0321	4.0317	4.0347	4.0343
C4B	4.2074	4.2336	4.2193	4.2395	4.2379	4.2564	4.2518	4.2721	4.2543	4.2720
H2Ba	0.7359	0.7359	0.7480	0.7480	0.7624	0.7624	0.7732	0.7732	0.7781	0.7782
H2Bb	0.7304	0.7304	0.7427	0.7427	0.7578	0.7579	0.7709	0.7709	0.7826	0.7827
H4Ba	0.7083	0.7083	0.7215	0.7215	0.7370	0.7370	0.7491	0.7491	0.7570	0.7570
H4Bb	0.7168	0.7168	0.7290	0.7290	0.7442	0.7443	0.7574	0.7575	0.7699	0.7699

Table II-21 (continued)

BAMO + AMMOH⁺Gross Atomic Populations
Ab-Initio MODPOT/VRDDO $\delta = 10^\circ$

R (bohrs)	2.3		2.9		3.6		4.6		10.0	
	SCF	CI								
O1A	6.4988	6.4544	6.5075	6.4589	6.5102	6.4530	6.5057	6.4361	6.4984	6.4171
C2A	4.2386	4.2559	4.2347	4.2523	4.2265	4.2436	4.2170	4.2290	4.2101	4.2173
C3A	4.0432	4.0434	4.0462	4.0511	4.0538	4.0629	4.0590	4.0703	4.0620	4.0771
C4A	4.1059	4.1047	4.1042	4.1134	4.0834	4.1014	4.0576	4.0702	4.0651	4.0781
H2Aa	0.7603	0.7604	0.7529	0.7530	0.7438	0.7439	0.7347	0.7348	0.7277	0.7278
H2Ab	0.7649	0.7650	0.7573	0.7574	0.7481	0.7482	0.7389	0.7390	0.7316	0.7317
H4Aa	0.7477	0.7548	0.7320	0.7428	0.7040	0.7179	0.6770	0.6913	0.6639	0.6803
H4Ab	0.7397	0.7475	0.7240	0.7353	0.6963	0.7107	0.6699	0.6845	0.6574	0.6741
H+	0.6516	0.6756	0.6358	0.6598	0.6159	0.6381	0.5961	0.6129	0.5814	0.5936
O1B	6.3669	6.3009	6.3689	6.2981	6.3910	6.3228	6.4148	6.3657	6.3811	6.3466
C2B	4.1896	4.2168	4.2051	4.2253	4.2277	4.2423	4.2496	4.2673	4.2568	4.2736
C3B	4.0362	4.0358	4.0342	4.0341	4.0333	4.0334	4.0324	4.0322	4.0346	4.0342
C4B	4.1871	4.2145	4.2024	4.2232	4.2246	4.2400	4.2463	4.2651	4.2544	4.2722
H2Ba	0.7286	0.7287	0.7387	0.7388	0.7529	0.7529	0.7681	0.7682	0.7780	0.7781
H2Bb	0.7246	0.7246	0.7348	0.7349	0.7497	0.7497	0.7666	0.7667	0.7825	0.7826
H4Ba	0.7015	0.7016	0.7126	0.7126	0.7278	0.7278	0.7443	0.7443	0.7569	0.7569
H4Bb	0.7108	0.7109	0.7210	0.7210	0.7359	0.7359	0.7531	0.7531	0.7698	0.7698

Table II-21 (cont inued)

BAMO + AMMOH⁺Gross Atomic Populations
Ab-Initio MODPOT/VRDDO $\delta = 15^\circ$

R(bohrs)	2.3		2.9		3.6		4.6		10.0	
	SCF	CI								
O1A	6.4978	6.4578	6.5048	6.4634	6.5105	6.4662	6.5132	6.4634	6.5123	6.4566
C2A	4.2446	4.2595	4.2436	4.2584	4.2400	4.2545	4.2340	4.2465	4.2284	4.2368
C3A	4.0418	4.0438	4.0492	4.0554	4.0593	4.0700	4.0661	4.0775	4.0690	4.0814
C4A	4.1369	4.1330	4.1294	4.1332	4.0965	4.1099	4.0430	4.0444	4.0234	4.0107
H2Aa	0.7624	0.7625	0.7563	0.7564	0.7490	0.7491	0.7404	0.7405	0.7327	0.7328
H2Ab	0.7670	0.7670	0.7607	0.7608	0.7532	0.7533	0.7444	0.7445	0.7363	0.7365
H4Aa	0.7385	0.7446	0.7272	0.7368	0.7020	0.7160	0.6701	0.6838	0.6473	0.6607
H4Ab	0.7304	0.7371	0.7191	0.7293	0.6945	0.7089	0.6635	0.6774	0.6418	0.6552
H+	0.6635	0.6883	0.6539	0.6792	0.6423	0.6679	0.6287	0.6520	0.6159	0.6360
O1B	6.3760	6.3091	6.3657	6.2934	6.3811	6.3058	6.4102	6.3529	6.3819	6.3471
C2B	4.1769	4.2049	4.1943	4.2156	4.2172	4.2298	4.2432	4.2575	4.2568	4.2739
C3B	4.0362	4.0358	4.0352	4.0351	4.0345	4.0348	4.0330	4.0331	4.0345	4.0341
C4B	4.1749	4.2030	4.1920	4.2139	4.2146	4.2281	4.2402	4.2560	4.2545	4.2726
H2Ba	0.7243	0.7243	0.7327	0.7327	0.7453	0.7453	0.7626	0.7626	0.7778	0.7779
H2Bb	0.7211	0.7212	0.7299	0.7299	0.7434	0.7434	0.7620	0.7621	0.7825	0.7825
H4Ba	0.6975	0.6976	0.7068	0.7069	0.7204	0.7205	0.7389	0.7390	0.7567	0.7568
H4Bb	0.7073	0.7073	0.7159	0.7160	0.7294	0.7295	0.7484	0.7484	0.7697	0.7698

Table II-21 (continued)

BAMO + AMMOH⁺Gross Atomic Populations
Ab-Initio MODPOT/VRDDO $\delta = 19^\circ$ (fully open)

R (bohrs)	2.3		2.9		3.6		4.6		10.0	
	SCF	CI								
O1A	6.4910	6.4526	6.4952	6.4566	6.4994	6.4601	6.5030	6.4626	6.5049	6.4625
C2A	4.2495	4.2629	4.2495	4.2625	4.2479	4.2604	4.2446	4.2563	4.2412	4.2511
C3A	4.0413	4.0439	4.0503	4.0561	4.0602	4.0724	4.0666	4.0793	4.0687	4.0796
C4A	4.1663	4.1615	4.1600	4.1646	4.1260	4.1386	4.0612	4.0618	4.0183	3.9892
H2Aa	0.7626	0.7627	0.7571	0.7572	0.7505	0.7506	0.7418	0.7419	0.7327	0.7328
H2Ab	0.7670	0.7671	0.7614	0.7615	0.7545	0.7546	0.7456	0.7457	0.7361	0.7362
H4Aa	0.7302	0.7357	0.7238	0.7322	0.7034	0.7176	0.6714	0.6858	0.6413	0.6535
H4Ab	0.7226	0.7286	0.7165	0.7252	0.6967	0.7111	0.6658	0.6804	0.6373	0.6495
H+	0.6684	0.6933	0.6616	0.6870	0.6535	0.6798	0.6432	0.6695	0.6319	0.6573
O1B	6.3841	6.3172	6.3633	6.2902	6.3718	6.2920	6.4023	6.3382	6.3823	6.3474
C2B	4.1693	4.1979	4.1875	4.2099	4.2101	4.2227	4.2378	4.2489	4.2568	4.2739
C3B	4.0366	4.0361	4.0360	4.0359	4.0355	4.0358	4.0337	4.0339	4.0345	4.0341
C4B	4.1675	4.1961	4.1855	4.2083	4.2077	4.2211	4.2350	4.2473	4.2545	4.2726
H2Ba	0.7215	0.7215	0.7286	0.7287	0.7400	0.7400	0.7579	0.7580	0.7777	0.7778
H2Bb	0.7191	0.7192	0.7268	0.7268	0.7391	0.7391	0.7583	0.7583	0.7825	0.7826
H4Ba	0.6950	0.6951	0.7031	0.7031	0.7153	0.7154	0.7344	0.7344	0.7566	0.7567
H4Bb	0.7052	0.7052	0.7127	0.7128	0.7250	0.7251	0.7445	0.7446	0.7697	0.7698

Table II-22

OXETANE + BAMOH⁺Gross Atomic Populations
Ab-Initio MODPOT/VRDDO $\delta = 0^\circ$ (fully closed)

R(bohrs)	2.3		2.9		3.6		4.6		10.0	
	SCF	CI								
O1A	6.4463	6.3860	6.4613	6.3940	6.4606	6.3870	6.4537	6.3760	6.4471	6.3690
C2A	4.2252	4.2480	4.2111	4.2360	4.1955	4.2200	4.1858	4.2100	4.1803	4.2050
C3A	4.0637	4.0530	4.0393	4.0340	4.0314	4.0300	4.0294	4.0300	4.0333	4.0350
C4A	4.0772	4.0900	4.1165	4.1380	4.1377	4.1520	4.1600	4.1670	4.1796	4.1850
H2Aa	0.7508	0.7500	0.7377	0.7370	0.7252	0.7250	0.7171	0.7170	0.7115	0.7110
H2Ab	0.7546	0.7540	0.7431	0.7430	0.7316	0.7310	0.7242	0.7240	0.7193	0.7190
H4Aa	0.7341	0.7440	0.7222	0.7340	0.7024	0.7150	0.6878	0.7000	0.6877	0.7000
H4Ab	0.7410	0.7520	0.7257	0.7380	0.7086	0.7210	0.6985	0.7100	0.7024	0.7130
H+	0.5864	0.6080	0.5563	0.5770	0.5285	0.5490	0.5117	0.5310	0.5021	0.5210
O1B	6.3795	6.3190	6.3924	6.3300	6.4056	6.3560	6.4027	6.3630	6.3773	6.3430
C2B	4.2616	4.2830	4.2657	4.2820	4.2761	4.2910	4.2815	4.2980	4.2729	4.2890
C3B	4.4552	4.4540	4.4492	4.4490	4.4487	4.4480	4.4491	4.4480	4.4502	4.4490
C4B	4.2492	4.2750	4.2230	4.2450	4.2198	4.2410	4.2390	4.2600	4.2695	4.2870
H2Ba	0.7412	0.7410	0.7464	0.7460	0.7533	0.7530	0.7585	0.7580	0.7661	0.7660
H2Bb	0.7515	0.7510	0.7532	0.7530	0.7566	0.7560	0.7598	0.7590	0.7665	0.7660
H4Ba	0.7714	0.7710	0.7716	0.7710	0.7720	0.7720	0.7721	0.7720	0.7746	0.7740
H4Bb	0.6452	0.6450	0.6874	0.6870	0.7357	0.7350	0.7672	0.7670	0.7760	0.7760

Table II-22 (continued)

OXETANE + BAMOH[†]Gross Atomic Populations
Ab-Initio MODPOT/VRDDO $\delta = 5^\circ$

R (bohrs)	2.3		2.9		3.6		4.6		10.0	
	SCF	CI								
O1A	6.4773	6.4260	6.4871	6.4280	6.4850	6.4140	6.4755	6.3940	6.4667	6.3790
C2A	4.2346	4.2540	4.2261	4.2460	4.2130	4.2320	4.2020	4.2170	4.1955	4.2090
C3A	4.0505	4.0450	4.0416	4.0410	4.0411	4.0450	4.0417	4.0490	4.0454	4.0550
C4A	4.0849	4.0900	4.1008	4.1180	4.1014	4.1270	4.1017	4.1190	4.1194	4.1360
H2Aa	0.7630	0.7630	0.7525	0.7520	0.7406	0.7400	0.7309	0.7300	0.7244	0.7240
H2Ab	0.7689	0.7690	0.7595	0.7590	0.7484	0.7480	0.7393	0.7390	0.7334	0.7330
H4Aa	0.7423	0.7510	0.7263	0.7380	0.6984	0.7120	0.6763	0.6920	0.6701	0.6860
H4Ab	0.7483	0.7580	0.7304	0.7430	0.7045	0.7180	0.6854	0.7010	0.6820	0.6980
H+	0.6249	0.6480	0.6009	0.6230	0.5728	0.5910	0.5505	0.5640	0.5376	0.5500
O1B	6.3711	6.3060	6.3770	6.3080	6.3933	6.3320	6.4012	6.3570	6.3779	6.3430
C2B	4.2313	4.2560	4.2418	4.2590	4.2609	4.2750	4.2757	4.2920	4.2728	4.2890
C3B	4.4523	4.4520	4.4490	4.4490	4.4487	4.4480	4.4487	4.4480	4.4502	4.4490
C4B	4.2082	4.2350	4.1982	4.2200	4.2117	4.2310	4.2405	4.2610	4.2696	4.2870
H2Ba	0.7335	0.7330	0.7380	0.7380	0.7467	0.7460	0.7556	0.7550	0.7659	0.7650
H2Bb	0.7413	0.7410	0.7430	0.7430	0.7492	0.7490	0.7570	0.7560	0.7664	0.7660
H4Ba	0.7558	0.7550	0.7557	0.7550	0.7609	0.7610	0.7679	0.7680	0.7746	0.7740
H4Bb	0.6534	0.6530	0.6909	0.6900	0.7333	0.7330	0.7650	0.7650	0.7761	0.7760

Table II- 22 (continued)

OXETANE + BAMOH⁺Gross Atomic Populations
Ab Initio MODPOT/VRDDO $\delta = 10^\circ$

R (bohrs)	2.3		2.9		3.6		4.6		10.0	
	SCF	CI								
O1A	6.4927	6.4490	6.5019	6.4540	6.5058	6.4500	6.5028	6.4360	6.4967	6.4190
C2A	4.2407	4.2570	4.2370	4.2530	4.2289	4.2450	4.2190	4.2310	4.2116	4.2190
C3A	4.0462	4.0430	4.0458	4.0480	4.0509	4.0580	4.0551	4.0640	4.0593	4.0710
C4A	4.1108	4.1100	4.1126	4.1220	4.0911	4.1110	4.0567	4.0710	4.0557	4.0670
H2Aa	0.7696	0.7690	0.7617	0.7610	0.7522	0.7520	0.7423	0.7420	0.7348	0.7340
H2Ab	0.7771	0.7770	0.7699	0.7700	0.7612	0.7610	0.7520	0.7520	0.7452	0.7450
H4Aa	0.7335	0.7410	0.7194	0.7310	0.6920	0.7070	0.6634	0.6780	0.6494	0.6650
H4Ab	0.7383	0.7460	0.7234	0.7350	0.6972	0.7120	0.6704	0.6850	0.6580	0.6730
H+	0.6495	0.6740	0.6348	0.6590	0.6159	0.6390	0.5961	0.6140	0.5817	0.5950
O1B	6.3718	6.3050	6.3647	6.2920	6.3770	6.3050	6.3966	6.3450	6.3790	6.3440
C2B	4.2111	4.2370	4.2240	4.2430	4.2452	4.2570	4.2676	4.2820	4.2728	4.2890
C3B	4.4504	4.4500	4.4491	4.4490	4.4491	4.4490	4.4486	4.4480	4.4501	4.4490
C4B	4.1813	4.2090	4.1824	4.2040	4.2037	4.2180	4.2393	4.2570	4.2699	4.2870
H2Ba	0.7284	0.7280	0.7318	0.7310	0.7397	0.7390	0.7513	0.7510	0.7656	0.7650
H2Bb	0.7335	0.7330	0.7349	0.7340	0.7414	0.7410	0.7525	0.7520	0.7662	0.7660
H4Ba	0.7437	0.7430	0.7432	0.7430	0.7495	0.7490	0.7618	0.7610	0.7744	0.7740
H4Bb	0.6624	0.6620	0.6937	0.6930	0.7284	0.7280	0.7601	0.7600	0.7761	0.7760

Table II- 22 (continued)

OXETANE + BAMOH⁺Gross Atomic Populations
Ab-Initio MODPOT/VRDDO $\delta = 15^\circ$

R (bohrs)	2.3		2.9		3.6		4.6		10.0	
	SCF	CI								
O1A	6.4934	6.4530	6.5004	6.4590	6.5062	6.4620	6.5094	6.4610	6.5090	6.4550
C2A	4.2429	4.2570	4.2419	4.2560	4.2381	4.2520	4.2317	4.2440	4.2254	4.2330
C3A	4.0455	4.0440	4.0501	4.0530	4.0586	4.0670	4.0660	4.0750	4.0720	4.0820
C4A	4.1388	4.1360	4.1363	4.1410	4.1052	4.1220	4.0450	4.0510	4.0164	4.0030
H2Aa	0.7717	0.7710	0.7652	0.7650	0.7575	0.7570	0.7480	0.7480	0.7395	0.7390
H2Ab	0.7801	0.7800	0.7742	0.7740	0.7672	0.7670	0.7586	0.7580	0.7509	0.7510
H4Aa	0.7262	0.7330	0.7160	0.7260	0.6923	0.7070	0.6607	0.6750	0.6384	0.6510
H4Ab	0.7301	0.7370	0.7196	0.7300	0.6965	0.7110	0.6658	0.6800	0.6442	0.6570
H+	0.6622	0.6870	0.6532	0.6780	0.6424	0.6680	0.6293	0.6530	0.6174	0.6380
O1B	6.3760	6.3090	6.3558	6.2830	6.3611	6.2820	6.3873	6.3270	6.3799	6.3450
C2B	4.1980	4.2250	4.2125	4.2330	4.2334	4.2430	4.2596	4.2700	4.2727	4.2890
C3B	4.4493	4.4480	4.4492	4.4490	4.4494	4.4490	4.4486	4.4480	4.4500	4.4490
C4B	4.1654	4.1930	4.1747	4.1970	4.1992	4.2120	4.2371	4.2510	4.2701	4.2870
H2Ba	0.7253	0.7250	0.7279	0.7270	0.7346	0.7340	0.7470	0.7460	0.7653	0.7650
H2Bb	0.7282	0.7280	0.7296	0.7290	0.7355	0.7350	0.7479	0.7470	0.7660	0.7660
H4Ba	0.7344	0.7340	0.7343	0.7340	0.7406	0.7400	0.7556	0.7550	0.7744	0.7740
H4Bb	0.6710	0.6710	0.6967	0.6960	0.7246	0.7240	0.7546	0.7540	0.7761	0.7760

Table II- 22 (continued)

OXETANE + BAMOH[†]Gross Atomic Populations
Ab-Initio MODPOT/VRDDO $\delta = 19^\circ$ (fully open)

R (bohrs)	2.3		2.9		3.6		4.6		10.0	
	SCF	CI								
O1A	6.4883	6.4490	6.4926	6.4540	6.4967	6.4570	6.4998	6.4590	6.5010	6.4590
C2A	4.2439	4.2570	4.2437	4.2560	4.2416	4.2540	4.2373	4.2480	4.2323	4.2420
C3A	4.0456	4.0450	4.0523	4.0550	4.0615	4.0710	4.0695	4.0800	4.0763	4.0840
C4A	4.1655	4.1620	4.1645	4.1700	4.1332	4.1500	4.0640	4.0720	4.0167	3.9880
H2Aa	0.7721	0.7720	0.7662	0.7660	0.7591	0.7590	0.7496	0.7490	0.7395	0.7390
H2Ab	0.7806	0.7800	0.7754	0.7750	0.7690	0.7690	0.7604	0.7600	0.7513	0.7510
H4Aa	0.7196	0.7260	0.7138	0.7230	0.6952	0.7100	0.6650	0.6800	0.6377	0.6490
H4Ab	0.7231	0.7290	0.7172	0.7260	0.6989	0.7140	0.6689	0.6840	0.6415	0.6530
H+	0.6683	0.6930	0.6618	0.6870	0.6543	0.6800	0.6446	0.6710	0.6343	0.6600
O1B	6.3808	6.3140	6.3499	6.2760	6.3485	6.2660	6.3769	6.3070	6.3804	6.3450
C2B	4.1894	4.2170	4.2048	4.2260	4.2255	4.2360	4.2533	4.2610	4.2726	4.2890
C3B	4.4492	4.4480	4.4496	4.4490	4.4498	4.4500	4.4488	4.4490	4.4500	4.4490
C4B	4.1570	4.1850	4.1708	4.1940	4.1965	4.2090	4.2347	4.2450	4.2702	4.2880
H2Ba	0.7237	0.7230	0.7256	0.7250	0.7312	0.7310	0.7436	0.7430	0.7652	0.7650
H2Bb	0.7252	0.7250	0.7264	0.7260	0.7316	0.7310	0.7444	0.7440	0.7659	0.7650
H4Ba	0.7285	0.7280	0.7285	0.7280	0.7346	0.7340	0.7507	0.7500	0.7743	0.7740
H4Bb	0.6767	0.6760	0.6983	0.6980	0.7217	0.7210	0.7501	0.7500	0.7762	0.7760

III. Ab-Initio MRD-CI Calculations for Breaking a Chemical Bond in a Crystal or Other Solid Environment

Breaking a $>C-NO_2$ or $>N-NO_2$ bond is the initial step leading to detonation of explosives and also the initial step in fractoemission of explosives. To describe properly breaking of a chemical bond in a molecule it is necessary to carry out ab-initio MRD-CI (multireference double excitation - configuration interaction) calculations of the isolated molecule. To describe properly breaking of a chemical bond in a molecule in a crystal or other solid environment it is necessary to carry out ab-initio MRD-CI calculations on dissociation of the molecule surrounded by other molecules as in the crystal or solid arrangement. Even this generation of supercomputers still does not have the space to carry out such calculations on large nitroexplosive molecules especially since many of them (such as RDX and HMX) have a large number of molecules in the unit cell.

Last year we derived, implemented and used successfully a new computational strategy for dissociation of large molecules based on localized/local orbitals. The localized molecular orbitals in the region of the bond breaking are included explicitly in the MRD-CI. The remainder of the occupied and virtual orbitals are folded into an "effective" CI Hamiltonian.

The technique is described below. The method is completely general and can be used for bond breaking and also for subsequent reactions of the species in the solid leading to detonation.

A. Methodology

MRD-CI calculations are absolutely necessary to describe bond breaking processes correctly in the ground state and especially in the excited states.

Our technique involves solving a quantum chemical ab-initio SCF explicitly for a system of a molecule surrounded by a number of other molecules (the unit reference cell or larger assemblage) in the multipole environment of yet more further out surrounding molecules. Multipoles in the environmental region affect the one-electron term in the Hamiltonian. This Hamiltonian is solved for the SCF for all the molecules in the space treated explicitly quantum chemically. The resulting canonical molecular orbitals are localized. All of the occupied and virtual localized orbitals in the region of interest are included explicitly in the MRD-CI and the remaining occupied localized orbitals are folded into an "effective" CI Hamiltonian. The advantage is that the transformations from integrals over atomic orbitals to integrals over molecular orbitals (the computer time-, computer core- and external storage - consuming part of the CI calculations) only have to be carried out for the localized molecular orbitals included explicitly in the MRD-CI calculations.

Space is broken up into three regions:



- A Localized space treated explicitly in ab-initio MRD-CI calculations. (This can be an entire molecule or the localized dissociation region of a large molecule.)
- B + A + B' Space treated explicitly quantum chemically (ab-initio SCF) for supermolecule B A B'
- C + C' Space represented by multipoles of additional molecules taken into account by inclusion of multipole interactions (up through quadrupoles) into one-electron part of SCF Hamiltonian.

This method is completely general. The space treated explicitly quantum chemically and the surrounding space can have voids, defects, deformations, dislocations, impurities, dopants, edges and surfaces, boundaries, etc.

To be able to carry out such MRD-CI calculations for breaking a chemical bond in a molecule or a crystal (or other solid environment) represents a significant breakthrough.

B. Calculations Carried Out for Nitromethane

The previous year we carried out extensive test calculations by this new technique for the dissociation of the $\text{H}_3\text{C} - \text{NO}_2$ bond in nitromethane for various numbers of molecules treated explicitly in the SCF in the multipole field of varying numbers of additional CH_3NO_2 molecules as in the crystal arrangement followed by localization and ab-initio MRD-CI calculations on breaking the $\text{H}_3\text{C} - \text{NO}_2$ bond in a specific nitromethane molecule. Since this technique is new we are still carrying out extensive testing to ascertain how many molecules must be treated in each region for reliable results.

One of the pertinent questions we posed initially for decomposition of molecules in crystals was did it take more or less energy to break the bond when the molecule was in a crystal compared to breaking the bond of an isolated molecule. The MRD-CI results for breaking the $\text{H}_3\text{C} - \text{NO}_2$ bond of nitromethane in the presence of other explicit nitromethane molecules and the multipoles of still farther distant nitromethane molecules compared to the MRD-CI results for breaking the $\text{H}_3\text{C} - \text{NO}_2$ bond in an isolated nitromethane molecule indicate that it takes more energy to break the $\text{H}_3\text{C} - \text{NO}_2$ bond when nitromethane is in the field of the additional nitromethane molecules.

When we presented a paper at the Working Group Meeting on Synthesis of High Energy Density Materials, June 1988, on our MRD-CI calculations for breaking the bond in nitromethane in a nitromethane crystal Dr. Thomas Brill raised the question of the effect of voids in the nitromethane crystal on the energy necessary to break the $\text{H}_3\text{C} - \text{NO}_2$ bond.

Thus, we subsequently carried out extensive investigations of the effects of voids (both in the nitromethane molecules treated explicitly in the SCF and those in the environment represented by multipoles) on the calculated $H_3C - NO_2$ bond dissociation energies.

From our previous studies last year we showed that a calculation involving five nitromethane molecules surrounded by eight more multipolar neighbors arranged as in a crystal is a reliable representation of the molecule in a periodic lattice; and these results compare favorably with ab-initio crystal-orbital calculations.

For the present study we examined the effect of voids on the system of the Real Crystal - Extended Cluster described by five nitromethane molecules treated explicitly in the SCF in the multipole environment of eight more nitromethane molecules (Figure III-1).

There are four nitromethane molecules per unit cell. These four nitromethane molecules are unique and not related by translation. We have designated these four nitromethane molecules classes a,b,c,d. The central unit cell is designated as (555). The unit cells along the x axis are (455) and (655), along the y axis (545) and (565) and along the z axis are (554) and (556). For nitromethane Real Crystal - Extended Cluster Table III-1 shows the cell/cluster designations of the nitromethane molecules included in the calculations.

The bond dissociation energy of a molecule in a crystal, in contrast to the bond dissociation energy in a free molecule, includes interactions with other molecules in crystal. The energy of the cluster before the decomposition can be written

$$\epsilon_1 = E_A + E_B + E_{AB} + E_{AC} + E_{CB} + E_{ABC} \quad \text{III-1}$$

(A,B,C correspond to spaces of cluster, where here B space = B + B'; C = C + C') and after decomposition

$$\epsilon_2 = \tilde{E}_A + E_B + E_{BC} + \dots \quad \text{III-2}$$

where E_A, \tilde{E}_A energy of molecule A before and after decomposition

E_B energy of molecules B

($E_B = E_B + E_{B'} + E_{BB'}$, in our case)

E_{ij} two body interactions

E_{ijk} three body interactions

The bond dissociation energy

$$\Delta E = \epsilon_1 - \epsilon_2 = \epsilon_1 - E_A - E_B$$

III-3

Assuming the decomposition of the bond to infinity, E_A is the energy of a completely decomposed free molecule and E_B is the energy of the cluster without A molecule.

The value

$$E_R(r) = \epsilon_1(r) - E_B,$$

III-4

is called the reduced energy and represents the energy of reference molecule in the field of other species in the crystal. The $E_R(r)$ can be used to compare energy surfaces (reaction surfaces in different assumed models).

In Table III-2 are presented the $E(\text{SCF})$, $E(\text{CI})$, $E(\text{CI,EX})$, $E(\text{CI,DAV})$, number of symmetry adapted functions used and total CSF's generated, the c^2 of the ground state configuration, the Σc^2 , E_B , E_R , and the bond dissociation energy ΔE {calculated from E_R at equilibrium distance $R_{\text{CN}} = 3.0$ bohrs, E_R [based on $E(\text{CI,EX})$] - $E_{\text{free molecule}}$ at $R_{\text{CN}} = 10.0$ bohrs from $E(\text{CI,EX})$ } in a.u. and in kcal/mole as a function of variously placed voids in the nitromethanes in the multipole field. Here the ΔE is defined as indicated above.

In Table III-3 are presented the $E(\text{SCF})$, $E(\text{CI})$, $E(\text{CI,EX})$, $E(\text{CI,DAV})$ number of symmetry adapted functions used and total CSF's generated, the c^2 of the ground state configuration, the Σc^2 , E_B , E_R , and the bond dissociation energy ΔE in a.u. and in kcal/mole as a function of variously placed voids in the nitromethanes in the multipole field. Here the ΔE is defined as

$$\Delta E = E(\text{CI,EX}; R_{\text{CN}} = 3.0 \text{ bohrs}) - E(\text{CI,EX}; R_{\text{CN}} = 5.6 \text{ bohrs}) \quad \text{III-5}$$

In Table III-4 are presented the $E(\text{SCF})$, $E(\text{CI})$, $E(\text{CI,EX})$, $E(\text{CI,DAV})$, number of symmetry adapted functions used and total CSF's generated, the c^2 of the ground state configuration, the Σc^2 , E_B , E_R , and the bond dissociation energy ΔE {calculated from E_R at equilibrium distance $R_{\text{CN}} = 3.0$ bohrs, E_R [based on $E(\text{CI,EX})$] - $E_{\text{free molecule}}$ at $R_{\text{CN}} = 10.0$ bohrs from $E(\text{CI,EX})$ } in a.u. and in kcal/mole as function of variously placed voids in the nitromethanes treated explicitly in the SCF. Here ΔE is defined as

$$\Delta E = E(\text{CI,EX}; R_{\text{CN}} = 3.0 \text{ bohrs}) - E_B - E(\text{CI,EX}; \text{free molecule}, R_{\text{CN}} = 10.0 \text{ bohrs}) \quad \text{III-6}$$

In Table III-5 are presented the $E(\text{SCF})$, $E(\text{CI})$, $E(\text{CI,EX})$, $E(\text{CI,DAV})$ number of symmetry adapted functions used and total CSF's generated, the c^2 of the ground state configuration, the Σc^2 , E_B , E_R , and the bond dissociation energy ΔE as a function of variously placed voids in the nitromethanes treated explicitly in the SCF. ΔE is defined as

$$\Delta E = E(\text{CI,EX}; R_{\text{CN}} = 3.0 \text{ bohrs}) - E(\text{CI,EX}; R_{\text{CN}} = 5.6 \text{ bohrs}) \quad \text{III-7}$$

In Table III-6 are presented the $E(\text{SCF})$, $E(\text{CI,EX})$, $E(\text{CI,DAV})$, number of symmetry adapted functions used and total CSF's generated, the c^2 of the ground state configuration, the Σc^2 , E_B , E_R and the bond dissociation energy ΔE {calculated from E_R at the equilibrium distance $R_{\text{CN}} = 3.0$ bohrs, E_R [based on $E(\text{EX,CI})$] - $E_{\text{free molecule}}$ at $R_{\text{CN}} = 10.0$ bohrs} in a.u. and in kcal/mole as a function of variously placed voids both in the explicit nitromethanes treated in the SCF and in the nitromethanes treated as multipoles in the surrounding environment.

Here ΔE is defined as in equation III-6.

In Table III-7 are presented the $E(\text{SCF})$, $E(\text{CI,EX})$, $E(\text{CI,DAV})$, number of symmetry adapted functions used and total CSF's generated, the c^2 of the ground state configuration, the Σc^2 , E_B , E_R and the bond dissociation energy ΔE in a.u. and in kcal/mole as a function of variously placed voids both in the explicit nitromethanes treated in the SCF and in the nitromethanes treated as multipoles in the surrounding environment.

Here ΔE is defined as in equation III-5.

Tables III-8 and III-9 present a summary of the calculated $\text{H}_3\text{C} - \text{NO}_2$ bond dissociation energies in the full extended cluster representation of the nitromethane crystal with variously placed voids in the nitromethane molecules represented by multipoles and/or in the nitromethane molecules treated explicitly in the SCF.

Examination of Tables III-8 and III-9 indicates that in the large majority of cases where there are voids in the nitromethanes represented by multipoles or in the nitromethanes treated explicitly in the SCF, the calculated bond dissociation energies are somewhat smaller than in the case of a full extended cluster representation of the nitromethane crystal (5 nitromethanes treated explicitly in the SCF in the multipole field of 8 additional nitromethane molecules where the arrangement of the molecules is as it is in the crystal structure). There are a few cases of voids where the calculated bond dissociation energies are a little larger than in the case of the full extended cluster representation of the nitromethane crystal. The effect of voids in the calculated bond dissociation energies has a dependence on the position of the voids as well as on the numbers and types of the voids. In all cases where there are voids in both the

nitromethanes represented by multipoles and the nitromethanes treated explicitly, the calculated $\text{H}_3\text{C} - \text{NO}_2$ bond dissociation energies are less than for the case of a full extended cluster representation of the nitromethane crystal.

To investigate more extensively the question of the effect of voids we are in the process of extending the implementation of this method to include hundreds of multipole molecules properly located as in the crystal environment.

The major thrust of this present study and our previous one last year was to ascertain the relative energies for breaking the $\text{H}_3\text{C} - \text{NO}_2$ bond under various crystal conditions (different representations of the crystal, voids, etc.) compared to breaking the $\text{H}_3\text{C} - \text{NO}_2$ bond in a nitromethane in an isolated molecule. All of the results in the previous year and this present research indicate it will take more energy to break the $\text{H}_3\text{C} - \text{NO}_2$ bond when the molecule is in a nitromethane crystal. To calculate accurate absolute bond dissociation energies for these various cases would merely require larger basis sets, more configurations for correlation in the MRD-CI wave functions and zero point energy corrections. However, based on our experience with other comparison larger and smaller MRD-CI calculations, the overall relative energies are expected to remain very similar.

Moreover, our method is completely general and the effect of impurities, dopants, etc. in the molecules treated explicitly or in the multipole field can be studied in the same manner as we have studied the problem including voids. In the computers used in the present study the limitation on available CPU size for a run was several million words. In computers such as the CRAY II several hundred million words are available and the newer computers are scheduled to have gigawords of memory. Our method is well suited to take advantage of these large memories since we will be able to handle both more molecules explicitly in the SCF and MRD-CI and also to handle much larger molecules and molecular systems. Most of the energetic compounds of interest are polynitrosubstituted {heterocyclics, polyheterocyclics or polyhedranes}, often with as many as eight large molecules per unit cell.

To understand and predict the initiation of dissociation in energetic molecules in crystals or solids requires a knowledge of the bond dissociation energy of the molecule in a crystal or other solid environment. At present the only experimental bond dissociation energy data available at best for such systems is experimental gas phase thermochemical data for isolated molecules or theoretical calculated data for isolated molecules and this is what is being used. Our results have demonstrated the need for multireference calculations (MRD-CI). We have shown conclusively that it will take a significantly amount more energy to dissociate the bond in the molecule when the molecule is in a crystal. We have also shown the effects of voids in the crystal on the calculated bond dissociation energies.

Figure III-1

THE CLUSTER OF 5 NITROMETHANES
FROM EXTENDED CLUSTER

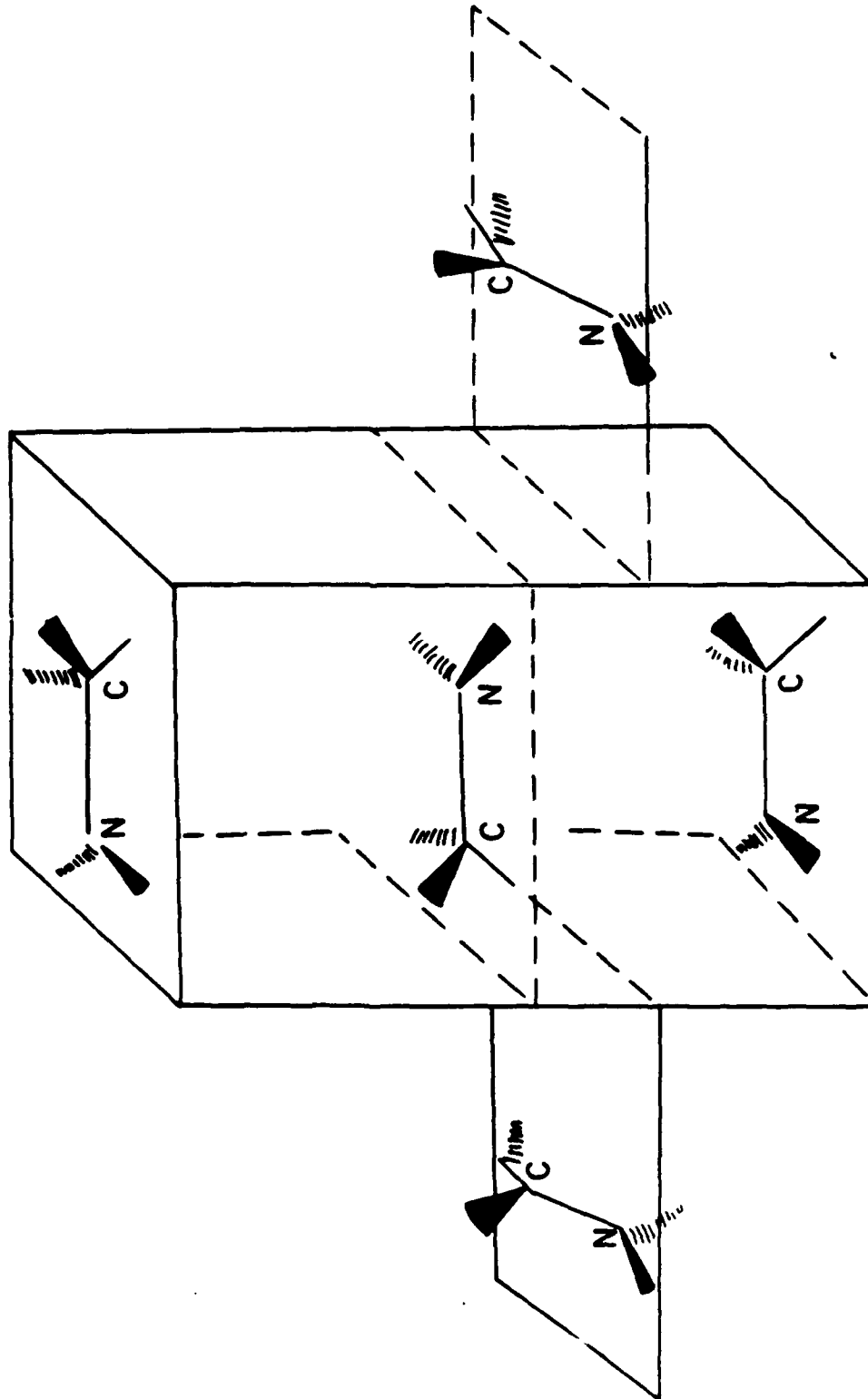


Table III-1. NITROMETHANE EXTENDED CLUSTER
CELL/CLASS DESIGNATIONS

CENTRAL MOLECULE	555	a
EXPLICIT MOLECULES		
	554	b
	555	b
	555	d
	645	d
MULTIPOLE MOLECULES		
	455	a
	655	a
	456	c
	556	c
	546	c
	446	c
	545	d
	655	d

Table III-2. Nitromethane $R_{CN} = 3.0$ bohrs MRD-CI Ab-Initio MODPOT/VRDDO

Energies (a.u.), SAF's, c^2 and Bond Dissociation Energies as a Function of Nitromethane Multipoles Removed

CELL	455	655	456	556	446	545	655
CLASS	a	a	c	c	c	d	d
SCF	-240.251793	-240.251996	-240.250395	-240.254662	-240.251472	-240.251548	-240.251050
CI	-240.486628	-240.483295	-240.484733	-240.486943	-240.486673	-240.486737	-240.486034
# CSF's	692	692	698	695	699	696	703
CI(EX)	-240.499872	-240.500806	-240.498186	-240.500330	-240.500582	-240.500255	-240.499584
CI(DAV)	-240.510863	-240.511940	-240.509153	-240.511434	-240.511895	-240.511464	-240.510653
total # SAF's generated	39946	39946	39946	39946	39946	39946	39946
c^2 gs	0.864688	0.863744	0.865230	0.864257	0.863186	0.863798	0.864321
Σc^2	0.926472	0.925793	0.926648	0.925933	0.924954	0.925452	0.926202
E_B	-192.184232	-192.186074	-192.179784	-192.186489	-192.180357	-192.180996	-192.183949
E_R	-48.315640	-48.314732	-48.318402	-48.313841	-48.319586	-48.319304	-48.315635
ΔE (a.u.)	-0.089224	-0.088316	-0.091986	-0.087425	-0.093170	-0.092888	-0.089219
ΔE (kcal/mol)	-55.989	-55.420	-57.723	-54.861	-58.466	-58.289	-55.986

Start with cluster of five nitromethanes with eight more molecules represented by multipoles. Remove one multipole molecule from the cluster at a time. The removed molecule is identified by its unit cell designation and its class. E_B is the SCF energy of the cluster with the multipole and the central molecule removed.

Definition ΔE see equation III-6
 gs - ground state configuration

Table III-3. Nitromethane $R_{CN} = 5.6$ bohrs MRD-CI Ab-Initio MDDPOT/VRDDO

Energies (a.u.), SAF's, c^2 and Bond Dissociation Energies as a Function of Nitromethane Multipoles Removed

CELL	455	655	456	556	546	446	545	655
CLASS	a	a	c	c	c	c	d	d
SCF	-240.098879	-240.097627	-240.099541	-240.102722	-240.098535	-240.105752	-240.097944	-240.100517
CI	-240.373366	-240.375685	-240.370092	-240.376060	-240.372490	-240.375226	-240.371153	-240.373132
# CSF's	718	718	717	719	716	713	714	715
CI(EX)	-240.394765	-240.399742	-240.389730	-240.397047	-240.393816	-240.394529	-240.391450	-240.393642
CI(DAV)	-240.425837	-240.432228	-240.419837	-240.427777	-240.424819	-240.424401	-240.421977	-240.424403
total # SAF's generated	39946	39946	39946	39946	39946	39946	39946	39946
c^2 gs	0.742675	0.733434	0.750433	0.745251	0.743036	0.752758	0.745489	0.747433
Σc^2	0.843315	0.839748	0.845247	0.844242	0.843324	0.845765	0.844583	0.844408
E_B	-192.184232	-192.186074	-192.179784	-192.186489	-192.180357	-192.180996	-192.180951	-192.183949
E_R	-48.210533	-48.213668	-48.209946	-48.210516	-48.213439	-48.213533	-48.210499	-48.209693
ΔE (a.u.)	-0.105017	-0.101064	-0.108456	-0.103283	-0.106845	-0.106053	-0.108805	-0.105942
ΔE (kcal/mol)	-65.956	-63.419	-68.058	-64.812	-67.047	-66.550	-68.277	-66.480

Start with cluster of five nitromethanes with eight more molecules represented by multipoles. Remove one multipole molecule from the cluster at a time. The removed molecule is identified by its unit cell designation and its class. E_B is the SCF energy of the cluster with the multipole and the central molecule removed.

Definition ΔE see equation III-6
gs - ground state configuration

Table III-4. Nitromethane $R_{CN} = 3.0$ bohrs MRD-CI Ab-Initio MODPOT/VRDDO

Energies(a.u.), SAF's, c^2 and Bond Dissociation Energies as a Function of Explicit Nitromethane Molecules Removed

CELL	554	555	555	645
CLASS	b	b	d	d
SCF	-192.207008	-192.205536	-192.206949	-192.204170
CI	-192.442648	-192.441224	-192.441907	-192.439280
# CSF's	690	696	696	694
CI(EX)	-192.455855	-192.454880	-192.455454	-192.452659
CI(DAV)	-192.466895	-192.466016	-192.466515	-192.463700
total # SAF's generated	39946	39946	39946	39946
c^2 gs	0.864048	0.863694	0.964270	0.864374
Σc^2	0.926267	0.925906	0.926200	0.926270
E_B	-144.142527	-144.140904	-144.137635	-144.136290
E_R	-48.313328	-48.313976	-48.317819	-48.316369
ΔE (a.u.)	-0.086912	-0.087560	-0.091403	-0.089953
ΔE (kcal/mol)	-54.539	-54.945	-57.357	-56.447

Start with cluster of five nitromethanes with eight more molecules represented by multipoles. Remove one explicit molecule from the cluster at a time. The removed molecule is identified by its unit cell designation and its class. E_B is the SCF energy of the cluster with the explicit molecule and the central molecule removed.

Definition ΔE see equation III-6
gs - ground state configuration

Table III-5. Nitromethane $R_{CN} = 5.6$ bohrs MRD-CI Ab-Initio MODPOT/VRDDO

Energies (a.u.), SAF's, c^2 and Bond Dissociation Energies as a Function of Explicit Nitromethane Molecules Removed

CELL	554	555	555	555	645
CLASS	b	b	d	d	d
SCF	-192.051508	-192.050497	-192.054641	-192.058596	
CI	-192.332210	-192.330648	-192.336979	-192.337244	
# CSF's	718	716	718	719	
CI(EX)	-192.357786	-192.355887	-192.362196	-192.362842	
CI(DAV)	-192.390600	-192.388620	-192.395297	-192.395779	
total # SAF's generated	39946	39946	39946	39946	
c^2 gs	0.729102	0.729635	0.725562	0.731271	
Σc^2	0.840103	0.840063	0.839226	0.838922	
E_B	-144.142527	-144.140904	-144.137635	-144.136290	
E_R	-48.215259	-48.214983	-48.224561	-48.226552	
ΔE (a.u.)	-0.098069	-0.098993	-0.093258	-0.089817	
ΔE (kcal/mol)	-61.540	-62.120	-58.521	-56.362	

Start with cluster of five nitromethanes with eight more molecules represented by multipoles. Remove one explicit molecule from the cluster at a time. The removed molecule is identified by its unit cell designation and its class. E_B is the SCF energy of the cluster with the explicit molecule and the central molecule removed.

Definition ΔE see equation III-5
gs - ground state configuration

Table III-6. Nitromethane $R_{CN} = 3.0$ bohrs MRD-CI Ab-Initio MODPOT/VRD00

Energies (a.u.), SAF's, c^2 and Bond Dissociation Energies as a Function of Nitromethane Multipoles Removed

The explicit nitromethane molecule removed is 554 b in all cases.

Nitromethane Multipoles Removed

CELL	556	655	556 and 655
CLASS	c	d	c d
SCF	-192.207388	-192.202856	-192.203131
CI	-192.443188	-192.438904	-192.439355
# CSF's	687	695	694
CI(EX)	-192.456769	-192.452262	-192.453070
CI(DAV)	-192.467922	-192.463377	-192.464301
total # SAF's generated	39946	39946	39946
c^2 gs	0.863285	0.863492	0.862841
Σc^2	0.925753	0.925983	0.925453
E_B	-144.144193	-144.140796	-144.142439
E_R	-48.312576	-48.311466	-48.310631
ΔE (a.u.)	-0.086160	-0.085050	-0.084215
ΔE (kcal/mol)	-54.067	-53.370	-52.846

Start with cluster of five nitromethanes with eight more molecules represented by multipoles. Remove one explicit molecule and either one or two multipole molecules from the cluster at a time. Each removed molecule is identified by its unit cell designation and its class. E_B is the SCF energy of the cluster with the explicit molecule, the multipole molecules and the central molecule removed.

Definition ΔE see equation III-6

Table III-7. Nitromethane $R_{CN} = 5.6$ bohrs MRD-CI Ab-Initio MODPOT/VRDDO

Energies (a.u.), SAF's, c^2 and Bond Dissociation Energies as a Function of Nitromethane Multipoles Removed

The explicit nitromethane molecule removed is 554 b in all cases.

Nitromethane Multipoles Removed

CELL	556	655	556 and 655
CLASS	c	d	c d
SCF	-192.052125	-192.048888	-192.049414
CI	-192.370888	-192.329568	-192.330443
# CSF's	790	717	717
CI(EX)	-192.361586	-192.354523	-192.355384
CI(DAV)	-192.386298	-192.387267	-192.388062
total # SAF's generated	52507	33946	33946
c^2 gs	0.69235933	0.73050592	0.73020441
Σc^2	0.88558098	0.84018197	0.84047878
E_B	-144.144193	-144.140796	-144.142439
E_R	-48.217393	-48.213727	-48.212945
ΔE (a.u.)	-0.095183	-0.097739	-0.097686
ΔE (kcal/mol)	-59.727	-61.357	-61.300

Start with cluster of five nitromethanes with eight more molecules represented by multipoles. Remove one explicit molecule and either one or two multipole molecules from the cluster at a time. Each removed molecule is identified by its unit cell designation and its class. E_B is the SCF energy of the cluster with the explicit molecule, the multipole molecules and the central molecule removed.

Definition ΔE see equation III-6

Table III-8. Summary of $H_3C - NO_2$ Bond Dissociation Energies (kcal/mol) in Nitromethane in Nitromethane Crystal as a Function of Voids in the 5 Nitromethane Molecules Treated Explicitly in SCF and/or in the Nitromethane Molecules Treated as Multipoles [Based on ΔE using E_R from $R_{CN} = 3.0$ bohrs - $R_{CN}(\text{free molecule}) = 10.0$ bohrs]

Bond Dissociation Energy (kcal/mol)				
no voids				-57.090
Voids in Multipoles		Voids in Molecules Treated Explicitly		ΔE (Bond Dissociation Energy kcal/mol)
Cell	Class	Cell	Class	
455	a			-55.989
655	a			-54.420
456	c			-57.723
556	c			-54.861
546	c			-58.916
446	c			-58.466
545	d			-58.289
655	d			-55.986
		554	b	-54.539
		555	b	-54.945
		555	d	-57.357
		645	d	-56.447
556	c	554	b	-54.067
655	d	554	b	-53.370
556	c	554	b	-52.846
655	d			
Free Molecule				-49.340

Table III-9. Summary of $H_3C - NO_2$ Bond Dissociation Energies (kcal/mol) in Nitromethane in Nitromethane Crystal as a Function of Voids in the 5 Nitromethane Molecules Treated Explicitly in the SCF and/or in the Nitromethane molecule treated as Multipoles [Based on $\Delta E(CI,EX; R = 3.0 \text{ bohrs} - E(CI,EX; R = 5.6 \text{ bohrs})]$

Bond Dissociation Energy (kcal/mol)				
no voids				-67.132
Voids in Multipoles		Voids in Molecules Treated Explicitly		ΔE (Bond Dissociation Energy kcal/mol)
Cell	Class	Cell	Class	
455	a			-65.956
655	a			-63.419
456	c			-68.058
556	c			-64.812
546	c			-67.047
446	c			-66.550
545	d			-68.277
655	d			-66.480
		554	b	-61.540
		555	b	-62.120
		555	d	-58.521
		645	d	-56.362
556	c	554	b	-59.729
655	d	554	b	-61.333
556	c	554	b	-61.300
655	d			
Free Molecule				-42.310

C. Calculations Carried Out for Dimethylnitramine

As a prototype for breaking $>N - NO_2$ bonds we initiated MRD-CI calculations for breaking the $Me_2N - NO_2$ bond in dimethylnitramine.

We first carried out the MRD-CI calculations for the $Me_2N - NO_2$ dissociation of the isolated molecule from 2.40 to 7.00 bohrs from a crystal structure geometry [B. Krebs, J. Mandt, R. E. Cobbledick and R. W. H. Small, Acta Cryst. B35, 402-404 (1979)] stretched about the bond midpoint. The equilibrium $Me_2N - NO_2$ bond distance was found at 3.00 bohrs. A very large number of reference configurations was found to be necessary along the dissociation pathway. The lowest 3 roots were extracted from the MRD-CI Hamiltonian matrix. $E_{(CI,EX)}$ energies vs. $Me_2N - NO_2$ distances are plotted in Figure III-2 for root 1, root 2 and root 3. It can be seen that there is an avoided crossing of roots 2 and 3. This avoided crossing is verified by examination of the coefficients of the various SAF's. In Tables III-10 to III-16 are tabulated the Energies (a.u.), SAF's, $\sum c^2$ and c^2 of the major SAF contributions to roots 1, 2, and 3 at N-N distances from 2.40 bohrs to 4.40 bohrs. In Tables III-17 to III-19 are tabulated the same quantities for Root 1 at 5.60, 6.20 and 7.00 bohrs. The contributions of all SAF's with $c^2 > 0.005$ are listed in the tables. It can be seen from the c^2 of the contributions of the various SAF's that even at the ground state equilibrium geometry 3.00 bohrs, Table III-13, the wave function of dimethylnitramine is not describable as a single determinant. The c^2 of the SCF wave function is only 0.864. There are other contributions which are identified in the Tables by the types of their excitations. Our dissociation energy of the $Me_2N - NO_2$ bond calculated as follows [$E_{(CI,EX)7.00 \text{ bohrs}} - E_{(CI,EX)3.00 \text{ bohrs}}$] = -54.66 kcal/mole] compares closely with the estimated BAC dissociation energy of Melius, 47.2 kcal/mole. {The BAC-MP4 method of Melius [C.F. Melius and J.S. Binkley, "Thermochemistry of the Decomposition of Nitramines in the Gas Phase," Twenty-first Symposium (International on Combustion) The Combustion Institute, 1986, pp 1953-1963] calculates single determinant unrestricted Hartree-Fock (UHF) SCF wavefunctions followed by MP4 corrections. For molecular systems which are UHF unstable (molecular configurations which contain significant biradical character Melius adds 104.65 kcal/mole.)}

In Table III-20, our calculated excitation energies are tabulated: root 1 + 2, root 1 + 3, root 2 + 3.

We are now carrying out preliminary MRD-CI calculations for breaking the $Me_2N - NO_2$ bond in a dimethylnitramine crystal.

Figure III-2

DIMETHYLNITRAMINE $\text{Me}_2\text{N-NO}_2$ ISOLATED MOLECULE
MRD-CI ENERGIES (Extrapolated) (a.u.) vs. $R_{\text{N-N}}$ (bohrs)
Ab-Initio MODPOT/VRDDO

C root 3
B root 2
A root 1

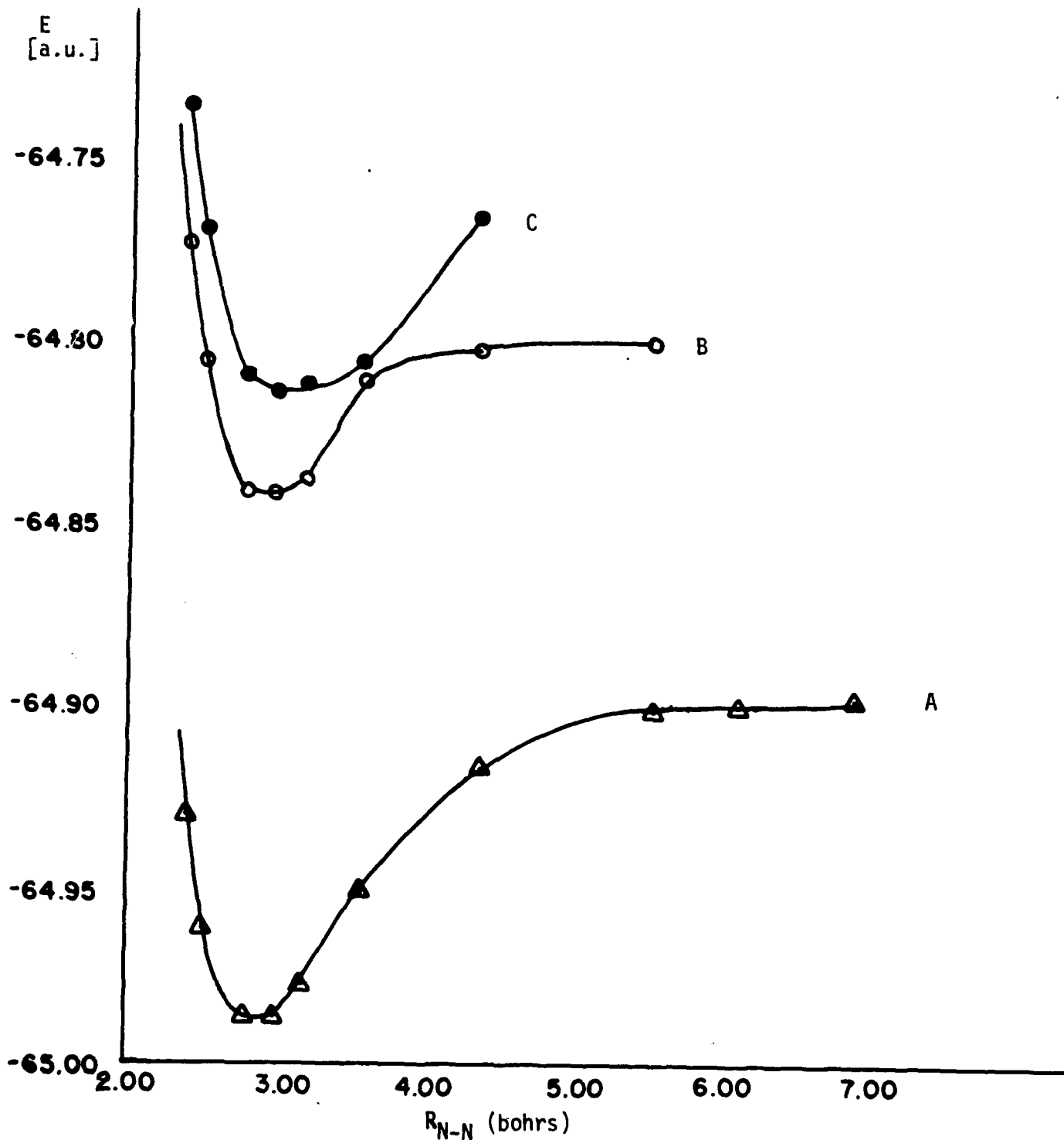


TABLE III-11

ENERGIES (a.u.), SAFs, $\sum c^2$, MAJOR CONTRIBUTIONS AS A FUNCTION OF Me₂N - NO₂ DISTANCE (bohrs)

R_{NN} = 2.51 bohrs

139073 SAFs generated

SCF	root 1	root 2	root 3
	-64.720672	-64.790015	-64.753006
CI (2741)	-64.950080	-64.807646	-64.771392
CI ^{EX}	-64.962207	-64.826409	-64.793668
CI ^{DAV}	-64.982531		
$\sum c^2$	0.9018838	0.8987052	0.8836967
0.8742	scf	kp ₀₁ + n ₁ n ₂ o ₁ o ₂ *	0.2510 kp ₀₂ ' + n ₁ n ₂ o ₁ o ₂ *
0.0608	n ₂ o ₂ ,n ₂ o ₂ ' + n ₁ n ₂ o ₁ o ₂ *	kp ₀₂ + n ₁ n ₂ o ₁ o ₂ *	0.2446 kp ₀₁ ' + n ₁ n ₂ o ₁ o ₂ *
0.0607	n ₂ o ₁ ,n ₂ o ₁ ' + n ₁ n ₂ o ₁ o ₂ *	kp ₀₁ ' + n ₁ n ₂ o ₁ o ₂ *	0.1251 kp ₀₂ + n ₁ n ₂ o ₁ o ₂ *
		kp ₀₂ ' + n ₁ n ₂ o ₁ o ₂ *	0.1147 kp ₀₁ + n ₁ n ₂ o ₁ o ₂ *
		n ₂ o ₂ ' + n ₁ n ₂ o ₁ o ₂ *	0.0558 n ₁ n ₂ + n ₁ n ₂ o ₁ o ₂ *
		n ₂ o ₂ + n ₁ n ₂ o ₁ o ₂ *	0.0065 n ₂ o ₂ + n ₁ n ₂ o ₁ o ₂ *
		n ₂ o ₁ + n ₁ n ₂ o ₁ o ₂ *	0.0065 n ₂ o ₂ ' + n ₁ n ₂ o ₁ o ₂ *
		n ₂ o ₁ ' + n ₁ n ₂ o ₁ o ₂ *	0.0074 n ₂ o ₁ ' + n ₁ n ₂ o ₁ o ₂ *
		kp ₀₂ ,n ₂ o ₂ + n ₁ n ₂ o ₁ o ₂ *	0.0074 n ₂ o ₁ + n ₁ n ₂ o ₁ o ₂ *
		kp ₀₂ ,n ₂ o ₂ ' + n ₁ n ₂ o ₁ o ₂ *	0.0060 kp ₀₂ ,n ₂ o ₂ + n ₁ n ₂ o ₁ o ₂ *
		kp ₀₁ ,n ₂ o ₁ + n ₁ n ₂ o ₁ o ₂ *	0.0060 kp ₀₂ ,n ₂ o ₂ ' + n ₁ n ₂ o ₁ o ₂ *
		kp ₀₁ ,n ₂ o ₁ ' + n ₁ n ₂ o ₁ o ₂ *	0.0057 kp ₀₁ ,n ₂ o ₁ + n ₁ n ₂ o ₁ o ₂ *
		kp ₀₂ ',n ₂ o ₂ + n ₁ n ₂ o ₁ o ₂ *	0.0057 kp ₀₁ ,n ₂ o ₁ ' + n ₁ n ₂ o ₁ o ₂ *
		kp ₀₂ ',n ₂ o ₂ ' + n ₁ n ₂ o ₁ o ₂ *	0.0090 kp ₀₂ ',n ₂ o ₂ + n ₁ n ₂ o ₁ o ₂ *
		kp ₀₁ ',n ₂ o ₁ + n ₁ n ₂ o ₁ o ₂ *	0.0090 kp ₀₂ ',n ₂ o ₂ ' + n ₁ n ₂ o ₁ o ₂ *
		kp ₀₁ ',n ₂ o ₁ ' + n ₁ n ₂ o ₁ o ₂ *	0.0087 kp ₀₁ ',n ₂ o ₁ + n ₁ n ₂ o ₁ o ₂ *
			0.0087 kp ₀₁ ',n ₂ o ₁ ' + n ₁ n ₂ o ₁ o ₂ *

TABLE III-13

ENERGIES (a.u.), SAFs, $\sum c^2$, MAJOR CONTRIBUTIONS AS A FUNCTION OF Me₂N - NO₂ DISTANCE (bohrs)

R_{NN} = 3.00 bohrs

134858 SAFs generated

	root 1	root 2	root 3
SCF	-64.732545	-64.825706	-64.798026
CI (2962)	-64.979182	-64.842791	-64.815684
CI ^{EX}	-64.987170	-64.870837	-64.842860
CI ^{DAV}	-65.008358		
$\sum c^2$	0.9001621	0.8758028	0.8745300
0.8630	scf	kpz + n ₁ n ₂ o ₁ o ₂ *	kpz' + n ₁ n ₂ o ₁ o ₂ *
0.0112	(n ₁ n ₂) ² + (n ₁ n ₂ *) ²	kpz	kpz'
0.0063	n ₂ o ₁ ,n ₂ o ₁ ' + n ₁ n ₂ o ₁ o ₂ *	kpz'	kpz'
0.0062	n ₂ o ₂ ,n ₂ o ₂ ' + n ₁ n ₂ o ₁ o ₂ *	kpz'	n ₁ n ₂
		kpz'	kpz
		kpz',n ₂ o ₂ + n ₁ n ₂ o ₁ o ₂ *	kpz
		kpz',n ₂ o ₂ ' + n ₁ n ₂ o ₁ o ₂ *	n ₂ o ₁
		kpz',n ₂ o ₁ + n ₁ n ₂ o ₁ o ₂ *	n ₂ o ₁ '
		kpz',n ₂ o ₁ ' + n ₁ n ₂ o ₁ o ₂ *	n ₂ o ₂
		kpz',n ₂ o ₂ + n ₁ n ₂ o ₁ o ₂ *	n ₂ o ₂
		kpz',n ₂ o ₂ ' + n ₁ n ₂ o ₁ o ₂ *	n ₂ o ₂
		(n ₁ n ₂) ²	(n ₁ n ₂) ²
		kpz',n ₂ o ₂ + n ₁ n ₂ o ₁ o ₂ *	kpz',n ₂ o ₂ + n ₁ n ₂ o ₁ o ₂ *
		kpz',n ₂ o ₂ ' + n ₁ n ₂ o ₁ o ₂ *	kpz',n ₂ o ₂ ' + n ₁ n ₂ o ₁ o ₂ *
		kpz',n ₂ o ₁ + n ₁ n ₂ o ₁ o ₂ *	kpz',n ₂ o ₁ + n ₁ n ₂ o ₁ o ₂ *
		kpz',n ₂ o ₁ ' + n ₁ n ₂ o ₁ o ₂ *	kpz',n ₂ o ₁ ' + n ₁ n ₂ o ₁ o ₂ *
		kpz',n ₂ o ₂ + n ₁ n ₂ o ₁ o ₂ *	kpz',n ₂ o ₂ + n ₁ n ₂ o ₁ o ₂ *
		kpz',n ₂ o ₂ ' + n ₁ n ₂ o ₁ o ₂ *	kpz',n ₂ o ₂ ' + n ₁ n ₂ o ₁ o ₂ *

TABLE III-14

ENERGIES (a.u.), SAFs, $\sum c^2$, MAJOR CONTRIBUTIONS AS A FUNCTION OF Me₂N - NO₂ DISTANCE (bohrs) $R_{NN} = 3.20$ bohrs

134858 SAFs generated

	root 1	root 2	root 3
SCF	-64.716834	-64.819525	-64.795543
CI (3036)	-64.970002	-64.836944	-64.813635
CI ^{EX}	-65.001187	-64.856988	-64.836850
CI ^{DAV}	0.8975205	0.8947545	0.8835092
$\sum c^2$	0.8534	0.2524	0.2180
	(n ₁ n ₂) ²	kp ₀₁ + n ₁ n ₂ o ₁ o ₂ *	kp ₀₂ ' + n ₁ n ₂ o ₁ o ₂ *
	0.1568	(n ₁ n ₂ *) ²	kp ₀₁ ' + n ₁ n ₂ o ₁ o ₂ *
	0.0061	n ₂ o ₂ , n ₂ o ₂ ' + n ₁ n ₂ o ₁ o ₂ *	n ₁ n ₂ + n ₁ n ₂ o ₁ o ₂ *
	0.0061	n ₂ o ₁ , n ₂ o ₁ ' + n ₁ n ₂ o ₁ o ₂ *	kp ₀₂ + n ₁ n ₂ o ₁ o ₂ *
		0.0070	kp ₀₁ + n ₁ n ₂ o ₁ o ₂ *
		0.0070	kp ₀₂ , n ₂ o ₂ + n ₁ n ₂ o ₁ o ₂ *
		0.0070	kp ₀₂ , n ₂ o ₂ ' + n ₁ n ₂ o ₁ o ₂ *
		0.0076	kp ₀₁ , n ₂ o ₁ + n ₁ n ₂ o ₁ o ₂ *
		0.0076	kp ₀₁ , n ₂ o ₁ ' + n ₁ n ₂ o ₁ o ₂ *
		0.0063	kp ₀₁ ', n ₂ o ₁ + n ₁ n ₂ o ₁ o ₂ *
		0.0063	kp ₀₁ ', n ₂ o ₁ ' + n ₁ n ₂ o ₁ o ₂ *
		0.0057	kp ₀₂ ', n ₂ o ₂ + n ₁ n ₂ o ₁ o ₂ *
		0.0057	kp ₀₂ ', n ₂ o ₂ ' + n ₁ n ₂ o ₁ o ₂ *
			(n ₁ n ₂) ² + n ₁ n ₂ *, n ₁ n ₂ o ₁ o ₂ *
		0.0082	kp ₀₂ ', n ₂ o ₂ + n ₁ n ₂ o ₁ o ₂ *
		0.0082	kp ₀₂ ', n ₂ o ₂ ' + n ₁ n ₂ o ₁ o ₂ *
		0.0076	kp ₀₁ ', n ₂ o ₁ + n ₁ n ₂ o ₁ o ₂ *
		0.0076	kp ₀₁ ', n ₂ o ₁ ' + n ₁ n ₂ o ₁ o ₂ *
		0.0050	kp ₀₂ , n ₂ o ₂ + n ₁ n ₂ o ₁ o ₂ *
		0.0050	kp ₀₂ , n ₂ o ₂ ' + n ₁ n ₂ o ₁ o ₂ *
		0.0069	kp ₀₂ , n ₁ n ₂ + n ₁ n ₂ *, n ₁ n ₂ o ₁ o ₂ *
		0.0067	kp ₀₁ ', n ₁ n ₂ + n ₁ n ₂ *, n ₁ n ₂ o ₁ o ₂ *

TABLE III-15 DIMETHYLNITRAMINE ISOLATED MOLECULE MRD-CI Ab-Initio MODPOT/VRDDO
 ENERGIES (a.u.), SAFs, $\sum c^2$, MAJOR CONTRIBUTIONS AS A FUNCTION OF Me₂N - NO₂ DISTANCE (bohrs)

R_{NN} = 3.60 bohrs

134858 SAFs generated

	root 1	root 2	root 3
SCF	-64.675560		
CI (3333)	-64.943190	-64.793257	-64.786242
CI _{EX}	-64.953368	-64.811549	-64.806180
CI _{DAV}	-64.977697	-64.833989	-64.831118
$\sum c^2$	0.8909997	0.8870427	0.8805038
0.8249	scf	kp ₀₁ + n ₁ n ₂ o ₁ o ₂ *	0.2247 n ₁ n ₂ + n ₁ n ₂ o ₁ o ₂ *
0.0300	(n ₁ n ₂) ² + (n ₁ n ₂ *) ²	kp ₀₂ + n ₁ n ₂ o ₁ o ₂ *	0.1954 kp ₀₂ ' + n ₁ n ₂ o ₁ o ₂ *
0.0057	n ₂ o ₁ , n ₂ o ₁ ' + n ₁ n ₂ o ₁ o ₂ *	kp ₀₁ ' + n ₁ n ₂ o ₁ o ₂ *	0.1411 kp ₀₁ ' + n ₁ n ₂ o ₁ o ₂ *
0.0057	n ₂ o ₂ , n ₂ o ₂ ' + n ₁ n ₂ o ₁ o ₂ *	kp ₀₂ ' + n ₁ n ₂ o ₁ o ₂ *	0.0806 kp ₀₂ + n ₁ n ₂ o ₁ o ₂ *
		kp ₀₁ + n ₁ n ₂ o ₁ o ₂ *	0.0409 kp ₀₁ ' + n ₁ n ₂ o ₁ o ₂ *
	(n ₁ n ₂) ² + (n ₁ n ₂ *) ²		0.0127 n ₂ o ₁ + n ₁ n ₂ o ₁ o ₂ *
0.0071	kp ₀₂ ' + n ₁ n ₂ o ₁ o ₂ *		0.0127 n ₂ o ₁ ' + n ₁ n ₂ o ₁ o ₂ *
	(n ₁ n ₂) ² + (n ₁ n ₂ *) ²		0.0103 n ₂ o ₂ + n ₁ n ₂ o ₁ o ₂ *
0.0066	kp ₀₁ ' + n ₁ n ₂ o ₁ o ₂ *		0.0102 n ₂ o ₂ ' + n ₁ n ₂ o ₁ o ₂ *
	(n ₁ n ₂) ² + (n ₁ n ₂ *) ²		0.0356 (n ₁ n ₂) ² + n ₁ n ₂ *, n ₁ n ₂ o ₁ o ₂ *
0.0073	kp ₀₁ , n ₂ o ₁ + n ₁ n ₂ o ₁ o ₂ *		0.0071 kp ₀₂ ', n ₂ o ₂ + n ₁ n ₂ o ₁ o ₂ *
0.0073	kp ₀₁ , n ₂ o ₁ ' + n ₁ n ₂ o ₁ o ₂ *		0.0071 kp ₀₂ ', n ₂ o ₂ ' + n ₁ n ₂ o ₁ o ₂ *
0.0067	kp ₀₁ ', n ₂ o ₁ + n ₁ n ₂ o ₁ o ₂ *		0.0052 kp ₀₁ ', n ₂ o ₁ + n ₁ n ₂ o ₁ o ₂ *
0.0067	kp ₀₁ ', n ₂ o ₁ ' + n ₁ n ₂ o ₁ o ₂ *		0.0052 kp ₀₁ ', n ₂ o ₁ ' + n ₁ n ₂ o ₁ o ₂ *
0.0057	kp ₀₂ , n ₂ o ₁ + n ₁ n ₂ o ₁ o ₂ *		0.0207 kp ₀₂ ', n ₁ n ₂ + n ₁ n ₂ o ₁ o ₂ *
0.0057	kp ₀₂ , n ₂ o ₁ ' + n ₁ n ₂ o ₁ o ₂ *		0.0197 kp ₀₁ ', n ₁ n ₂ + n ₁ n ₂ o ₁ o ₂ *
			0.0065 kp ₀₂ ', kp ₀₁ ' + n ₁ n ₂ *, n ₁ n ₂ o ₁ o ₂ *
			0.0053 kp ₀₂ ', n ₁ n ₂ + n ₁ n ₂ *, n ₁ n ₂ o ₁ o ₂ *

TABLE III-17

ENERGIES (a.u.), SAFs, $\sum c^2$, MAJOR CONTRIBUTIONS AS A FUNCTION OF $Me_2N - NO_2$ DISTANCE (bohrs)

$R_{NN} = 5.60$ bohrs

134858 SAF's generated		
SCF	-64.4939414	
	<u>root 1</u>	
CI (4548)	-64.889345	
CI EX	-64.902746	
CI DAV	-64.938242	
$\sum c^2$	0.8788997	scf
0.5379		
0.1860	$(n_1 n_2)^2 + (n_1 n_2^*)^2$	
0.0255	$n_1 n_2 + n_1 n_2^*$	
0.0283	$n_2 o_1', n_1 n_2' + n_1 n_2^*$	
0.0143	$n_2 o_1, n_1 n_2 + n_1 n_2^*$	
0.0087	$n_2 o_2, n_1 n_2' + n_1 n_2^*$	
0.0057	$n_2 o_2, n_1 n_2 + n_1 n_2^*$	

ENERGIES (a.u.), SAFs, $\sum c^2$, MAJOR CONTRIBUTIONS AS A FUNCTION OF $Me_2N - NO_2$ DISTANCE (bohrs)

$R_{NN} = 6.20$ bohrs

134858 SAFs generated

SCF -64.474679

root 1

CI (4771) -64.888953

CI^{EX} -64.900102

CI^{DAV} -64.935445

$\sum c^2$ 0.8682240

0.4921 scf

0.2207 $(n_1 n_2)^2 + (n_1 n_2^*)^2$

0.0319 $n_1 n_2 + n_1 n_2^*$

0.0327 $1p_{01}, n_1 n_2 + n_1 n_2^*$

0.0330 $1p_{02}, n_1 n_2 + n_1 n_2^*$

0.0063 $n_{201}, n_1 n_2 + n_1 n_2^*$

0.0062 $n_{201'}, n_1 n_2 + n_1 n_2^*$

0.0059 $n_{202}, n_1 n_2 + n_1 n_2^*$

0.0060 $n_{202'}, n_1 n_2 + n_1 n_2^*$

TABLE III-19

ENERGIES (a.u.), SAFs, $\sum c^2$, MAJOR CONTRIBUTIONS AS A FUNCTION OF Me₂N - NO₂ DISTANCE (bohrs)

R_{NN} = 7.00 bohrs

134858 SAFs generated

SCF -64.4746793

root 1

CI (4282) -64.881443

CI_{EX} -64.900055

CI_{DAV} -64.934694

$\sum c^2$ 0.8723250

0.4612 scf

0.2654 (n₁n₂)² + (n₁n₂^{*})²

0.0400 n₁n₂ + n₁n₂^{*}

0.0305 λ po₁' , n₁n₂ + n₁n₂^{*}

0.0300 λ po₂' , n₁n₂ + n₁n₂^{*}

0.0061 n₂o₁' , n₁n₂ + n₁n₂^{*}

0.0056 n₂o₂' , n₁n₂ + n₁n₂^{*}

TABLE 20

DIMETHYLNITRAMINE

ISOLATED MOLECULE

Extrapolated CI Dissociation Energies (D_e)

	Root 1				
D_e	[7.00 - 3.00]	-	0.0871 au	-	2.370 eV - 54.664 kcal
D_e	[5.60 - 3.00]	-	0.0844 au	-	2.298 eV - 52.975 kcal
D_e	[4.40 - 3.00]	-	0.0676 au	-	1.838 eV - 42.395 kcal

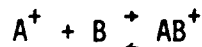
Excitation energies, r_e (3.00) of root 1:

root 1	+	root 2	-	0.144 au	-	3.929 eV	-	90.596 kcal
root 1	+	root 3	-	0.171 au	-	4.666 eV	-	107.606 kcal
root 2	+	root 3	-	0.0271 au	-	0.738 eV	-	17.009 kcal

IV. Ab-Initio Multireference Coupled Cluster and Multireference CI Calculations for Protonation NH_3 / Deprotonation NH_4^+

Protonation is the initiation step in cationic polymerization.

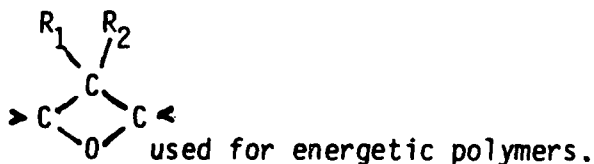
Protonation/deprotonation reactions of organic and most inorganic molecules are ion-molecule reactions of the type



where the ionization potential of A (the H atom; 13.6 eV) is higher than that of B. At the dissociation asymptote the separated pair $A^+ + B$ will be higher in energy than the separated pair $A + B^+$; thus even if $A^+ + B$ are both closed-shell ground state systems, a single determinant ab-initio SCF calculation will be neither a sufficient nor a proper description of the system. From the separated lowest energy pair $H(2S_g) + B^+(2Y_z)$ an open-shell singlet state and open-shell triplet state of symmetry $1,3Y_z$ will arise. If the symmetry $1Y_z$ is of the most symmetrical representation of B^+ the singlet state HB^+ that arises from the dissociation asymptote will be totally symmetric but the potential energy surface will not connect smoothly to the ground state singlet totally symmetric state at an equilibrium geometry.

However, the protonation energy of oxetane cannot be measured directly because the protonated ring opens. Our experimental colleague, Professor Walter S. Koski of the Johns Hopkins University, had earlier tried this experiment for us in this double tandem mass spectrometer.

Last year we had carried out ab-initio MRD-CI calculations on this protonation of an epoxide ring ($>C \begin{array}{c} \diagup \\ \diagdown \\ O \end{array} / C<$) the 3 member correlate of the 4-member oxetane ring



These results clearly showed the multideterminant character of the two potential energy surfaces for protonation and deprotonation.

The dissociation of NH_4^+ is of interest in the energetic field because the NH_4^+ ion occurs in energetic materials such as ammonium perchlorate. The ionization potential of NH_3 [NH_3^+ (\bar{X}^2A_1) 10.166 eV] is such that its protonation/deprotonation will behave as described above.

Thus to compare multireference coupled cluster (MR-CCM) results against multireference configuration interaction (MRD-CI) calculations we chose the system protonation NH_3 / deprotonation NH_4^+ which is well defined experimentally.

We have therefore carried out both multireference coupled cluster (MR-CCM) by the method of Kaldor [1] and multireference double excitation-configuration interaction (MRD-CI) calculations (by the method of Buenker and Peyerimhoff) [2] for the lowest singlet states and the lowest triplet state that arise from the separated pairs $\text{H}(^2S_g) + \text{NH}_3^+(\bar{X} \ ^2A_1)$ and $\text{H}^+(^1S_g) + \text{NH}_3^+(\bar{X} \ A_1)$.

The major advantage of the coupled cluster method (CCM) is the ability to sum numerous perturbation terms to infinite order, thus enabling the inclusion of large classes of virtual excitations, while being size-consistent.

Single-reference CCM has been used extensively in recent years, but until this past year there had been little experience with multireference MR-CCM especially when there were avoided crossings of ground and electronically excited potential energy surfaces. There are still theoretical problems to be studied such as the structure of the model space and its effect on the linked-diagram theorem. Our previous preliminary applications of MR-CCM gave encouraging results (agreement to 0.15eV or better with experiment in most cases [3]). Single and double excitations were included to all orders, and triples were calculated to lowest order.

Since there is so little experience with the MR-CCM, one of the objectives of our research is to make detailed comparisons, point by point, on the ground and electronically excited potential energy surfaces between these results and those of multireference double excitation configuration interaction (MRD-CI) results (including a Davidson type correction to the MRD-CI results to account for size consistency). These comparisons will help to establish guidelines for the types of excitations which must be included in MR-CCM and the range of problems handled well by it.

The protonation/deprotonation process is an excellent and stringent test of MR-CCM since it has clearly identifiable avoided crossings.

A. Methodology - Multireference Coupled Cluster Method (MR-CCM)

1. General Discussion of Coupled Cluster Method

The exp(s) or coupled cluster method (CCM) [4-8] has been used widely in recent years for ab-initio electronic structure calculations in closed-shell, non-degenerate systems, with highly satisfactory results [9]. Physically it amounts to the inclusion of certain types of excitations to all orders. From a perturbation theory point of view, infinite-order summation of large classes of linked perturbation diagrams is accomplished. CCM has proved competitive with the widely-used configuration-interaction (CI) method, and it has the advantage of being

size consistent [9]. The CCSD approximation [10], in which single and double excitations are included to all orders, is usually employed; a few calculations approximating the effect of triple excitations have appeared recently [11,12].

Closed-shell CCM is applicable only when the system of interest can be approximately described by a single Slater determinant. Even the very accurate calculations require multireference theories, as has been shown in recent years by developments in CI methodology. Most molecular states cannot be treated properly (or not at all) by a single-reference method. Shavitt, who has made seminal contributions to both CI and CCM theory, has predicted recently that [13] MR-CCM would ultimately prove the single most promising approach to molecular structure calculations.

A variety of multireference or open-shell coupled-cluster methods (OSCCM) have been described in the literature [14-17], but only few applications to real systems are available. The method of Lindgren differs from most others by employing the time-ordered formalism, which considerably reduces the number of diagrams needed. Lindgren's formalism has recently been adapted by Kaldor [1] to the direct calculation of atomic and molecular transition energies, including electron affinities [1a,1b,1f], ionization potentials [1c] and excitation energies [1e]. These preliminary results were encouraging (agreement of 0.15eV or better with experiment in most cases). In our laboratory at the Johns Hopkins University we had also derived another alternative approach to MR-CCM where single and double excitations were included [18].

2. Specific Methodology

The Hamiltonian, H , of a system is separated in the conventional way into H_0 , with known eigenfunctions, and a perturbation V ,

$$H = H_0 + V \quad \text{IV-1}$$

$$H_0 |\alpha\rangle = E_0 |\alpha\rangle \quad \text{IV-2}$$

A d -dimensional model space P is defined by the projection operator P , and Q is its complement:

$$P = \sum_{\alpha \in P} |\alpha\rangle \langle \alpha|, \quad Q = 1 - P \quad \text{IV-3}$$

There will usually be d eigenfunctions of H with major components in the model space,

$$H \psi^a = E^a \psi^a \quad \text{IV-4}$$

$$P \psi^a = \psi_0^a \quad a = 1, 2, \dots, d \quad \text{IV-5}$$

where ψ_0^a are linear combinations of $|\alpha\rangle \alpha \in P$. the wave operator Ω transforms the model functions into exact ones

$$\Omega \Psi_0^a = \Psi^a, \quad a=1, 2, \dots, d \quad \text{IV-6}$$

The key equation in Lindgren's derivation [17] is the generalized Bloch equation

$$[\Omega, H]P = WP - \Omega PWP \quad \text{IV-7}$$

where W is the effective interaction

$$W = V\Omega \quad \text{IV-8}$$

Alternatively, one may rewrite (7) as

$$[\chi, H_0]P = QWP - \chi PWP \quad \text{IV-9}$$

where the correlation operator χ is defined by

$$\Omega = 1 - \chi \quad \text{IV-10}$$

The energies of interest are obtained by diagonalizing the effective Hamiltonian in the model space

$$H_{\text{eff}} \Psi_0^a = E^a \Psi_0^a \quad \text{IV-11}$$

where

$$H_{\text{eff}} = PH\Omega P = P(H_0 + W)P \quad \text{IV-12}$$

The correlation operator χ includes single, double, etc., excitations and may be written as

$$\chi = C_1 + C_2 + \dots = \sum_{ij} \{a_i^+ a_j\} t_j^i + 1/2 \sum_{ijkl} \{a_i^+ a_j^+ a_l a_k\} t_{kl}^{ij} \quad \text{IV-13}$$

$t_j^i, t_{kl}^{ij}, \dots$, are excitation amplitudes, and the curly brackets denote normal order with respect to a reference (core) determinant. All terms, connected and disconnected, are included in (13). The operator used in CCM is the excitation operator T , related to Ω by

$$\Omega = \{\exp(T)\} = 1 + T + 1/2\{T^2\} + \dots \quad \text{IV-14}$$

T is obtained by summing the rhs of (13) over connected terms only.

Perturbative and non-perturbative schemes for calculating the excitation operator and correlation energies may be derived from either of the following two equations, which include connected terms only [14]

$$[T, H_0] = (QV\Omega - \chi P V \Omega)_{\text{conn}} \quad \text{IV-15}$$

or

$$[T, H_0] = W_{op,conn} - (XW_{C1})_{conn} \quad IV-16$$

$W_{op,conn}$ describes all connected diagrams which have some open (non-valence) lines, corresponding to P+Q transitions. W_{C1} diagram, with no external non-valence lines, describe P+P transitions. The latter also appear in the effective Hamiltonian, which may be written as

$$H_{eff} = PH_0P + W_{C1} \quad IV-17$$

The second term in equation (15) or (16) gives rise to the so-called folded diagrams.

The T operator for an open-shell system may be partitioned according to the number of valence orbitals excited,

$$T = T^{(0)} + T^{(1)} + T^{(2)} + \dots \quad IV-18$$

Haque and Mukherjee [19] have shown that partial decoupling of the equations is then possible, as the equation for $T^{(n)}$ involves only $T^{(m)}$ elements with $m \leq n$. This decoupling is helpful in reducing the computational effort, and has been used by Kaldor [1a-1e]. The H_{eff} or W_{C1} diagrams may be separated into core and valence parts

$$H_{eff} = H_{eff}^{core} + H_{eff}^{val} \quad IV-19$$

where the first term on the rhs consists of diagrams without any external lines. The eigenvalues of H_{eff}^{val} will then give directly the transition energies from the core, with correlation effects included for both core and valence electrons. The physical significance of these energies depends of course on the model space. Thus electron affinities may be calculated by constructing a model space with valence particles only [1a,1b], ionization potentials are given using valence holes [1c], and both types are included for the purpose of getting excitations from a closed-shell system [1d,1e].

The open-shell multireference coupled cluster (MR-CCM) package, written by Kaldor for the Tel Aviv University CYBER 180/990, was adapted by him at the Johns Hopkins University to the SDSC SCS-40 and the CRAY XMP-48 and vectorized. The integral, SCF and transformation routines already in use at the Johns Hopkins University for MRD-CI calculations (including the desirable computational options for ab-initio calculations on large molecules) [20-26] we had developed over the years at the Johns Hopkins University were also meshed into the open-shell MR-CCM package.

Multireference CSD calculations, including excited and ionized states would represent a major increase in the potential usefulness of the method. It should be noted that commonly used packages such as GAUSSIAN 82 [27a], 86

[27b] etc. are limited to single reference many body perturbation theory (MBPT) Møller Plesset {MP(2) - second order, MP(3) third order, MP(4) - fourth order.}

3. Computational Details of the $(\text{H}_3\text{N} \text{---} \text{H})^+$ MR-CCM Calculations

These open-shell MR-CCM programs contain routines for calculating the diagrams for closed shell, or for systems obtained from a closed shell, by ionizing electron(s) and for systems with electron(s) outside a closed shell.

Thus the MR-CCM calculations on $(\text{H}_3\text{N} \text{---} \text{H})^+$ where an open-shell system was required [$R(\text{H}_3\text{N} \text{---} \text{H})^+ \geq 4.0$ bohrs] were carried out using a closed-shell NH_4^{+3} core.

The MR-CCM scheme as implemented by us requires a closed-shell reference configuration, from which the states of interest can be obtained by adding and/or subtracting electrons. The selection of the reference states depends mainly on the orbital energy spectrum and on the states under investigation. The energies of the highest occupied ($3a_1$) and lowest unoccupied ($4a_1$) orbitals, calculated in both the NH_4^+ and NH_4^{3+} ions, are given in Table IV-1 as functions of $R(\text{H}_3\text{N} \text{---} \text{H})^+$. The angle θ minimizing the MRD-CI energy for each R is also given. The gap between the two orbitals closes with increasing R , so that quasidegeneracy effects must be considered for $R > 4$ bohr. The quasidegeneracy may not be evident from the orbital energies alone. However, a simple inspection of the lowest-energy determinant at different separations will show that the closed-shell system is lowest around R_{eq} , whereas $3a_1 4a_1$ is lowest at large R ($\text{NH}_3^+ + \text{H}$ is lower than $\text{NH}_3 + \text{H}^+$). A recent study on excited states of atomic Be has shown that degeneracies and "intruder states" may be caused by two-electron interactions, even if not predicted by orbital energies. In the present case, the expected curve crossing is manifested by convergence difficulties of the single-reference CCM at $R > 4$ bohr. The potential surface is therefore obtained by carrying out single-reference CCM for NH_4^+ below $R = 4$ bohr, and MR-CCM, with the $(3a_1)^2$ and $3a_1 4a_1$ determinants in the model space, for larger distances. The latter calculation is done using the core (NH_4^{3+}) orbitals. This approach is valid only if the transition between the two regions is smooth. As similar transitions will occur in many potential surfaces, this point is crucial to the applicability of the method. MRD-CI calculations were also carried out with both NH_4^+ and NH_4^{3+} orbitals to provide additional checks on the results.

The basis set was a Dunning $9^S5^P \rightarrow 5^S3^P$ plus a polarization function on the N and a $4^S + 3^S$ plus a p polarization function on the H.

The potential energy surfaces for $(\text{H}_3\text{N} \cdots \text{H})^+$ dissociation were run in C_3 symmetry to allow for possible geometrical distortions. The symmetries of both the HOMO (highest occupied molecular orbital - orbital 3) and the LUMO (lowest unoccupied molecular orbital - orbital 4) in NH_4^+ are of the totally symmetric irreducible representation.

At each different $(\text{H}_3\text{N} \cdots \text{H})^+$ distance the geometry of the system was optimized by MRD-CI calculations at the lowest singlet state of $(\text{H}_3\text{N} \cdots \text{H})^+$. For expediency, the subsequent MR-CCM and MRD-CI calculations for the lowest and second singlet state and for the triplet state were then carried out at these optimized geometries.

B. Results and Discussion

We made a very detailed and intensive study of the protonation of NH_3 and deprotonation of NH_4^+ . This was a stringent test for the open-shell multireference coupled cluster method for the following reason.

The lowest energy state of the separated fragments from NH_4^+ at the dissociation asymptote is not $\text{H}^+(^1S_g) + \text{NH}_3(^1A_1)$ but rather $\text{H}(^2S_g) + \text{NH}_3^+(^2A_1)$. The single determinant SCF for the lowest singlet state of NH_4^+ at equilibrium does not dissociate properly to the asymptote. Thus, MR-CCM calculations are necessary but it is complicated by the fact that the ground and excited singlet state are of the same symmetry. We ran open-shell MR-CCM calculations for the ground and first excited singlet state for the lowest triplet state of NH_4^+ .

As a check on the accuracy of the MR-CCM calculations and as a guide to the type of excitations involved, we also ran MRD-CI calculations for this same system point-by-point for comparison.

We first ran the MRD-CI calculations for the ground and excited singlet states of $(\text{H}_3\text{N} \cdots \text{H})^+$ and for the triplet state. At the MRD-CI level we optimized the geometry of the lowest singlet state at each point on the potential surface. The subsequent MRD-CI and all of the MR-CCM calculations were carried out using these optimized geometries for both the lowest and first excited singlet state and for the triplet state.

The integrals, SCF and transformation were run first. Preliminary MRD-CI calculations were run for the ground and excited singlet state to identify the important configurations. Then the MRD-CI calculations were carried out as described in sections B.2 and c.3.

Then the MR-CCM calculations for the two lowest singlet states were run at this geometry using the identical integrals, SCF and transformed integrals. Similar MRD-CI and MR-CCM calculation were also run for the triplet state.

Figure IV-1 shows the MR-CCM and MRD-CI energies for the ground and first excited states and for the lowest triplet state. It may be seen that the MR-CCM did give the two correct singlet curves which dissociate properly at the asymptote. Furthermore the MR-CCM energies and the MRD-CI energies (including the Davidson type correction) are very close both for the two singlet and triplet states.

The energies of the ground 1A_1 state of the NH_4^+ molecule as a function of $R(H_3N---H)^+$ distance are shown in Table IV-2. Figure IV-1 presents the potential energy surface for the three states calculated. The avoided crossing is not apparent at first glance, as the interaction between the two diabatic curves corresponding to the $(3a_1)^2$ and $3a_1,4a_1$ configurations is very strong and leads to an unusually large separation between the curves. The crossing may be confirmed by looking at the CI or CCM excitation coefficients (see below), by observing the change in the character of the lowest state as explained in the previous section, or by comparing the correlated potential curves to the SCF curve. The latter is rather poor, as shown by the correlation energy increase from 0.21 hartree near equilibrium to 0.35 hartree at large $(H_3N --- H)^+$ separation. The SCF determinant corresponds at large separation to the second 1A_1 state, which has indeed a correlation energy of 0.20 hartree (Table IV-3) in this region. The SCF potential surface therefore approximates a diabatic, rather than an adiabatic, surface. When moved down by -0.2 hartree, the SCF potential overlaps the ground state at small R and the excited state at large R.

At present, the open-shell MR-CCM requires that a closed shell core be used and all excitable electrons be put into a model space. Both MRD-CI and MR-CCM calculations were carried out at every point from an $(H_3N --- H)^+$ reference. Additionally as mentioned in the previous section, the open-shell MR-CCM program used required the model space to have electrons outside a closed shell. Thus in the regions where open shell calculations were necessary, MR-CCM calculations were also run using reference $(H_3N --- H)^{+3}$ allowing electrons to occupy empty orbitals 3 and 4. The MRD-CI calculations allow all single and double excitations from the filled orbitals of $(H_3N --- H)^+$ itself and all single and double excitations from multireference configurations arising from this. For comparison with the

MR-CCM results for open-shell systems the MRD-CI calculations were also run at these points for a core of $(\text{H}_3\text{N} \text{---} \text{H})^{+3}$ calculations with the last two electrons allowed to occupy empty orbitals 3 and 4 and higher (all single and double excitations relative to reference configurations with a c^2 of 0.005 or higher).

In Table IV-4a are tabulated the CCM excitation amplitudes and mixing coefficients for $^1\text{A}_1$ states. In Table IV-4b are tabulated the MR-CCM mixing coefficients using NH_4^{3+} orbitals. In Table IV-5a are tabulated the MRD-CI coefficients for $^1\text{A}_1$ states using NH_4^+ orbitals as a reference; in Table IV-5b are tabulated the coefficients using NH_4^{+3} orbitals as a reference.

C. Conclusion

The MR-CCM and MRD-CI energies and wave functions are very close for the lowest and second singlet states and for the triplet for the entire potential surface of $(\text{H}_3\text{N} \text{---} \text{H})^+$. Moreover, the MRD-CI results (including the Davidson correction) are close to the MR-CC results over the entire calculated potential surface of $\text{H}_3\text{N} \text{---} \text{H})^+$.

Both the MR-CC and the MRD-CI results confirm that the lowest singlet state of NH_4^+ at equilibrium follows a diabatic singlet totally symmetric irreducible representation potential energy surface to the separated species $\text{H}^+ + \text{NH}_3$; however the adiabatic lowest singlet curve changes dominant configuration from 33 to a mixture of 34 + 44 at $R(\text{H}_3\text{N} \text{---} \text{H})^+ \geq 4.0$ bohrs.

These results are significant for dissociation of energetic compounds which contain $\text{R}_1\text{R}_2\text{R}_3\text{NH}^+$ species. These results also have profound implications for protonation and deprotonation of biomolecules, both endogenous and exogenous. Previous theoretical quantum chemical studies of protonation and deprotonation of biomolecules seem to have been based on single determinant closed shell SCF calculations, sometimes supplemented by MP_2 (or MP_3 or MP_4) corrections MP correlation correction to any order cannot correct for the deficiency of a single determinant wave function. MP corrections can only take into account correlation corrections to the particular wave function used.

A study of the deprotonation of NH_4^+ was carried out using the MR-CCM and MRD-CI methods. The reaction path goes through an avoided crossing of two potential surfaces, with the closed-shell NH_4^+ dissociating into the

open-shell $H(2S) + NH_3^+(2A_1)$ rather than the higher-energy closed-shell system $H^+ + NH_3(1A_1)$. The avoided crossing occurs near a $(H_3N \cdots H)^+$ separation of 4 bohr, and is accompanied by a change of the geometry of the NH_3 group from pyramidal to planar. The different methods used gave very similar energies, up to a few mhartree. This is probably the magnitude of the remaining error relative to the exact (full CI) energies in the Hilbert space spanned by the basis used. The MRD-CI errors are due to including the contribution of large numbers of configurations approximately, by extrapolation, and estimating the effect of higher than double excitations by the Davidson correction. The CCM errors come from ignoring the connected triple and higher excitations (i.e. those not described as products of single and double excitations).

The work reported above served as a test for the MR-CCM method. In particular, two questions were posed: how close does the method come to giving the full CI energy, and can it be used for potential surfaces which include an avoided crossing and necessitate a change of the model (P) space. The results are highly encouraging on both counts. The MR-CCM energies are only a few mhartree away from the MRD-CI, a difference similar to that given by MRD-CI calculations with different choices of molecular orbitals constructed from the same basis; and the avoided crossing with concomitant change of reference determinants did not cause any problems. The method seems therefore of great potential value.

Bibliography

- 1a. A. Haque and U. Kaldor, Chem. Phys. Lett. 117, 347 (1985).
- b. A. Haque and U. Kaldor, Chem. Phys. Lett. 120, 261 (1985).
- c. A. Haque and U. Kaldor, Intern. J. Quantum Chem. 29, 425 (1986).
- d. U. Kaldor and A. Haque, Chem. Phys. Lett. 128, 45 (1986).
- e. U. Kaldor, Intern. J. Quantum Chem. S20, 445 (1986).
- f. U. Kaldor, J. Comput. Chem. 8, 448-453 (1987).

- 2a. R. J. Buenker, S. D. Peyerimhoff and W. Butscher, Mol. Phys. 35, 771 (1978).
- b. R. J. Buenker, in STUDIES IN PHYSICAL AND THEORETICAL CHEMISTRY Vol. 21 (CURRENT ASPECTS OF QUANTUM CHEMISTRY 1981), Ed. R. Carbo, Elsevier Scientific Publishing Co., Amsterdam, 1982, pp. 17-34.
- c. R. J. Buenker, in PROCEEDINGS OF WORKSHOP ON QUANTUM CHEMISTRY AND MOLECULAR PHYSICS in Wollongong, Australia, Feb. 1980.
- d. R. J. Buenker and R. A. Phillips, J. Mol. Struct. Theochim. 123, 291 (1985).

- 3a. U. Kaldor, J. Chem. Phys. 87, 467 (1987).
- b. U. Kaldor, J. Comput. Chem. Symp. 8, 448 (1987).

4. J. Hubbard, Proc. Roy. Soc. (London) A240, 539 (1957); *ibid.* A243, 336 (1958).

- 5a. F. Coester, Nucl. Phys. 7, 421 (1958).
- b. F. Coester and H. Kuemmel, Nucl. Phys. 17, 477 (1960).
- c. H. Kuemmel, K. H. Luermann and J. G. Zabolitzky, Phys. Rept. 36, 1 (1978).

6. O. Sinanoglu, Adv. Chem. Phys. 6, 315 (1964).

7. J. Cizek, J. Chem. Phys. 45, 4256 (1966); Advan. Chem. Phys. 14, 35 (1969).

- 8a. J. Paldus, J. Cizek and I. Shavitt, Phys. Rev. A 5, 50 (1972).
- b. J. Paldus, J. Chem. Phys. 67, 303 (1977).
- c. B. G. Adams and J. Paldus, Phys. Rev. A 20, 1 (1979).

9. For a review see R. J. Bartlett, Ann. Rev. Phys. Chem. 32, 359 (1981).

10. The explicit closed-shell CCSD equations may be found in G. D. Purvis and R. J. Bartlett, J. Chem. Phys. 76, 1910 (1982); and in J. M. Cullen and M. C. Zerner, J. Chem. Phys. 77, 4088 (1982). The latter reference also shows the CCSD diagrams.

11. A. Haque and U. Kaldor, Chem. Phys. Lett. 120, 261 (1985)

- 12a. S. Pal, M. Rittby, R. J. Bartlett, D. Sinka and D. Mukherjee, Chem. Phys. Lett 137, 273 (87).
- b. Y. S. Lee and R. J. Bartlett, J. Chem. Phys. 80, 4371 (1984).
- c. Y. S. Lee, S. A. Kucharsky, and R. J. Bartlett, J. Chem. Phys. 81, 5906 (1984).
- d. M. Urban, J. Noga, S. J. Cole, and R. J. Bartlett, J. Chem. Phys. 83, 4041 (1985).
- e. See also M. R. Hoffmann and H. F. Schaefer, J. Chem. Phys. 83, 703 (1985).
13. I. Shavitt, in "Advanced Theories and Computational Approaches to the Electronic Structure of Molecules", ed. C. E. Dykstra, Reidel, 1984, p. 185 (quotation from p. 192).
- 14a. F. E. Harris, Intern. J. Quantum Chem. S11, 403 (1977);
- b. H. J. Monkhorst, Intern. J. Quantum Chem. S11, 421 (1977).
- 15a. J. Paldus, J. Cizek, M. Saute and A. Laforge, Phys. Rev. A 17, 805 (1978).
- b. M. Saute, J. Paldus and J. Cizek, Intern. J. Quantum Chem. 15, 463 (1979).
- 16a. D. Mukherjee, R. K. Moitra and A. Mukhopadhyay, Pramana 4, 247 (1975).
- b. Ibid., Mol. Phys. 30, 1861 (1975).
- c. A. Mukhopadhyay, R. K. Moitra and D. Mukherjee, J. Phys. B 12, 1 (1979).
- d. D. Mukherjee and P. K. Mukherjee, Chem. Phys. 39, 325 (1979).
- e. S. S. Adnan, S. Bhattacharyya and D. Mukherjee, Mol. Phys. 39, 519 (1980).
- f. Ibid., Chem. Phys. Lett. 85, 204 (1981).
- 17a. R. Offerman, W. Ey and H. Kummel, Nucl. Phys. A273, 349 (1976).
- b. R. Offerman, Nucl. Phys. A273, 368 (1976).
- c. W. Ey, Nucl. Phys. A296, 189 (1978).
- 18a. A. Laforge and S. Roszak, CR Acad. Sc. Paris, 297, 459 (1983).
- b. A. Laforge, M. Saute, S. Roszak, CR Acad. Sc. Paris, 299, 229 (1984).
- 19a. A. Haque and D. Mukherjee, J. Chem. Phys. 80, 5058 (1984).
- b. Ibid., Pramana 23, 651 (1984)
20. H. E. Popkie, "MOLASYS: A Computer Program for Molecular Orbital Calculations on Large Systems," The Johns Hopkins University, 1974.
- b. H. E. Popkie, "MOLASYS-MERGE," The Johns Hopkins University, 1978
21. H. E. Popkie, "GIPSY (Gaussian Integral Program System): A System of Computer Programs for the Evaluation of One- and Two- Electron Integrals Involving s-, p-, d- and f-type Contracted Cartesian Gaussian Functions," The Johns Hopkins University, 1975.

22. W.A. Sokalski, P.C. Hariharan, V. Lewchenko and Joyce J. Kaufman, MOLASYS-INTER: A Program to Calculate Ab-Initio Partitioned Energy contributions from Ab-Initio (or Ab-Initio MODPOT/VRDDO) SCF Wave Functions; s and p Orbitals. Also Includes Calculation of Electric Field at a Molecule from Surrounding Molecules and Procedures for Calculation of Dispersion Energy," The Johns Hopkins University, 1979-present. b. A less extensive version of this program was written and used as early as 1979. W.A Sokalski, P.C.Hariharan, Joyce J. Kaufman and C. Petrolongo, "Basis Set Superposition Effect on Difference Electrostatic Molecular Potential Contour Maps," Int. J. Quantum Chemi. 18, 165-171 (1980)
23. W.A. Sokalski, P.C.Hariharan, W. Lewchenko and Joyce J. Kaufman, "GIPSY-INTER: A Program to Calculate Ab-Initio Partitioned Energy Contributions from Ab-Initio (or Ab-Initio MODPOT/VRDDO) SCF Wave Functions; s, p, d, and f Orbitals. Also Includes Calculations of Electric Field at a Molecule from Surrounding Molecules and Procedures for Calculation of Dispersion Energy," The Johns Hopkins University, 1982-present.
24. Joyce J. Kaufman, H.E. Popkie and P.C. Hariharan, "New Optimal Strategies for Ab-Initio Quantum Chemical Calculations on Large Drugs, Carcinogens, Teratogens, and Bimolecules." An invited lecture presented at the Symposium on Computer Assisted Drug Design. Division of Computers in Chemistry at the American Chemical Society National Meeting, Honalulu, Hawaii, April 1979. In COMPUTER ASSISTED DRUG DESIGN, Eds. E.C. Olson and R.E. Christoffersen, ACS Symposium Series 112, Am. Chem. Soc., Washington, D.C., 1979, pp. 415-435
25. Joyce J. Kaufman, P.C. Hariharan, and H.E. Popkie, Int. J. Quantum Chem. S15, 199-201 (1981)
26. Joyce J. Kaufman, Presented at the Sanibel International Symposia Snowbel Satellite, Utah, April 1986. Int. J. Quantum Chem. 29, 179-184 (1987)
- 27a. J.S. Binkley, et al. and J. Pople, Gaussian 82, Department of Chemistry, Carnegie-Mellon University, Pittsburgh, PA.
- b. M.J. Frisch, et al. and J.A Pople, Gaussian 86, Carnegie-Mellon Quantum Chemistry Publishing Unit, Pittsburgh, PA, 1984

Figure IV-1

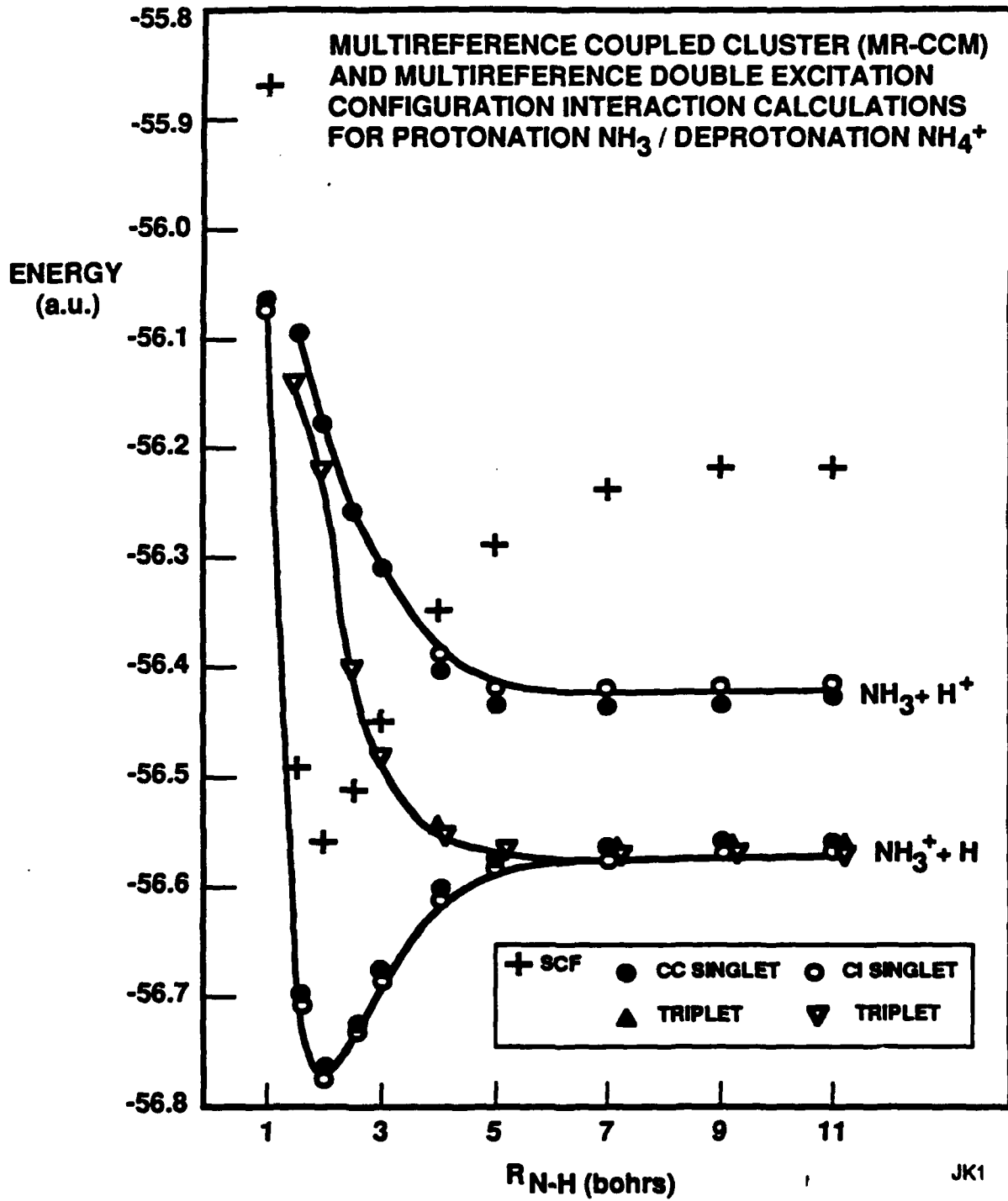


Table IV-1

NH_4^+ and NH_4^{3+} orbital energies (hartree).

R(bohr) ^a	θ^b	NH_4^+		NH_4^{3+}	
		$3a_1$	$4a_1$	$3a_1$	$4a_1$
1.000	109.4	-1.03096	-0.08750		
1.500	109.4	-1.01667	-0.08638		
1.750	109.4	-1.01018	-0.08727		
1.943	109.4	-1.00600	-0.08951	-1.44422	-0.72439
2.500	107.0	-0.89257	-0.13026	-1.31293	-0.83312
3.000	104.0	-0.81502	-0.19759	-1.21317	-0.88475
4.000	100.0	-0.70845	-0.30028	-1.06937	-0.90037
5.000	92.0	-0.64304	-0.35773	-0.98767	-0.86779
7.000	91.0	-0.57178	-0.40548	-0.91986	-0.77806
9.000	90.0	-0.53536	-0.41883	-0.88667	-0.71857
11.000	90.0	-0.51437	-0.42278	-0.86604	-0.67948

^a $\text{R}(\text{H}_3\text{N} \cdots \text{H})^+$. $\text{R}(\text{NH})$ in the NH_3 group is kept at 1.943 bohr.

^bThe angle between NH in the NH_3 group and the C_3 axis. All the results reported below are for these angles.

Table IV-2

 $\text{NH}_4^+ X^1A_1$ ground state energies (hartree) as a function of $R(\text{H}_3\text{N} \cdots \text{H})^+$.

R(bohr)	SCF	NH_4^+ orbs		NH_4^{3+} orbs	
		MRD-CI	CCM	MRD-CI	MR-CCM
1.000	-55.87003	-56.08092	-56.07795		
1.500	-56.49116	-56.70277	-56.69971		
1.750	-56.54932	-56.76284	-56.75946		
1.943	-56.55670	-56.77058	-56.76815	-56.77614	
2.500	-56.51006	-56.73165	-56.72794		
3.000	-56.44988	-56.68011	-56.67546		
4.000	-56.35185	-56.60863	-56.59887	-56.61039	-56.60263
5.000	-56.28961	-56.57932	-56.56307	-56.57940	-56.57424
7.000	-56.23844	-56.56954	---	-56.56862	-56.56585
9.000	-56.22349	-56.56960	---	-56.56836	-56.56604
11.000	-56.21908	-56.56960	---	-56.56818	-56.56620

Table IV-3

NH_4^+ excited state energies (hartree) as a function of $R(\text{H}_3\text{N} \cdots \text{H})^+$.

R(bohr)	$^1\text{A}_1$			$^3\text{A}_1$	
	MRD-CI ^a	MRD-CI ^b	MR-CCM ^b	MRD-CI ^a	MR-CCM ^b
1.000	-55.46380			-55.51202	
1.500	-56.09771			-56.14469	
1.750	-56.16444			-56.21064	
1.943	-56.18084	-56.18173		-56.22369	
2.500	-56.25877				
3.000	-56.31005				
4.000	-56.39159	-56.39925	-56.40282	-56.54613	-56.54461
5.000	-56.43570	-56.44096	-56.43175	-56.56336	-56.56159
7.000	-56.43800	-56.44279	-56.43405	-56.56702	-56.56548
9.000	-56.41651	-56.42207	-56.42826	-56.56635	-56.56603
11.000	-56.41651	-56.41972	-56.42601	-56.56664	-56.56620

^a NH_4^+ orbitals.

^b NH_4^{3+} orbitals.

Table IV-4

CCM excitation amplitudes and mixing coefficients for 1A_1 states.^a

A. CCM excitation amplitudes, NH_4^+ orbitals.						
R(bohr)	s_3^4	s_{33}^{44}				
1.000	0.000	0.010				
1.500	0.000	0.011				
1.750	0.000	0.011				
1.943	0.000	0.011				
2.500	0.000	0.065				
3.000	0.019	0.141				
4.000	0.098	0.311				
5.000	0.256	0.511				
B. MR-CCM mixing coefficients, NH_4^{3+} orbitals.						
R(bohr)	$C_1(33)$	$C_1(34)$	$C_1(44)$	$C_2(33)$	$C_2(34)$	$C_2(44)$
4.000	0.932	0.174	0.321	0.380	0.858	0.358
5.000	0.673	0.672	0.320	0.785	0.595	0.167
7.000	0.131	0.984	0.122	0.994	0.109	0.015
9.000	0.014	1.000	--	1.000	0.016	--
11.000	0.002	1.000	--	1.000	0.001	--

^aThe $3a_1$ and $4a_1$ orbitals are denoted by 3 and 4, respectively, and the subscript gives the molecular state. Thus, s_3^4 is the excitation amplitude from $3a_1$ to $4a_1$, and $C_2(44)$ is the coefficient of the $(4a_1)^2$ determinant in the second 1A_1 state function.

Table IV-5

MRD-CI coefficients for 1A_1 states.^a

R(bohr)	$C_1(33)$	$C_1(34)$	$C_1(44)$	$C_2(33)$	$C_2(34)$	$C_2(44)$
A. NH_4^+ orbitals						
1.000	0.952	0.000	0.000	0.000	0.924	0.000
1.500	0.950	0.000	0.000	0.000	0.922	0.000
1.750	0.948	0.000	0.000	0.000	0.920	0.000
1.943	0.947	0.000	0.000	0.000	0.919	0.000
2.500	0.938	0.000	0.000	0.000	0.888	0.000
3.000	0.920	0.001	0.000	0.005	0.842	0.000
4.000	0.823	0.023	0.092	0.080	0.667	0.182
5.000	0.630	0.110	0.194	0.267	0.526	0.141
7.000	0.345	0.334	0.249	0.564	0.329	0.047
9.000	0.260	0.430	0.237	0.656	0.260	0.026
11.000	0.260	0.430	0.237	0.656	0.260	0.026
B. NH_4^{3+} orbitals						
1.943	0.823	0.000	0.000	0.000	0.729	0.000
4.000	0.732	0.061	0.000	0.088	0.615	0.118
5.000	0.375	0.449	0.071	0.439	0.345	0.022
7.000	0.014	0.891	0.000	0.780	0.014	0.000
9.000	0.000	0.908	0.000	0.791	0.000	0.000
11.000	0.000	0.909	0.000	0.790	0.000	0.000

^a For notation see footnote to Table IV.

V. Lectures Presented and Publications on This ONR Research

Presentations given and/or scheduled and papers published and/or submitted during the fiscal year.

A. Presentations Given Dr. Joyce J. Kaufman

1. Already Presented (* denotes invited lecture)

a. At National and International Meetings

- * (1). "Ab-Initio MRD-CI Calculations for Breaking a Chemical Bond in a Molecule in a Crystal or Other Solid Environment I. $\text{H}_3\text{C} - \text{NO}_2$ Decomposition in Nitromethane", American Chemical Society/North American Chemical Congress, Division of Physical Chemistry, Toronto, Canada, June 1988.
- * (2). "Ab-Initio Multireference Coupled Cluster and Multireference CI Calculations for Protonation of NH_3 /Deprotonation of NH_4^+ Involve Multipotential Surfaces" American Chemical Society/North American Chemical Congress, Division of Physical Chemistry, Toronto, Canada, June 1988.
- * (3). "Ab-Initio MRD-CI Calculations for Breaking a Chemical Bond in a Molecule in a Crystal or Other Solid Environment I. $\text{H}_3\text{C} - \text{NO}_2$ Decomposition in Nitromethane", Working Group Meeting on Synthesis of High Energy Density Materials, U.S. Army Armament Research, Development and Engineering Center, Dover, New Jersey, June 1988. (An invited lecture)
- * (4). "Ab-Initio MRD-CI Calculations for Breaking a Chemical Bond in a Molecule or Other Solid Environment", Gordon Conference on Chemistry of Energetic Materials, New Hampton School, New Hampshire, June 1988. (An invited lecture; the organizers of that Gordon Conference paid Dr. Kaufman's registration fee and living expenses.)
- * (5). "Ab-Initio MRD-CI Calculations for Breaking a Chemical Bond in a Molecule in a Crystal or Other Solid Environment I. $\text{H}_3\text{C} - \text{NO}_2$ Decomposition in Nitromethane," 6th International Congress of Quantum Chemistry, Jerusalem, Israel, August 1988,

b. At DOD Meetings and Workshops

- * (1). "Ab-Initio MRD-CI calculations on the Propagation Step in Cationic Polymerization of Energetic Substituted Oxetanes," ONR Energetic Materials Workshop, Great Oak Landing, Maryland, September 1988,

In that paper Dr. Kaufman also mentioned briefly our results on the $\text{H}_3\text{C} - \text{NO}_2$ decomposition in a nitromethane crystal including preliminary results on treating voids in the nitromethane crystal.

2. To be presented

- *a. Ab-Initio MRD-CI Calculations for Breaking a Chemical Bond in a Molecule in a Crystal or Other Solid Environment. III. $\text{Me}_2\text{N} - \text{NO}_2$ Decomposition of Dimethylnitramine in a Large Crystalline Environment," Sanibel International Symposium on Atomic, Molecular and Solid State Physics, St. Augustine, Florida, March 1988.

B. Publications

1. Already Published

- a. "Ab-Initio MRD-CI Calculations for Breaking a Chemical Bond in a Molecule in a Crystal or Other Solid Environment I. $\text{H}_3\text{C}-\text{NO}_2$ Decomposition in Nitromethane", S. Roszak, P. C. Hariharan, P. B. Keegstra, and Joyce J. Kaufman, Int. J. Quantum Chem. S22, 619-635 (1988).
- b. "Ab-Initio Calculations on Large Molecules and Solids By Desirable Computational Procedures," an invited special lecture presented at the VIII International Conference on Computers in Chemistry Research and Education, Beijing, China, June 1987. Analytica Chimica Acta 210, 209-212 (1988).
- c. "Ab-Initio MRD-CI Calculations for the Propagation Step in the Cationic Polymerization of Oxetanes Based on Localized Orbitals," Joyce J. Kaufman, P. C. Hariharan and P. B. Keegstra. Int. J. Quantum Chem., S21, 623-643 (1987)
- d. "Comparison of Ab-Initio MODPOT and Ab-Initio Energy Partitioned Potential Functions for Nitromethane Dimer Against Large Basis Set Calculations," W. A. Sokalski, P. C. Hariharan and Joyce J. Kaufman. Int. J. Quantum Chem., S21 645-660 (1987).
- e. "Ab-Initio MRD-CI Calculations on Protonated Cyclic Ethers. I. Protonation Pathways Involve Multipotential Surfaces (Protonation of Oxetane) II. Differences from

SCF in Dominant Configurations Upon Opening Non-Protonated Oxirane Rings (epoxides)," Joyce J. Kaufman, P. C. Hariharan, S. Roszak and P. B. Keegstra, Int. J. Quantum Chem., QBS14 37-46 (1987).

2. Accepted for publication and in press

- a. "Ab-Initio MRD-CI Calculations for Breaking a Chemical Bond in a Molecule in a Crystal or Other Solid Environment. II. $H_3C - NO_2$ Decomposition of Nitromethane in a Nitromethane Crystal with Voids," S. Roszak, P. B. Keegstra, D. O'Neal, P. C. Hariharan, and Joyce J. Kaufman, an invited paper presented at the 6th International Congress of Quantum Chemistry, Jerusalem, Israel, August 1988. In press, Int. J. Quantum Chem., Congress Issue.
- b. "Ab-Initio Multireference Coupled Cluster (MR-CCM) and Ab-Initio Multireference Configuration Interaction (MRD-CI) Calculations for Protonation NH_3 / Deprotonation NH_4^+ Involve Multipotential Surfaces," U. Kaldor, S. Roszak, P. C. Hariharan and Joyce J. Kaufman. In press, J. Chem. Phys.

VI. Project Personnel

Joyce J. Kaufman, Ph.D.

Principal Investigator

P. C. Hariharan, Ph.D.

Research Scientist

Overall responsibility for implementing new program developments and conversion to Cray computers. Quantum chemical calculations on energetic polymers, breaking a chemical bond in a molecule in a crystal, MRD-CI calculations, GAMESS and POLY-CRYST calculations

Uzi Kaldor, Ph.D.

Visiting Scientist (Permanent position, Professor and Dean, University of Tel Aviv, Israel).

(at no salary cost to this ONR contract)

Rewriting, vectorizing and adapting the multireference coupled cluster method (MR-CCM) for the SCS-40 and the CRAY-XMP. Calculating MR-CCM potential energy surfaces for protonation NH_3 / deprotonation NH_4 .

Douglas W. O'Neal, Ph.D. (February 1988-October 1988)

Postdoctoral

Assistance with carrying out MRD-CI calculations on energetic polymers and breaking the $\text{H}_3\text{C} - \text{NO}_2$ bond in nitromethane in a nitromethane crystal with voids.

Douglas A. Chapman, Ph.D. (August 1988 - present)

Postdoctoral

Carrying out MRD-CI calculations on energetic polymers and MRD-CI calculations on breaking the $\text{Me}_2\text{N} - \text{NO}_2$ bond in dimethylnitramine in an isolated molecule and in a dimethylnitramine crystal.

(SYN)

DISTRIBUTION LIST

Dr. R.S. Miller
Office of Naval Research
Code 432P
Arlington, VA 22217
(10 copies)

Dr. A.L. Slafkosky
Scientific Advisor
Commandant of the Marine Corps
Code RD-1
Washington, DC 20380

JHU Applied Physics Laboratory
ATTN: CPIA (Mr. T.W. Christian)
Johns Hopkins Rd.
Laurel, MD 20707

Dr. Kenneth D. Hartman
Hercules Aerospace Division
Hercules Incorporated
Alleghany Ballistic Lab
P.O. Box 210
Washington, DC 21502

Mr. Otto K. Heiney
AFATL-DLJG
Elgin AFB, FL 32542

Dr. Merrill K. King
Atlantic Research Corp.
5390 Cherokee Avenue
Alexandria, VA 22312

Dr. R.L. Lou
Aerojet Strategic Propulsion Co.
Bldg. 05025 - Dept 5400 - MS 167
P.O. Box 15699C
Sacramento, CA 95813

Dr. R. Olsen
Aerojet Strategic Propulsion Co.
Bldg. 05025 - Dept 5400 - MS 167
P.O. Box 15699C
Sacramento, CA 95813

Dr. J. Pastine
Naval Sea Systems Command
Code 06R
Washington, DC 20362

Dr. Henry P. Marshall
Dept. 93-50, Bldg 204
Lockheed Missile & Space Co.
3251 Hanover St.
Palo Alto, CA 94304

Dr. Ingo W. May
Army Ballistic Research Lab.
ARRADCOM
Code DRXBR - 1BD
Aberdeen Proving Ground, MD 21005

Dr. R. McGuire
Lawrence Livermore Laboratory
University of California
Code L-324
Livermore, CA 94550

P.A. Miller
736 Leavenworth Street, #6
San Francisco, CA 94109

Dr. W. Moniz
Naval Research Lab.
Code 6120
Washington, DC 20375

Dr. K.F. Mueller
Naval Surface Weapons Center
Code R11
White Oak
Silver Spring, MD 20910

Prof. M. Nicol
Dept. of Chemistry & Biochemistry
University of California
Los Angeles, CA 90024

(SYN)

DISTRIBUTION LIST

Dr. Randy Peters
Aerojet Strategic Propulsion Co.
Bldg. 05025 - Dept 5400 - MS 167
P.O. Box 15699C
Sacramento, CA 95813

Dr. D. Mann
U.S. Army Research Office
Engineering Division
Box 12211
Research Triangle Park, NC 27709-2211

Mr. R. Geisler
ATTN: DY/MS-24
AFRPL
Edwards AFB, CA 93523

Naval Air Systems Command
ATTN: Mr. Bertram P. Sobers
NAVAIR-320G
Jefferson Plaza 1, RM 472
Washington, DC 20361

R.B. Steele
Aerojet Strategic Propulsion Co.
P.O. Box 15699C
Sacramento, CA 95813

Mr. M. Stosz
Naval Surface Weapons Center
Code R10B
White Oak
Silver Spring, MD 20910

Mr. E.S. Sutton
Thiokol Corporation
Elkton Division
P.O. Box 241
Elkton, MD 21921

Dr. Grant Thompson
Morton Thiokol, Inc.
Wasatch Division
MS 240 P.O. Box 524
Brigham City, UT 84302

Mr. L. Roslund
Naval Surface Weapons Center
Code R10C
White Oak, Silver Spring, MD 20910

Dr. David C. Sayles
Ballistic Missile Defense
Advanced Technology Center
P.O. Box 1500
Huntsville, AL 35807

Director
US Army Ballistic Research Lab.
ATTN: DRXBR-IBD
Aberdeen Proving Ground, MD 21005

Commander
US Army Missile Command
ATTN: DRSMI-RKL
Walter W. Wharton
Redstone Arsenal, AL 35898

T. Yee
Naval Weapons Center
Code 3265
China Lake, CA 93555

Dr. E. Zimet
Office of Naval Technology
Code 071
Arlington, VA 22217

Dr. Ronald L. Derr
Naval Weapons Center
Code 389
China Lake, CA 93555

T. Boggs
Naval Weapons Center
Code 389
China Lake, CA 93555

Lee C. Estabrook, P.E.
Morton Thiokol, Inc.
P.O. Box 30058
Shreveport, LA 71130

(SYN)

DISTRIBUTION LIST

Dr. R.F. Walker
Chief, Energetic Materials Division
DRSMC-LCE (D), B-3022
USA ARDC
Dover, NJ 07801

Dr. Janet Wall
Code 012
Director, Research Administration
Naval Postgraduate School
Monterey, CA 93943

R.E. Shenton
Atlantic Research Corp.
7511 Wellington Road
Gainesville, VA 22065

Mike Barnes
Atlantic Research Corp.
7511 Wellington Road
Gainesville, VA 22065

Dr. Lionel Dickinson
Naval Explosive Ordnance
Disposal Tech. Center
Code D
Indian Head, MD 20340

Prof. J.T. Dickinson
Washington State University
Dept. of Physics 4
Pullman, WA 99164-2814

M.H. Miles
Dept. of Physics
Washington State University
Pullman, WA 99164-2814

Dr. T.F. Davidson
Vice President, Technical
Morton Thiokol, Inc.
Aerospace Group
110 North Wacker Drive
Chicago, IL 60606

Dr. D.D. Dillehay
Morton Thiokol, Inc.
Longhorn Division
Marshall, TX 75670

G.T. Bowman
Atlantic Research Corp.
7511 Wellington Road
Gainesville, VA 22065

Brian Wheatley
Atlantic Research Corp.
7511 Wellington Road
Gainesville, VA 22065

Mr. G. Edwards
Naval Sea Systems Command
Code 62R32
Washington, DC 20362

C. Dickinson
Naval Surface Weapons Center
White Oak, Code R-13
Silver Spring, MD 20910

Prof. John Deutch
MIT
Department of Chemistry
Cambridge, MA 02139

Dr. E.H. deButts
Hercules Aerospace Co.
P.O. Box 27408
Salt Lake City, UT 84127

David A. Flanigan
Director, Advanced Technology
Morton Thiokol, Inc.
Aerospace Group
110 North Wacker Drive
Chicago, IL 60606

(SYN)

DISTRIBUTION LIST

Mr. J. Consaga
Naval Surface Weapons, Center
Code R-16
Indian Head, MD 20640

Naval Sea Systems Command
ATTN: Mr. Charles M. Christensen
NAVSEA62R2
Crystal Plaza, Bldg. 6, Rm 806
Washington, DC 20362

Mr. R. Beauregard
Naval Sea Systems Command
SEA 64E
Washington, DC 20362

Dr. Anthony J. Matuszko
Air Force Office of Scientific Research
Directorate of Chemical & Atmospheric
Sciences
Bolling Air Force Base
Washington, DC 20332

Dr. Michael Chaykovsky
Naval Surface Weapons Center
Code R11
White Oak
Silver Spring, MD 20910

J.J. Rocchio
USA Ballistic Research Lab.
Aberdeen Proving Ground, MD 21005-5066

G.A. Zimmerman
Aerojet Tactical Systems
P.O. Box 13400
Sacramento, CA 95813

B. Swanson
INC-4 MS C-346
Los Alamos National Laboratory
Los Alamos, NM 87545

Dr. L.H. Caveny
Air Force Office of Scientific
Research
Directorate of Aerospace Sciences
Bolling Air Force Base
Washington, DC 20332

W.G. Roger
Code 5253
Naval Ordnance Station
Indian Head, MD 20640

Dr. Donald L. Bell
Air Force Office of Scientific
Research
Directorate of Chemical &
Atmospheric Sciences
Bolling Air Force Base
Washington, DC 20332

Dr. H.G. Adolph
Naval Surface Weapons Center
Code R11
White Oak
Silver Spring, MD 20910

U.S. Army Research Office
Chemical & Biological Sciences
Division
P.O. Box 12211
Research Triangle Park, NC 27709

G. Butcher
Hercules, Inc.
MS X2H
P.O. Box 98
Magna, Utah 84044

W. Waesche
Atlantic Research Corp.
7511 Wellington Road
Gainesville, VA 22065

(SYN)

DISTRIBUTION LIST

Dr. James T. Bryant ,
Naval Weapons Center
Code 3205B
China Lake, CA 93555

Dr. L. Rothstein
Assistant Director
Naval Explosives Dev. Engineering Dept.
Naval Weapons Station
Yorktown, VA 23691

Dr. M.J. Kamlet
Naval Surface Weapons Center
Code R11
White Oak, Silver Spring, MD 20910

Dr. Henry Webster, III
Manager, Chemical Sciences Branch
ATTN: Code 5063
Crane, IN 47522

Dr. R.S. Valentini
United Technologies Chemical Systems
P.O. Box 50015
San Jose, CA 95150-0015

Administrative Contracting
Officer (see contract for
address)
(1 copy)

Defense Technical Information Center
Bldg. 5, Cameron Station
Alexandria, VA 22314
(12 copies)

Arpad Junasz
Code DRDAR-IBD
Ballistic Research Lab
Aberdeen, MD 21005

Mr. C. Gotzmer
Naval Surface Weapons Center
Code R-11
White Oak
Silver Spring, MD 20910

Dr. John S. Wilkes, Jr.
FJSRL/NC
USAF Academy, CO 80840

Dr. H. Rosenwasser
Naval Air Systems Command
AIR-320R
Washington, DC 20361

Dr. A. Nielsen
Naval Weapons Center
Code 385
China Lake, CA 93555

Dr. Joyce J. Kaufman
The Johns Hopkins University
Department of Chemistry
Baltimore, MD 21218

Dr. J.R. West
Morton Thiokol, Inc.
P.O. Box 30058
Shreveport, LA 71130

Director
Naval Research Laboratory
Attn: Code 2627
Washington, DC 20375
(6 copies)

Dr. Robert J. Schmitt
SRI International
333 Ravenswood Avenue
Menlo Park, CA 94025

Dr. Michael D. Coburn
Los Alamos National Lab
M-1, Explosives Technology
Mail Stop, C920
Los Alamos, NM 87545

(SYN)

DISTRIBUTION LIST

Dr. G. Neece
Office of Naval Research
Code 413
Arlington, VA 22217

Mr. C.M. Havlik
0/83-10, B/157-3W
Lockheed Missiles & Space Co., Inc.
P.O. Box 504
Sunnvale, CA 94086

Dr. Philip Howe
Ballistic Research Laboratory
Code DRXBR-TBD
Aberdeen Proving Ground, MD 21005

Prof. C. Sue Kim
Department of Chemistry
California State University, Sacramento
Sacramento, California 95819

Mr. J. Moniz
Naval Ordnance Station
Code 5253L
Indian Head, MD 20640

Dr. R. Reed Jr.
Naval Weapons Center
Code 38904
China Lake, CA 93555

L.H. Sperling
Materials Research Center #32
Lehigh University
Bethlehem, PA 18015

Dr. Kurt Baum
Fluorochem, Inc.
680 South Ayon Ave.
Azusa, CA 91702

Dr. Andrew C. Victor
Naval Weapons Center
Code 3208
China Lake, CA 93555

Dr. J.C. Hinshaw
Morton Thiokol Inc.
P.O. Box 524
Mail Stop 240
Brigham City, Utah 84302

Dr. V.J. Keenan
Anal-Syn Lab. Inc.
P.O. Box 547
Paoli, PA 19301

P. Politzer
Chemistry Department
University of New Orleans
New Orleans, Louisiana 70148

Mr. David Siegel
Office of Naval Research
Code 253
Arlington, VA 22217

Dr. Rodney L. Willer
Morton Thiokol, Inc.
P.O. Box 241
Elkton, MD 21921

Dr. R. Atkins
Naval Weapons Center
Code 3852
China Lake, CA 93555

(SY:)

DISTRIBUTION LIST

Prof. J.C. Chien University of Massachusetts Department of Chemistry Amherst, MA 03003	Dr. W.H. Graham Morton Thiokol, Inc. Hunstville Division Hunstville, AL 35807-7501
Dr. B. David Halpern Polysciences, Inc. Paul Valley Industrial Park Warrington, PA 18976	Dr. C. Coon Lawrence Livermore Lab. University of California P.O. Box 808 Livermore, CA 94550
Dr. M.B. Frankel Rockwell International Rocketdyne Division 6633 Canoga Avenue Canoga Park, CA 91304	Dr. R. Gilardi Naval Research Laboratory Code 6030 Washington, DC 20375
Dr. R.A. Earl Hercules, Inc. Magna, Utah 84109	Dr. Alan Marchand Dept. of Chemistry North Texas State University NTSU Station, Box 5068 Denton, Texas 76203
Dr. Robert R. Ryan INC-4, MS C346 Los Alamos National Laboratory Los Alamos, New Mexico 87545	T.B. Brill Department of Chemistry University of Delaware Newark, Delaware 19716
Dr. Robert D. Chapman AFRPL/LKLR Edwards AFB, CA 93525	Dr. A.A. Defusco Code 3858 Naval Weapons Center China Lake, CA 93555
Dr. L. Erwin MIT Room 35-008 Cambridge, MA 02139	Dr. Richard A. Hollins Naval Weapons Center Code 3853 China Lake, CA 93555
Dr. M. Farber Space Sciences, Inc. 135 W. Maple Avenue Monrovia, CA 91016	Dr. R. Armstrong MIT Room 66-505 Cambridge, MA 02139
	Professor Philip E. Eaton Department of Chemistry University of Chicago 5735 South Ellis Avenue Chicago, IL 60637

7/22/86

NEW ADDRESS:

G. E. Manser
Aerojet Strategic Propulsion Co.
P. O. Box 15699C
Bldg. 05025, Dept. 2139
Sacramento, CA 95852

Prof. J. H. Boyer
Chemistry Department
University of New Orleans
New Orleans, LA 70148

Dr. C. Bedford
Naval Surface Weapons Center
Code R11
White Oak
Silver Spring, MD 20910